

REPORT DOCUMENTATION PAGE

Form Approved
OMB NO. 0704-0188

Public Reporting burden for this collection of information is estimated to average 1 hour per response, including the time for reviewing instructions, searching existing data sources, gathering and maintaining the data needed, and completing and reviewing the collection of information. Send comment regarding this burden estimates or any other aspect of this collection of information, including suggestions for reducing this burden, to Washington Headquarters Services, Directorate for information Operations and Reports, 1215 Jefferson Davis Highway, Suite 1204, Arlington, VA 22202-4302, and to the Office of Management and Budget, Paperwork Reduction Project (0704-0188,) Washington, DC 20503.

1. AGENCY USE ONLY (Leave Blank)		2. REPORT DATE 31 Dec. 2003	3. REPORT TYPE AND DATES COVERED Final (June 2001 Nov 21, 2003) 01 Jul 00 - 31 Oct 03	
4. TITLE AND SUBTITLE Testing a High-Sensitivity ATR-FTIR Water Monitor for Ionic CWA Breakdown Products			5. FUNDING NUMBERS DAAD DAAD19-00-1-0417	
6. AUTHOR(S) Professor Steven H. Strauss				
7. PERFORMING ORGANIZATION NAME(S) AND ADDRESS(ES) Colorado State University Department of Chemistry Fort Collins, CO 80523			8. PERFORMING ORGANIZATION REPORT NUMBER	
9. SPONSORING / MONITORING AGENCY NAME(S) AND ADDRESS(ES) U. S. Army Research Office P.O. Box 12211 Research Triangle Park, NC 27709-2211			10. SPONSORING / MONITORING AGENCY REPORT NUMBER 41567.2-CH	
11. SUPPLEMENTARY NOTES The views, opinions and/or findings contained in this report are those of the author(s) and should not be construed as an official Department of the Army position, policy or decision, unless so designated by other documentation.				
12 a. DISTRIBUTION / AVAILABILITY STATEMENT Approved for public release; distribution unlimited.			12 b. DISTRIBUTION CODE	
13. ABSTRACT (Maximum 200 words) no abstract to report				
14. SUBJECT TERMS Detection, water monitor, terrorist weapons, CWA, ions, cyanide, G agents, ATR, FTIR, infrared spectroscopy			15. NUMBER OF PAGES 90 pages	
			16. PRICE CODE	
17. SECURITY CLASSIFICATION OR REPORT UNCLASSIFIED	18. SECURITY CLASSIFICATION ON THIS PAGE UNCLASSIFIED	19. SECURITY CLASSIFICATION OF ABSTRACT UNCLASSIFIED	20. LIMITATION OF ABSTRACT UL	

Table of Contents

Abstract	2
Table of Contents	3
Introduction	4
FTIR Detection of Aqueous Anions Using Coated ATR Crystals: A Mini Review	5
Experimental Details	7
Evanescent Wave Penetration Depth Calculations	11
Determination of Limits of Detection (LODs) in this Work	13
Calibration Curve for Aqueous Nitrate Using the Uncoated Silicon ATR Probe	21
The Limits of Detection for CN^- (cyanide)	22
Calibration Curves for CN^-	26
Table of Limits of Detection (LODs) for Analytes Other Than CN^-	30
The Limits of Detection for PMPA^- (pinacolylmethylphosphonate)	32
The Limits of Detection for ClO_4^- (perchlorate)	37
The Limits of Detection for ClO_3^- (chlorate)	41
The Limits of Detection for PFOS^- (perfluorooctanesulfonate)	44
The Limits of Detection for PFBS^- (perfluorobutanesulfonate)	46
The Limits of Detection for CF_3SO_3^- (trifluoromethanesulfonate)	48
The Limits of Detection for BF_4^- (tetrafluoroborate)	50
The Limits of Detection for PF_6^- (hexafluorophosphate)	54
Discussion of LODs	57
Detection of Aqueous MnO_4^- (permanganate)	60
Detection of Aqueous CF_3CO_2^- , $\text{C}_7\text{F}_{15}\text{CO}_2^-$, and $\text{C}_{11}\text{F}_{23}\text{CO}_2^-$ (perfluorocarboxylates)	61
Calibration Curves for PMPA^- , ClO_4^- , and PFOS^-	65
Synthesis and Use of the Alternate Extractant $\text{azaDEC}^+\text{NO}_3^-$	XX

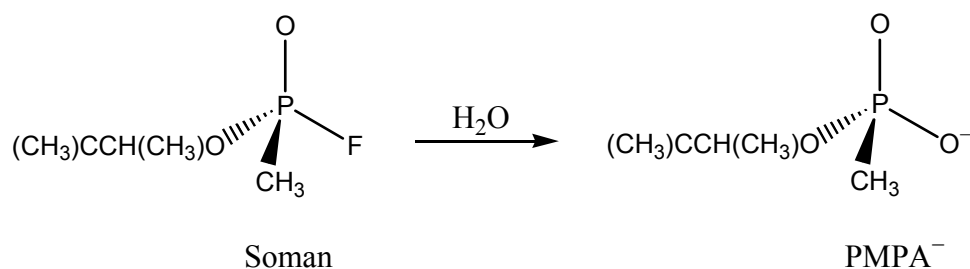
Testing a High-Sensitivity ATR-FTIR Water Monitor for Ionic CWA Breakdown Products

Introduction

We had already developed a sensitive infrared spectroscopy method for detecting monovalent anions in water¹ when we were approached by the US Army, through Janet Jensen, to work with the Joint Service Agency Water Monitor (JSAWM) program with the specific goal of detecting CWA agents such as G-agent hydrolysis products and cyanide in water in real time and at concentrations approaching 1–10 ppb.

This work was simultaneously supported, in part, by an NSF grant to Professor Strauss (*Detection, Separation, and Recovery of Aqueous Ions with Redox-Recyclable Extractants*, CST-0085892).

In consultation with Janet Jensen, we focused our efforts on the detection of cyanide (CN^-) and PMPA^- . The latter is the first hydrolysis product of the G-agent Soman. The hydrolysis is shown below.



However, in order to define and improve the detection limits for both CN^- and PMPA^- and to develop consistent procedures for developing linear calibration curves, it was also necessary to study additional anionic analytes as surrogates. Some of the surrogates were chosen, in consultation with Janet Jensen, because their detection and quantification in water might be of

interest to US military personnel from programs other than JSAWM. Surrogates for CN^- included azide, N_3^- , cyanate, OCN^- , and thiocyanate, SCN^- . Surrogates for PMPA^- included perchlorate, ClO_4^- , chlorate, ClO_3^- , perfluorooctanesulfonate (PFOS^-), $\text{C}_8\text{F}_{17}\text{SO}_3^-$, perfluorobutanesulfonate (PFBS^-), $\text{C}_4\text{F}_9\text{SO}_3^-$, trifluoromethanesulfonate, CF_3SO_3^- , permanganate, MnO_4^- , perrhenate, ReO_4^- , perfluorooctanoate, $\text{C}_7\text{F}_{15}\text{CO}_2^-$, perfluorododecanoate, $\text{C}_{11}\text{F}_{23}\text{CO}_2^-$, tetrafluoroborate, BF_4^- , and hexafluorophosphate, PF_6^- . The relevance of some of these is as follows. Azide is a component of blasting caps.² Perchlorate is a component of solid propellants for rockets and its presence in water has become a significant environmental concern in many western states.³ Perfluorooctanesulfonate was, for decades a key ingredient in aqueous film-forming foams (AFFFs) used to extinguish liquid fuel fires on aircraft carriers and military air bases as well as civilian airports.⁴

FTIR Detection of Aqueous Anions Using Coated ATR Crystals: A Mini Review

We searched the literature (CAS and Medline databases) for methods of detection similar to the one we were developing. The last search that we did was at the end of July 2003. Numerous authors have studied analytical uses of ATR-FTIR spectroscopy, but there are only a handful of publications, listed in Table 1 (next page), that focus on coated ATR crystals for the quantification and/or detection of aqueous anions. In most cases, the ATR-FTIR spectrometer was used to examine the properties of the coating, not as an anion sensor. As a result, all but two of the concentrations listed are the lowest concentration reported, not the LOD.

Table 1. List of references for the FTIR detection of aqueous anions using coated ATR crystals

corresponding author ^(ref)	anion(s)	lowest reported concentration	ATR coating material(s)
Hug ⁵	SO ₄ ²⁻	1 μM	hematite
Blesa ⁶	carboxylates	1 μM	TiO ₂
Martin ⁷	carboxylates	10 μM (LOD)	hematite
Elzinga ⁸	SO ₄ ²⁻	30 μM	goethite
Borda ⁹	oxalate	50 μM	goethite
Peak ¹⁰	borate	50 μM	hydrrous ferric oxide
Hug ¹¹	arsenate	90 μM	ferrihydrite
Mizaikoff ¹²	2,4-D ^a	210 μM (LOD)	MIPs ^b
McQuillan ¹³	SO ₄ ²⁻ , SO ₄ ²⁻ , S ₂ O ₃ ²⁻	1 mM	Cr ₂ O ₃
McQuillan ¹⁴	carboxylates	1 mM	metal oxides
McQuillan ¹⁵	CO ₃ ²⁻	1 mM	ZrO ₂ sol-gel
Schulthess ¹⁶	CO ₃ ²⁻	1 mM	goethite
Sheals ¹⁷	<i>N</i> -phosphonomethylglycine	0.7 μmol/m ²	goethite
Kellner ¹⁸	S ₂ O ₃ ²⁻	100 mM	PVC-membrane

^a 2,4-D, 2,4-dichlorophenoxyacetic acid. ^b MIPs, molecularly imprinted polymers.

Experimental Details

Apparatus. IR spectra were recorded using an ATR-FTIR spectrometer (ReactIR-1000, Applied Systems Inc., Millersville, MD) that was equipped with either a silicon (SiComp) or diamond (DiComp) ATR probe (Applied Systems Inc, Millersville, MD) and a liquid-nitrogen-cooled MCT detector. The spectral window was 4000 to 650 cm^{-1} with a nominal spectral resolution of 8 cm^{-1} . The electronic gain was 1 (SiComp probe) or 2 (DiComp probe). Happ-Ganzel apodization was used with no post-run spectral smoothing. The SiComp probe consisted of a 30-bounce silicon ATR crystal mated to a ZnSe optical focusing element and was housed in a 5.2 cm long \times 2.5 cm diameter cylindrical stainless-steel conduit. The DiComp probe consisted of a 18-bounce diamond ATR crystal mated to a ZnSe optical focusing element and housed in a 1.3 cm thick \times 7.6 cm diameter stainless-steel DuraDisk (Applied Systems Inc., Millersville, MD). The wetted surface of both the silicon and diamond ATR crystals was a circular area 0.9 cm in diameter.

Reagents. Unless otherwise specified, the reagents used for this project were reagent grade or better and were used as received from Sigma/Aldrich or similar vendors. The polyalkylated ferrocenium salts 1,1',3,3'-tetrakis(2-methyl-2-nonyl)ferrocenium nitrate ($\text{DEC}^+\text{NO}_3^-$) and DEC^+Cl^- were synthesized by literature methods.^{19,20} Potassium perfluoro-*n*-octanesulfonate (K(PFOS)) was synthesized from perfluorooctanesulfonyl fluoride (3M Company, St. Paul, MN) by adding it to potassium hydroxide in water and recrystallizing the resultant salt five times from water to a final purity of >99%.²¹ Potassium perfluoro-*n*-butanesulfonate (K(PFBS)) was synthesized from perfluorobutanesulfonyl fluoride (3M Company, St. Paul, MN) in the same manner. CAUTION: the preparation of K(PFOS) and K(PFBS) should be carried out in a fume hood by trained personnel due to the generation of HF.

A synthetic tap water recipe was given to us by Janet Jensen, and solutions for some experiments were prepared using the recipe shown in Table 2.

Table 2. Recipe for Synthetic Tap Water (from Janet Jensen)

compound	final concentration (mg/L)
NaHCO ₃	100
MgSO ₄	6.7
CaSO ₄	27.0
K ₂ HPO ₄	0.71
KH ₂ PO ₄	0.30
(NH ₄) ₂ SO ₄	0.01
NaCl	0.01
FeSO ₄	0.0015
Humic Acid	1.0
Fulvic Acid	1.0
NaNO ₃	1.0

Procedure. All aqueous stock solutions were prepared in Class A volumetric glassware using distilled deionized water (Barnstead NANOpure, Dubuque, IA) that had an initial resistivity of 18 M Ω cm. All experiments were performed at 24 ± 1 °C (room temperature) unless otherwise noted. Aqueous stock solutions were made from the K⁺, Li⁺, or Na⁺ salts of each anion except for PMPA⁻ where H(PMPA) was used. Since the pK_a of H(PMPA) is 2.4,²² the concentration ratio [PMPA⁻]/[H(PMPA)] is ca. 400 when [PMPA⁻] + [H(PMPA)] = 10 μ M.

The exposed surface of the ATR crystal was treated with 20 ± 3 μ L of a fresh (<1 week old) dichloromethane solution of either DEC⁺NO₃⁻ or DEC⁺Cl⁻. Evaporation of dichloromethane (ca. 30 s) left a dry thin-film coating on the surface of the crystal. A nominal film thickness of 0.2 μ m was calculated assuming a uniform cylinder of 0.9 cm diameter and using the density of DEC⁺NO₃⁻ determined by X-ray crystallography (1.1 g cm⁻³).²⁰ Ellipsometry (WVASE32, J. A. Wollman Co. Inc. Lincoln, NE) was used to estimate the actual film thickness (ca. 0.1 μ m) and index of refraction for a silicon wafer coated with DEC⁺NO₃⁻. Using the experimentally determined index of refraction for the DEC⁺NO₃⁻ film, ca. 1.5, the

evanescent wave extends 1.0, 0.4, or 0.2 μm beyond the surface of the ATR crystal at 650, 1555, or 4000 cm^{-1} respectively (see next section). Therefore, the entire thickness of the film was sensed by the evanescent wave below 1555 cm^{-1} .

The coated ATR probe was used for a single analysis, after which the thin-film coating was removed by washing with acetone. The bare ATR crystal was re-coated with a thin film of extractant for each subsequent analysis. A single spectrum of each film was collected prior to its use and the absolute and relative absorbance of the observed IR bands were compared to previous films. For 46 films prepared from 20 μL of a 3 mM dichloromethane solution of $\text{DEC}^+\text{NO}_3^-$ on the silicon crystal, the absolute absorbance of the 2926 cm^{-1} $\nu(\text{CH})$ band and the 1332 cm^{-1} $\nu(\text{NO})$ band varied by only $\pm 5\%$ and $\pm 6\%$, respectively. These data are displayed in Table 3 (below and continued on next page). For nine $\text{DEC}^+\text{NO}_3^-$ films, the initial dA/dt rates for solutions of 5.0 μM ClO_4^- were reproducible to within $\pm 11\%$.

Table 3. Reproducibility of the Absorbance Values of the $\text{DEC}^+\text{NO}_3^-$ -Coated Silicon Probe^a

absorbance of $\nu(\text{CH})$ at 2926 cm^{-1}	absorbance of $\nu(\text{NO})$ at 1332 cm^{-1}	ratio of $\nu(\text{CH})/\nu(\text{NO})$ absorbances
1.07552	1.02550	1.049
1.14979	1.10149	1.044
1.09480	1.03961	1.053
1.14328	1.10144	1.038
1.04346	0.973823	1.072
1.05895	1.02104	1.037
1.09580	1.05249	1.041
1.09303	1.03467	1.056
1.13891	1.09950	1.036
1.11588	1.06903	1.044
1.10047	1.05341	1.045
1.09961	1.03958	1.058
1.10233	1.04308	1.057
1.12473	1.06946	1.052
1.08815	1.01821	1.069
1.04588	0.99044	1.056
1.13347	1.08252	1.047
1.13782	1.09580	1.038
1.06323	0.991293	1.073

1.11972	1.07413	1.042
1.12652	1.07328	1.050
1.10616	1.04949	1.054
1.13713	1.08028	1.053
1.13806	1.08202	1.052
1.12118	1.09805	1.021
1.07691	1.04596	1.030
1.15893	1.11425	1.040
1.13043	1.07322	1.053
1.17572	1.14723	1.025
1.16416	1.11521	1.044
1.05459	0.91956	1.147
1.09551	0.969367	1.130
1.18743	1.03604	1.146
1.07599	0.907701	1.185
1.08523	0.914866	1.186
1.07856	0.93066	1.159
1.16029	1.11945	1.036
1.16526	1.11445	1.046
1.15317	1.08410	1.064
1.01684	1.03705	0.981
1.04445	1.01487	1.029
1.06020	1.03194	1.027
1.02866	0.991616	1.037
1.01641	1.01634	1.000
1.02395	1.00046	1.023
1.04622	1.02553	1.020

^a Each trial listed is for a separate film made from 20 μL of a 3 mM dichloromethane solution of $\text{DEC}^+\text{NO}_3^-$. The mean $\nu(\text{CH})$ absorbance value is 1.10(5) (5% RSD). The mean $\nu(\text{NO})$ absorbance value is 1.04(6) (6% RSD). The mean $\nu(\text{CN})/\nu(\text{NO})$ abs. ratio is 1.06(4) (4% RSD).

The film thickness was optimized by coating the silicon probe with 20 μL of dichloromethane solutions of $\text{DEC}^+\text{NO}_3^-$ ranging in concentration from 0.1 to 10 mM. The more concentrated extractant solutions resulted in more intense $\nu(\text{CH})$ and $\nu(\text{NO})$ IR bands due to the thicker coatings on the ATR crystal. For each experiment, the coated probe was immersed in 5.0 μM aqueous LiClO_4 and spectra were recorded every minute for 15 minutes. Films prepared from the 3 mM $\text{DEC}^+\text{NO}_3^-$ solution resulted in the largest initial dA/dt values while films made from both higher and lower concentrations of $\text{DEC}^+\text{NO}_3^-$ had smaller initial dA/dt values. Therefore, unless otherwise noted, 3 mM $\text{DEC}^+\text{NO}_3^-$ solutions were used for all analyses.

ATR crystals were coated with $\text{DEC}^+\text{NO}_3^-$ for the analysis of all of the anions studied except PMPA^- , which, because its hydration energy is apparently larger than that of nitrate, was not extracted by $\text{DEC}^+\text{NO}_3^-$. Coating the diamond ATR crystal with DEC^+Cl^- enabled the extraction of PMPA^- from aqueous solution as a result of the higher hydration energy of Cl^- relative to NO_3^- . The film thickness of DEC^+Cl^- was not optimized.

In a typical analysis, the coated ATR probe was immersed in 100 mL of water which was stirred at ca. 200 rpm for the silicon probe and at ca. 75 rpm for the diamond probe. The film was allowed to equilibrate with water for 10 minutes, at which time a background spectrum was collected. An appropriate amount of an analyte stock solution was then added to the water with stirring to achieve the desired final analyte concentration and FTIR spectra (64 co-added scans) of this solution were collected every minute for an appropriate amount of time (usually 10–60 minutes). The solution was stirred continuously during the entire experiment. Control experiments with a colored dye showed that dispersion of the added aliquot occurred within 10 s for both probes.

Entirely analogous procedures were developed for the analysis of CN^- and its surrogates using *cis*-1,3-bis(diphenylphosphino)propanedichloronickel(II), $\text{NiCl}_2(\text{dppp})$.

Evanescent Wave Penetration Depth Calculations

The theory of ATR spectroscopy is available in monographs by Harrick and by Urban.^{23,24} The distance (d_p) that the evanescent wave penetrates beyond the exposed surface of the ATR crystal is given by equation 1, where ν is the wavenumber, θ is the angle of incidence of

$$d_p = \frac{1}{2\pi\nu\sqrt{n_1^2 \sin^2 \theta - n_2^2}} \quad (1)$$

the light at the interface, and n_1 and n_2 are the refractive indexes of the two materials.²³ The intensity of the evanescent wave at the calculated d_p value is 37% of the original intensity at the crystal surface.

Table 4 lists d_p values at four different IR wavenumbers. Two of these points, 4000 and 650 cm^{-1} , were chosen since they are the boundaries over which all the IR spectra in this study were collected. The other two points, 1555 and 1000 cm^{-1} , are the boundaries for the useful part of the fingerprint region that is most commonly examined when using either the silicon or diamond ATR probes. Data are presented for experiments in which the ATR probes were not coated and for experiments in which the ATR crystals were coated by evaporation of 20 μL of a 1 mM dichloromethane solution of $\text{DEC}^+\text{NO}_3^-$. The index of refraction of a thin film of $\text{DEC}^+\text{NO}_3^-$ was determined to be ca. 1.5 by ellipsometry. Both of the ASI probes used have a manufacturer-specified θ value of 45°.

Table 4. Calculated evanescent wave penetration depths (d_p)

interface	n_1	n_2	d_p (μm) at the indicated wavenumber			
			4000 cm^{-1}	1555 cm^{-1}	1000 cm^{-1}	650 cm^{-1}
silicon/water	3.5	1.3	0.15	0.39	0.61	0.93
silicon/ $\text{DEC}^+\text{NO}_3^-$	3.5	1.5	0.16	0.40	0.62	0.96
diamond/water	2.4	1.3	0.26	0.67	1.05	1.61
diamond/ $\text{DEC}^+\text{NO}_3^-$	2.4	1.5	0.28	0.73	1.14	1.75

These penetration depths were compared with the measured and calculated thicknesses of the $\text{DEC}^+\text{NO}_3^-$ film. An approximate film thickness of 0.2 μm was calculated using the equation for the volume of a cylinder and the known density of $\text{DEC}^+\text{NO}_3^-$, which was previously determined by X-ray crystallography. An actual film thickness of ca. 0.1 μm was estimated by ellipsometry. The evanescent wave penetrates from 0.40 to 1.75 μm beyond the surface of the

ATR crystal in the fingerprint region of the IR spectrum for $\text{DEC}^+\text{NO}_3^-$ -coated ATR crystals. Therefore, the entire thickness of the film, 0.1–0.2 μm , is sensed by the evanescent wave. In addition, the evanescent wave also penetrates into the aqueous solution in contact with the thin-film coating. However, since the analyte concentrations used for the thin-film experiments are much too dilute, by orders of magnitude, for the analyte to be detected in aqueous solution, only analyte that has undergone ion exchange with nitrate or chloride in the thin-film can be detected. In other words, the aqueous analyte is "invisible" in the thin-film experiments.

Determination of Limits of Detection (LODs) in this Work

The limit of detection (LOD) is commonly defined as the analyte concentration that gives a signal intensity three times higher than the intensity of the noise. As we will show, this definition is ambiguous for IR spectra. Consider the spectrum of aqueous 1 mM LiClO_4 shown in Figure 1 (2,500 scans, 8 cm^{-1} resolution). The perchlorate $\nu(\text{ClO})$ signal at ca. 1108 cm^{-1} is obvious and by visual inspection is undoubtedly greater than three times the intensity of the noise. However, the peak (i.e., signal) position (to $\pm 4 \text{ cm}^{-1}$ at 8 cm^{-1} resolution), the intensity (absorbance) at that position, and the noise in the vicinity of that position need to be determined from the experimental data for the signal-to-noise ratio (*SNR*) to be calculated. It should be clear that the peak position and absorbance become increasingly difficult to measure as the concentration of analyte is lowered and the true LOD is approached.

To address these issues, we first consulted the LOD literature. Reported definitions of limits of detection vary widely and have been heavily disputed.²⁵⁻³² These papers culminated in the publication of an IUPAC resolution in 1975 that attempted to standardize procedures for determining LODs.^{27,28} The IUPAC defined the LOD as the concentration, c_L , derived from the smallest signal, x_L , that can be detected with reasonable certainty. The quantity x_L is defined by

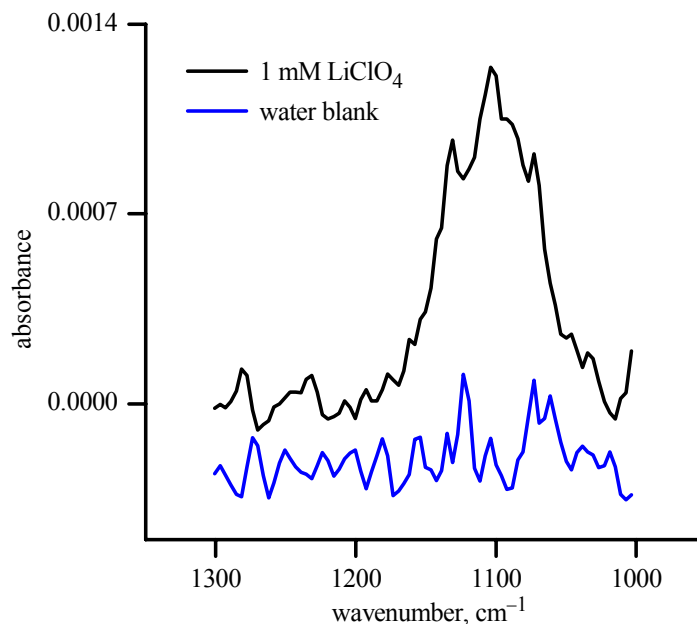


Figure 1. ATR-FTIR spectra of 1 mM aqueous LiClO_4 and a distilled, deionized water blank. Both spectra were collected over fifteen minutes (2,500 scans, 8 cm^{-1} resolution). The peak position and SNR for the LiClO_4 spectrum were determined as described in this section, to be 1108 cm^{-1} and 8, respectively.

equation 2, in which x_b is the mean of the signal intensity from the blanks, s_b is the standard deviation of these blank signal intensities, and k is a numerical factor corresponding to a specific

$$x_L = x_b + ks_b \quad (2)$$

confidence level. The quantity x_b should be determined from a blank that does not intentionally contain the analyte and has essentially the same composition as the sample to be analyzed. The concentration, c_L , is a function of x_L , as shown in equation 3, where m is the slope of a calibration curve of analyte signal, x , versus concentration, c .

$$c_L = (x_L - x_b)/m \quad (3)$$

Substituting equation 3 into equation 2 results in equation 4, which defines the LOD.

$$c_L = ks_b/m \quad (4)$$

This approach is only valid if m is well-defined and has a very small error associated with it *and* if the intercept of the calibration curve is essentially zero. The value $k = 3$ defines a confidence level of 99.6% for the quantity x_L (see equation 5) and has been generally accepted.^{26,27,29,30}

$$x_L = (x_b + 3s_b) \quad (5)$$

Values of x_b and s_b should be experimentally determined from a sufficiently large number of blanks (≥ 20).

As an alternative, the IUPAC suggested that s_b can be determined from a single measurement when using techniques that involve counting statistics. This simplification can be used with FTIR spectroscopy, since a typical spectrum is the result of multiple scans (e.g., either 64, 1660, 2500, or 5000 scans per spectrum in our experiments). Several authors have defined s_b to be equal to the root-mean-square of the noise (N_{RMS}) from a blank spectrum.^{25,32,33} This assumes that the noise in the spectrum is essentially white noise (i.e., random noise with no drift). Since white noise follows a normal probability error distribution, it can be used to define the standard deviation.²⁵ If N_{RMS} is substituted into equation 2 for s_b then equation 6 results for $k = 3$. When a typical sample FTIR spectrum is collected, the signal from the blank, x_b , is

$$x_L - x_b = 3N_{\text{RMS}} \quad (6)$$

ratioed out as the background so the measured signal, S , from the sample spectrum of an analyte can be defined as shown in equation 7.

$$S = x_L - x_b \quad (7)$$

Substituting equation 7 into equation 6 gives $S = 3N_{\text{RMS}}$, leading to the familiar definition that the LOD is the concentration for which $S/N_{\text{RMS}} = 3$. It should be noted that N_{RMS} is typically calculated using software that accompanies a spectroscopic instrument. This software first squares all the signal values within a designated range resulting in all the values being positive. The square root of the average of these positive values is then calculated giving the root-mean-square of the selected data. The N_{RMS} can also be approximated manually as 1/5 of the peak-to-peak noise.^{25,32,33}

The definition of LOD can now be applied to the spectrum of 1 mM aqueous LiClO_4 shown in Figure 1. Using least-squares fitting in the graphing/analysis software Origin, the peak was fit to a Gaussian using equation 8, in which m is the slope of the linear baseline, y_0 is the

$$y = mx + y_0 + \left(\frac{A}{w(\pi/2)^{1/2}} \right) \exp\left(-2 \left(\frac{x-x_c}{w} \right)^2\right) \quad (8)$$

y intercept of the baseline, A is the integrated area under the peak, w is the peak width at half maximum, and x_c is the x value with the highest absorbance. An iterative approach was used to minimize the calculated residuals. Good fits resulted in residual plots with a slope close to zero. A fairly good Gaussian fit to the 1 mM LiClO_4 spectrum was achieved, as shown in Figure 2.

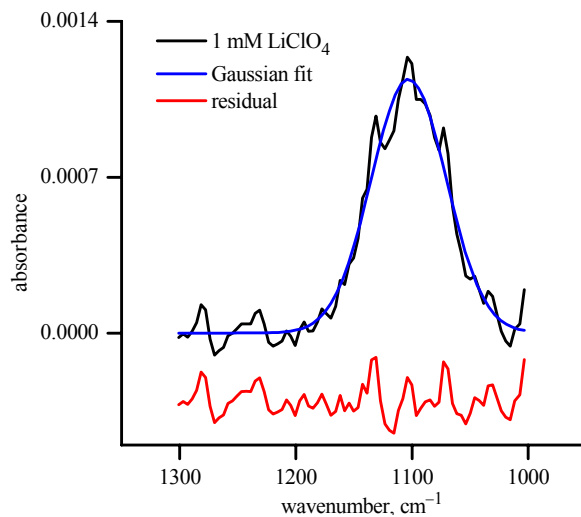


Figure 2. ATR-FTIR spectrum (2,500 scans, 8 cm^{-1} resolution) of 1 mM aqueous LiClO_4 fitted to a Gaussian curve as described in the text. A plot of the residuals of the fit is shown offset.

In order to obtain the true intensity (absorbance) of the peak, the baseline from the Gaussian fit ($y = (-1.8275 \times 10^{-7})x + 0.00016$) was subtracted from both the least-squares fit and from the spectrum. The resulting curves are shown in Figure 3. Using this baseline-adjusted spectrum, the signal, 1.14×10^{-3} , and the peak position, 1108 cm^{-1} , were determined.

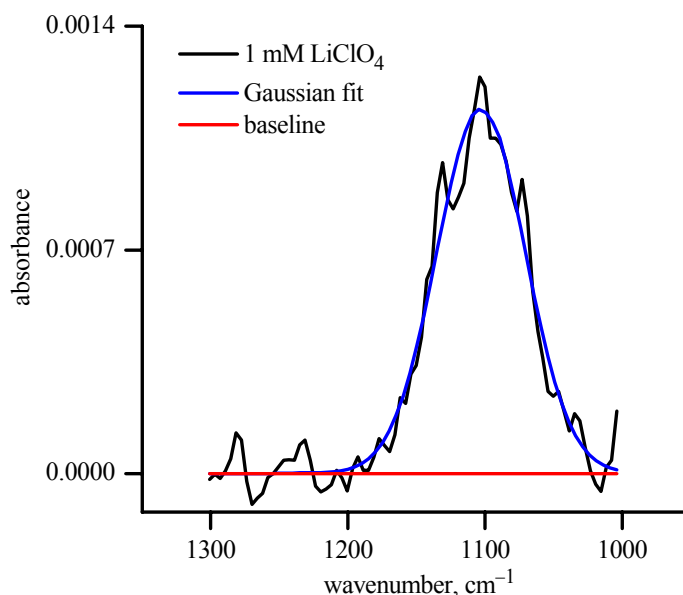


Figure 3. ATR-FTIR spectrum of 1 mM LiClO_4 and its Gaussian fit after subtraction of a baseline ($y = (-1.8275 \times 10^{-7})x + 0.00016$) to yield a horizontal baseline ($y = 0$).

Deciding on the proper wavenumber region over which the noise of an IR spectrum should be measured (the noise window) is also problematic. In the older literature, the noise on either side of a peak was averaged. This assumes, however, that one can determine where the peak "ends" and the baseline "begins", and this is clearly difficult at concentrations approaching the LOD. In addition to that, what wavenumber regions of baseline on either side of the peak should be used? $\pm 20 \text{ cm}^{-1}$? $\pm 50 \text{ cm}^{-1}$? $\pm 100 \text{ cm}^{-1}$?

For our LOD experiments, the noise window was chosen as follows. The spectrum of a high concentration of analyte (or of the thin film at complete ion exchange) was recorded. The noise window for LOD spectra was chosen so that it was centered at the peak maximum in the

high-concentration spectrum and included those wavenumbers on either side of the peak position where the peak intensity was 1% or greater of the peak maximum. This window, which was 198 cm^{-1} ($1200\text{--}1002\text{ cm}^{-1}$) in the case of aqueous perchlorate, was used as the noise window for all uncoated probe perchlorate LOD experiments. It was subsequently determined for several of the anions that the corresponding noise window was frequently within $\pm 20\text{ cm}^{-1}$ of the window defined in the same manner but using the fitted LOD spectra instead of high-concentration spectra.

The N_{RMS} for each LOD experiment was calculated from at least 10 blank spectra over this window using the root-mean-square noise function in the ReactIR software (Applied Systems Inc., Millersville, MD) that operates the particular spectrometer used in our study. In the case of ClO_4^- , N_{RMS} over the range $1200\text{--}1002\text{ cm}^{-1}$ was $1.5(2) \times 10^{-4}$. Control experiments confirmed that N_{RMS} is approximately equal to 1/5 of the peak-to-peak noise over a given spectral window, as previously reported in the literature.^{32,33}

With the signal intensity and noise determined as described above, the *SNR* for the peak shown in Figure 1 was determined to be 8. The average *SNR* for 1 mM ClO_4^- was 7 ± 1 (4 trials). Thus, 1 mM was determined to be above the LOD for ClO_4^- for this particular spectrometer, ATR probe, and set of spectral acquisition parameters. Lower concentrations were examined next. For 0.8 mM ClO_4^- , the average *SNR* was 4.0 ± 0.6 (3 trials). For 0.7 mM ClO_4^- , the average *SNR* was 2.9 ± 0.7 (3 trials). Therefore, the LOD for perchlorate using the uncoated silicon probe was determined to be 0.8 mM.

The process just described for determining a *SNR* becomes more complex for analytes that have multiple IR bands in the region of interest. For example, the FTIR spectrum of the DEC^+Cl^- -coated diamond ATR crystal after 30 minutes in contact with 1 mM aqueous PMPA^- is shown in Figure 4 (64 scans, 8 cm^{-1} resolution). There are at least six major peaks present, not counting the small bands at 1116 and 934 cm^{-1} .

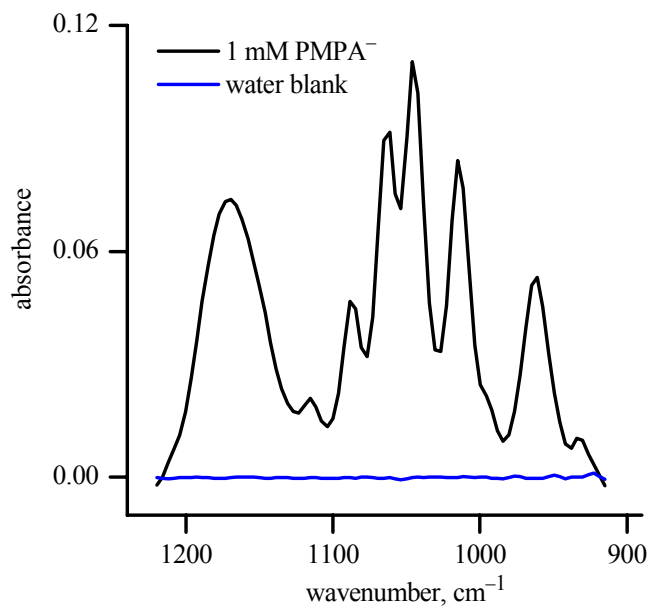


Figure 4. ATR-FTIR spectra (64 scans and 8 cm^{-1} resolution) of the DEC^+Cl^- -coated diamond ATR crystal immersed in distilled deionized water (blank) and after 30 minutes in contact with a 1 mM aqueous solution of PMPA^- .

The $\text{DEC}^+\text{PMPA}^-(s)$ spectrum was least-squares fitted to a combination of seven Gaussian peaks, all but one of which overlap each other, as shown in Figure 5. Contrary to what was done to fit of the perchlorate peaks, an integer baseline (i.e., $y_0 = \text{constant}$) was used for simplicity.

The integer baseline ($y_0 = 4.36 \times 10^{-3}$) was subtracted from both the combined fit and the $\text{DEC}^+\text{PMPA}^-(s)$ spectrum resulting in a new baseline ($y_0 = 0$) as shown in Figure 6. Using this baseline-adjusted spectrum, the signal was measured from the absorbance of the most intense peak ($S = 0.1060$ at 1046 cm^{-1} for this case). The noise value of 1.9×10^{-4} was calculated from 18 blank spectra over the noise window, which ranged from 1212 to 926 cm^{-1} . The SNR was calculated to be 560 for 1 mM aqueous PMPA^- in contact with the DEC^+Cl^- -coated diamond ATR crystal after 30 minutes. Note that the LODs listed below in Table 13 were determined for 10-minute experiments, not 30-minute experiments. The spectra displayed here are for illustrative purposes only.

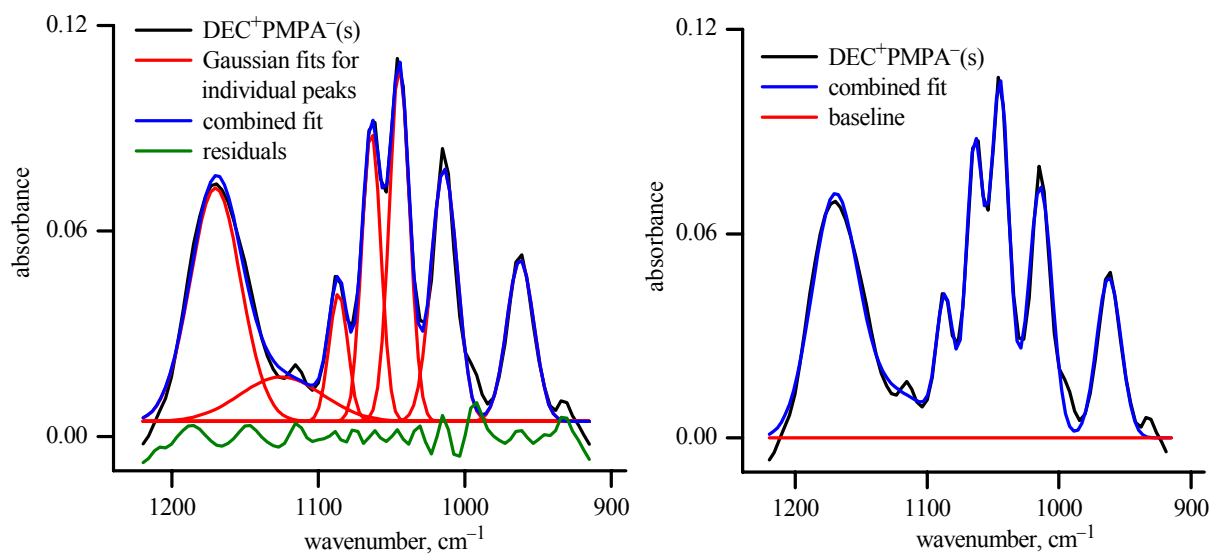


Figure 5 (left). ATR-FTIR spectrum of the DEC⁺Cl⁻-coated diamond ATR crystal after 30 minutes in contact with a 1 mM aqueous solution of PMPA⁻. The seven Gaussian fits of each individual peak are shown and were combined into one overall fit of the spectrum with a baseline of $y_0 = 4.36 \times 10^{-3}$. A plot of the residuals is offset for clarity.

Figure 6 (right). ATR-FTIR spectrum of 1 mM PMPA⁻ after 30 minutes in contact with the DEC⁺Cl⁻-coated diamond ATR probe. The spectrum was fit to a combination of seven Gaussian curves, and a baseline of $y_0 = 4.36 \times 10^{-3}$ was subtracted from both the spectrum and the combined Gaussian fit.

In 1980, a special ACS committee published an extension of the IUPAC LOD definitions.³⁰ They also proposed definitions for a limit of quantification (LOQ) and a region of detection. Some of these limits had been previously used under different names, and the ACS was hoping to provide a uniform terminology for future reports.^{29,30} The LOQ was defined as the analyte concentration for which $SNR = 10$. Three regions of analyte measurement were defined: if $SNR < 3$, the analyte is not detected; if $3 < SNR < 10$, the analyte is in the region of detection; if $SNR \geq 10$, the analyte is in the region of quantitation.³⁰

Calibration Curve for Aqueous Nitrate Using the Uncoated Silicon ATR Probe

The Beer-Lambert law can generally be used in spectroscopic experiments to produce linear calibration curves of absorbance versus analyte concentration. An ATR-FTIR calibration curve for aqueous solutions of nitrate was described by Wilhite and Ellis in 1963, but the plot was not displayed.³⁴ We have redetermined this calibration curve over the range 10–400 mM for the $\nu_{\text{asym}}(\text{NO})$ band of aqueous NaNO_3 using the 30-bounce silicon ATR-FTIR probe. Figure 7 shows this calibration curve (correlation coefficient = 0.999).

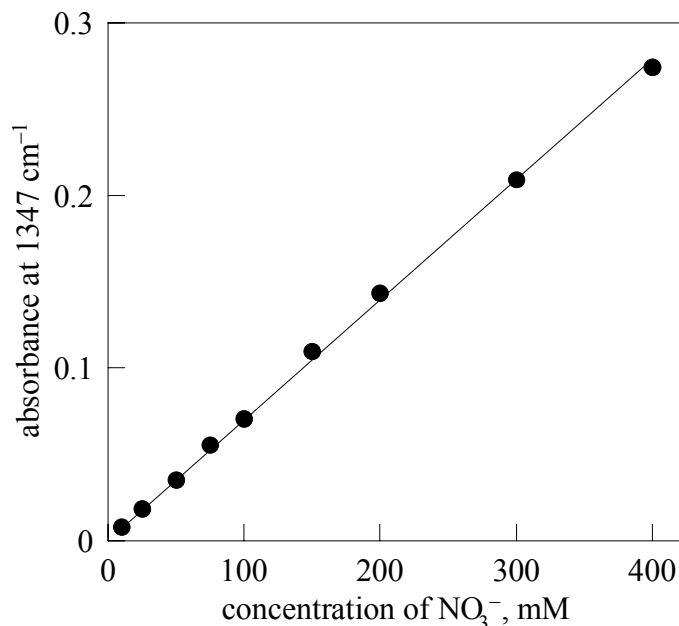


Figure 7. Calibration curve for aqueous nitrate ($\nu(\text{NO})$ at 1347 cm^{-1} ($7.42 \mu\text{m}$)). A set of three spectra (64 co-added scans) were averaged for each concentration and the error bars ($\pm 1\sigma$) are smaller than the points. Wilhite and Ellis monitored the same band but reported its position as $7.46 \mu\text{m}$.

The Limits of Detection for CN^-

At the end of the project period, the 10-minute LOD for cyanide in distilled/deionized water with the $NiCl_2(dppp)$ -coated silicon probe was $2.3 \mu g L^{-1}$ with a SNR of 4 ± 1 . The 10-minute LOD for cyanide in the same medium using the uncoated silicon probe was found to be $52 mg L^{-1}$ with a SNR of 4 ± 1 . The 10-minute LOD for cyanide in synthetic tap water with the $NiCl_2(dppp)$ -coated silicon probe was $5.2 \mu g L^{-1}$ with a SNR of 4.2 ± 0.9 . The 10-minute LOD for cyanide in synthetic tap water with the uncoated silicon probe was $195 \mu g L^{-1}$ with a SNR of 4.5 ± 1.3 . The data are presented in the Figures and Tables below

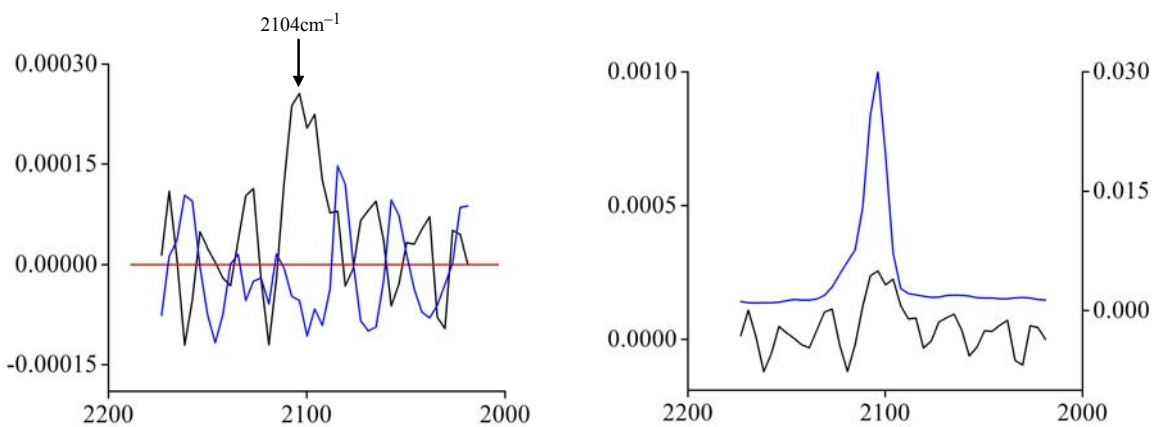


Figure 8 (left). ATR-FTIR spectrum of $2.3 \mu g L^{-1} CN^-$ after 10 minutes in contact with the $NiCl_2(dppp)$ -coated silicon probe is shown in black. A blank spectrum is shown in blue, and the baseline ($y = 0$) is shown in red.

Figure 9 (right). ATR-FTIR spectrum of the same $2.3 \mu g L^{-1} CN^-$ after 10 minutes in contact with the $NiCl_2(dppp)$ -coated silicon probe is shown in black. A spectrum of $260 \mu g L^{-1} CN^-$ after 10 minutes in contact with the $NiCl_2(dppp)$ -coated silicon probe is overlaid in blue.

Table 5. Determination of the 10-minute CN⁻ LOD using the NiCl₂(dppp)-coated silicon probe^a

concentration, μg L ⁻¹	v(CN) signal ^b	average signal (σ) ^c	average SNR ± error ^d
260	0.02385	0.023(4)	330 ± 110
260	0.01895		
260	0.01799		
260	0.02471		
260	0.02856		
260	0.020057		
13	0.001204	0.0015(2)	21 ± 7
13	0.00161		
13	0.00166		
7.8	0.000847	0.00095(8)	14 ± 4
7.8	0.00105		
7.8	0.000966		
5.2	0.000621	0.00069(7)	10 ± 3
5.2	0.000681		
5.2	0.00078		
2.6	0.000314	0.00031(4)	4.4 ± 1.4
2.6	0.000259		
2.6	0.000345		
2.3	0.000256	0.00027(7)	4 ± 1
2.3	0.000393		
2.3	0.000251		
2.3	0.000199		
2.1	0.00018	0.00017(1)	2.4 ± 0.7
2.1	0.000177		
2.1	0.000153		

^a Each trial was done using the silicon probe coated with 20 μL of a 5 mM dichloromethane solution of NiCl₂(dppp). ^b Absorbance at 2104 cm⁻¹. ^c σ = Standard deviation. ^d Signal-to-noise ratio (SNR) where the average noise = 7(2) × 10⁻⁵ and the error was propagated from the signal and noise standard deviations.

Table 6. Determination of the 10-minute CN⁻ LOD using the uncoated silicon probe^a

concentration, mg L ⁻¹	v(CN) signal ^b	average signal (σ) ^c	average SNR \pm error ^d
260	0.000357		15.5
104	0.0001901		8.3
78	0.000188	0.00018(2)	8 \pm 3
78	0.000154		
78	0.000196		
52	0.000095	0.00010(1)	4 \pm 1
52	0.000117		
52	0.000083		

^a Each 10-minute spectrum was the result of 1660 co-added scans. ^b Absorbance at 2081 cm⁻¹.

^c σ = Standard deviation. ^d Signal-to-noise ratio (SNR) where the average noise = $2.3(7) \times 10^{-5}$ and the error was propagated from the signal and noise standard deviations.

Table 7. Determination of the 10-minute CN⁻ LOD in synthetic tap water using the NiCl₂(dppp)-coated silicon probe^a

concentration, μ g L ⁻¹	v(CN) signal ^b	average signal (σ) ^c	average SNR \pm error ^d
26	0.001361		17 ^e
13	0.001189		15
7.8	0.000618		7.8
5.2	0.00033	0.00034(6)	4.2 \pm 0.9
5.2	0.000273		
5.2	0.000414		

^a Each trial was done using the silicon probe coated with 20 μ L of a 5 mM dichloromethane solution of NiCl₂(dppp). ^b Absorbance at 2104 cm⁻¹. ^c σ = Standard deviation. ^d Signal-to-noise ratio (SNR) where the average noise = $8(1) \times 10^{-5}$ and the error was propagated from the signal and noise standard deviations. ^e No error is listed for those concentrations for which only one experiment was performed.

Table 8. Determination of the 10-minute CN^- LOD in synthetic tap water using the uncoated silicon probe^a

concentration, $\mu\text{g L}^{-1}$	$\nu(\text{CN})$ signal ^b	average signal (σ) ^c	average $\text{SNR} \pm \text{error}$ ^d
651	0.000445	na	
325	0.000205	na	
195	0.0000711	0.00008(2)	4.5 \pm 1.3
195	0.000101		
195	0.0000785		
130	0.0000433	na	

^a Each trial was done using the silicon probe coated with 20 μL of a 5 mM dichloromethane solution of $\text{NiCl}_2(\text{dppp})$. ^b Absorbance at 2080 cm^{-1} . ^c σ = Standard deviation. ^d Signal-to-noise ratio (SNR) where the average noise = $1.8(4) \times 10^{-5}$ and the error was propagated from the signal and noise standard deviations.

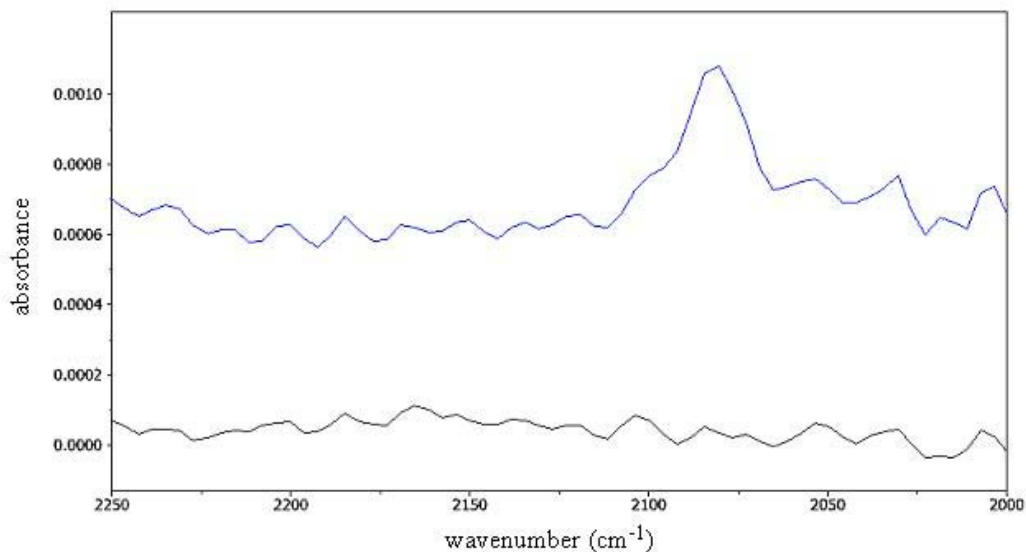


Figure 10. ATR-FTIR spectrum of $130 \text{ mg L}^{-1} \text{CN}^-$ (5.00 mM) in synthetic tap water taken with the uncoated silicon ATR probe ($\nu(\text{CN}) = 2080 \text{ cm}^{-1}$). A blank spectrum is shown at the bottom.

Calibration Curves for CN^-

The development of the calibration curve for CN^- over time is shown in the Tables and Figures in this section.

Table 9. Data for the September 2000 CN^- calibration curve using a film formed by evaporation of 83 μL of 1 mM $\text{NiCl}_2(\text{dppp})$ on the silicon probe

concentration, $\mu\text{g L}^{-1}$	average dA/dt at 2104 cm^{-1}	sigma (std. dev.)	RSD ^a
2.6	0.00004	0.00003	75
26	0.0001	0.00002	20
130	0.00054	0.00009	17
260	0.001	0.0001	10
1300	0.0017	0.0005	29
2600	0.001254		

^a Relative standard deviation (RSD). Three trials were done for all concentrations except 260 $\mu\text{g L}^{-1}$ where six trials were done and 2600 $\mu\text{g L}^{-1}$ where only one trial was done.

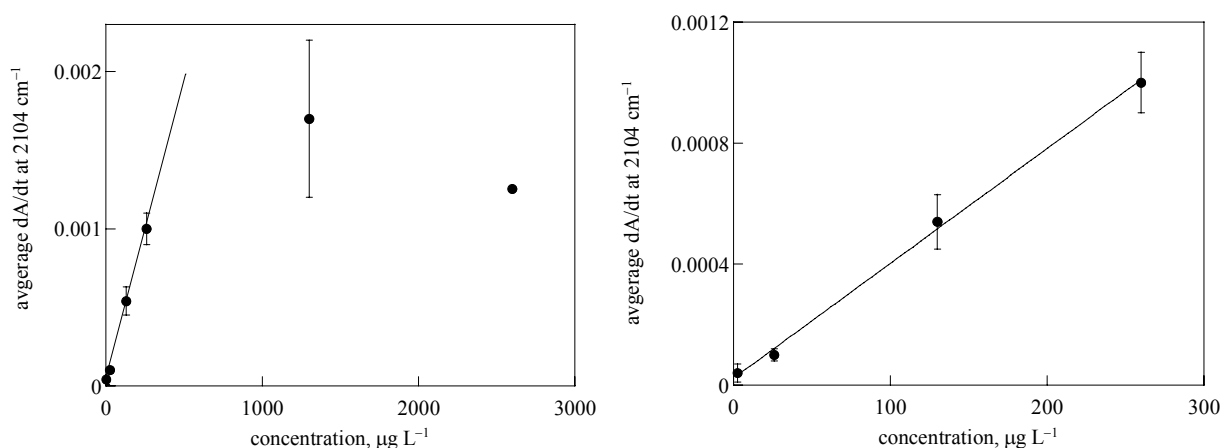


Figure 11. Cyanide calibration curve made September 2000. The films were made on the silicon probe from 83 μL of a 1 mM dichloromethane solution of $\text{NiCl}_2(\text{dppp})$. The error bars represent \pm one standard deviation. The equation of the line is: $y = 3.8(1) \times 10^{-6}x + 2(1) \times 10^{-5}$. The line shown in the right graph is the same as the equation of the line in the left graph.

Table 10. Data for the July 2001 CN^- calibration curve using a film formed by evaporation of 20 μL of 5 mM $\text{NiCl}_2(\text{dppp})$ on the silicon probe

concentration, $\mu\text{g L}^{-1}$	average dA/dt at 2104 cm^{-1}	sigma (std. dev.)	RSD ^a
2.6	0.00002	0.000006	30
13	0.00005	0.00002	40
26	0.000129	0.000006	5
130	0.00056	0.00007	13
260	0.001	0.0002	20

^a Relative standard deviation (RSD). At least three trials were done for all concentrations.

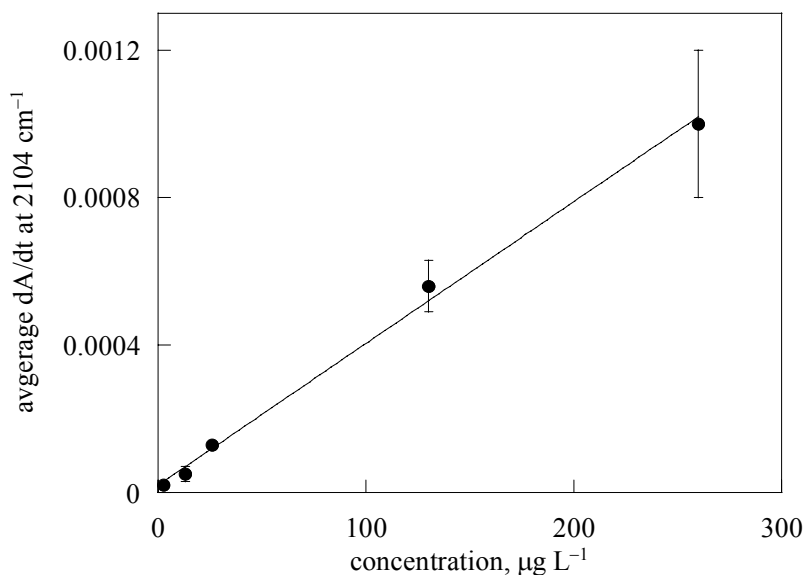


Figure 12. Cyanide calibration curve made July 2001. The films were made on the silicon probe from 20 μL of a 5 mM dichloromethane solution of $\text{NiCl}_2(\text{dppp})$. The error bars represent \pm one standard deviation. The equation of the line is: $y = 3.8(1) \times 10^{-6}x + 2(1) \times 10^{-5}$. Note this data was collected by undergraduate student Karen Wendling and the data very closely agree with the September 2000 data collected by Gretchen Hebert. The least-squares linear fit to the data are exactly the same within error.

Table 11. Data for the May 2003 CN^- calibration curve using a film formed by evaporation of 20 μL of 5 mM $\text{NiCl}_2(\text{dppp})$ on the silicon probe

concentration, $\mu\text{g L}^{-1}$	average dA/dt at 2104 cm^{-1}	sigma (std. dev.)	RSD ^a
2.6	0.000014	0.000002	14
26	0.00015	0.00002	13
130	0.00068	0.00008	12
260	0.0011	0.0002	18

^a Relative standard deviation (RSD). At least three trials were done for all concentrations.

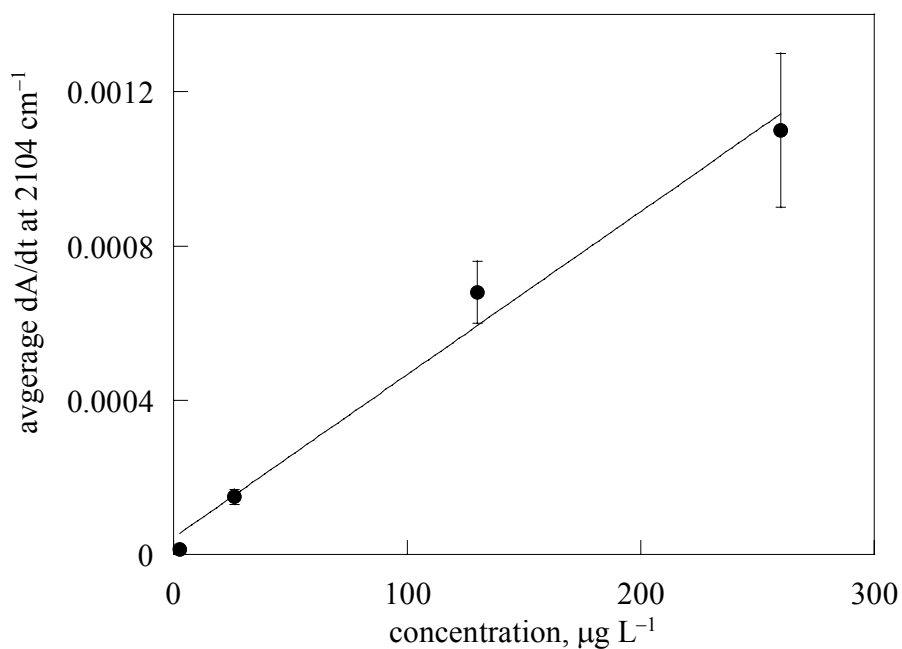


Figure 13. Cyanide calibration curve made May 2003. The films were made on the silicon probe from 20 μL of a 5 mM dichloromethane solution of $\text{NiCl}_2(\text{dppp})$. The error bars represent \pm one standard deviation. The equation of the line is: $y = 4.2(4) \times 10^{-6} x + 4(5) \times 10^{-5}$.

Table 12. Data for the June 2003 cyanide calibration curve using 20 μL of 5 mM $\text{NiCl}_2(\text{dppp})$ on the silicon probe

concentration, $\mu\text{g L}^{-1}$	average dA/dt at 2104 cm^{-1}	sigma (std. dev.)	RSD ^a
0	0.00002	0.00004	200
2.6	0.00002	0.00001	50
13	0.00009	0.00003	33
26	0.00014	0.00002	14
130	0.00059	0.00009	15
260	0.0012	0.0001	8

^a Relative standard deviation (RSD). At least three trials were done for all concentrations.

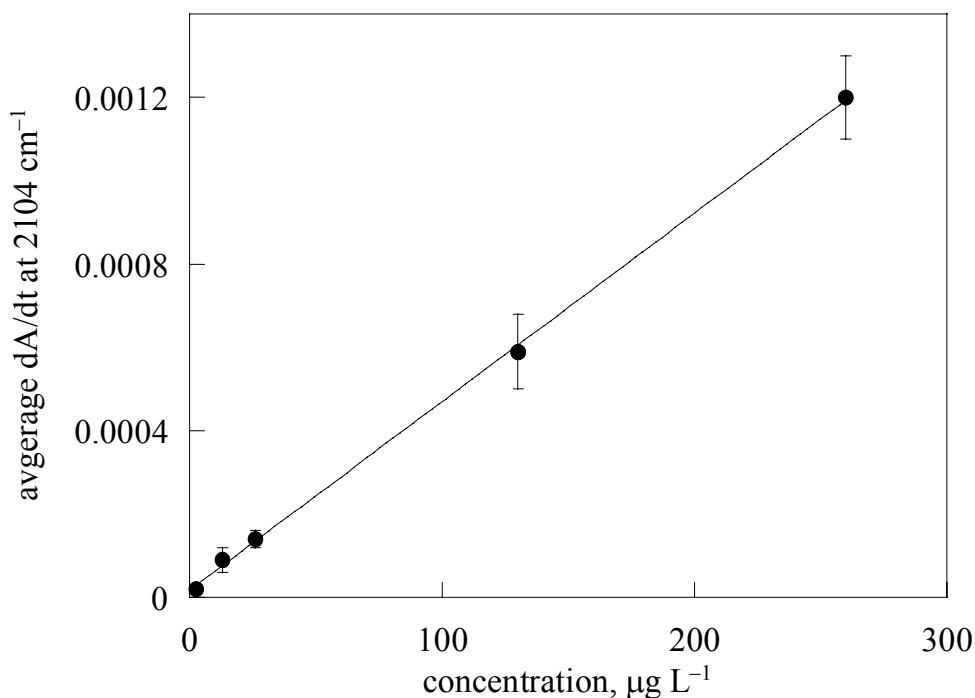


Figure 14. Cyanide calibration curve made June 2003. This is the final calibration curve for CN^- made as part of this project. The films were made on the silicon probe from 20 μL of a 5 mM dichloromethane solution of $\text{NiCl}_2(\text{dppp})$. The error bars represent \pm one standard deviation. The equation of the line is: $y = 4.52(6) \times 10^{-6}x + 1.8(8) \times 10^{-5}$.

Table of Limits of Detection (LODs) for Analytes Other Than CN⁻

In this section, we will present the LODs that we have measured using either DEC⁺NO₃⁻ or DEC⁺Cl⁻. Then, in the following sections, each analyte will be treated separately and nearly all of the relevant data that we collected will be presented (along with representative IR spectra).

As discussed above, the standard spectroscopic definition of an LOD is the analyte concentration for which the signal is three times the intensity of the noise in the region of the signal (i.e., when the signal-to-noise ratio, *SNR*, is equal to 3). Since *SNRs* have experimental errors associated with them, the LOD can only be determined within certain error limits. In this work, we define an LOD as the analyte concentration for which $SNR \geq 3 \pm x$ and $x \leq 1$, where x is the estimated standard deviation of the *SNR*. All *SNRs* reported are averages of three or more trials at that concentration.

For any Fourier-transform method, the *SNR* is dependent on the collection time (in principle, it is proportional to the square root of the number of scans that are averaged). Therefore, an LOD determined by FTIR is not a fixed quantity because it is time dependent. LODs in this work are defined as $SNR \geq 3 \pm 1$ for a 10-minute analysis. The choice of 10 minutes was arbitrary. In the case of perchlorate, a 30-minute LOD was also determined for comparison. Spectral noise was taken to be the root mean square of the points in a blank spectrum over a range of wavenumbers that was centered at the peak absorbance maximum and extended to wavenumbers on either side of the peak where only 1% of the maximum peak absorbance remained. The peak position and maximum absorbance (i.e., signal intensity) were determined by least-squares fitting the experimental spectrum to a Gaussian function, as previously discussed.

For a given analyte, the most meaningful comparison of the LOD for a coated silicon or diamond probe with the LOD for the same probe without the extractant coating would be one that involved equal *total* analysis times, not equal numbers of scans (interferograms) averaged. For a coated-probe LOD, the probe was allowed to undergo ion exchange with the aqueous

analyte solution for 10 minutes followed by the collection of only 64 co-added scans. For an uncoated-probe LOD, the probe was immersed in the analyte solution and 1660 co-added scans were collected over the ten-minute interval. The LODs are listed in Table 13.

Table 13. Ten-minute limits of detection (LODs) for aqueous anions determined by ATR-FTIR using uncoated or DEC⁺X⁻-coated probes^a

anion	uncoated probe ^b			ATR crystal	extractant coated probe ^c			ratio
	ν , cm ⁻¹	LOD ₂ , mg L ⁻¹	SNR(σ)		ν , cm ⁻¹	LOD ₂ , μ g L ⁻¹	SNR(σ)	
ClO ₄ ⁻	1108	70	4(1)	Di ^d	1096	3	2.8(6)	23,000
ClO ₄ ⁻	1108	80	4.0(6)	Si ^d	1096	4	3.5(8)	20,000
ClO ₃ ⁻	973	84	4(1)	Di ^d	973	17	3.2(7)	5,000
ClO ₃ ⁻	992	167	3.0(7)	Si ^d	988	58	3.4(6)	2,860
BF ₄ ⁻	1073	26	4(1)	Di ^d	1057	5	4(1)	5,000
PF ₆ ⁻	861	245	4(1)	Di ^d	841	86	3.1(8)	2,830
CF ₃ SO ₃ ⁻	1258	45	3.7(7)	Si ^e	1266	7.5	2.9(5)	6,000
PFBS ⁻	1254	75	3.5(7)	Si ^e	1270	21	3.5(8)	7,140
PFOS ⁻	1243	5	4(1)	Si ^e	1270	30	3(1)	170
PMPA ⁻	1042	54	4(1)	Di ^f	1046	125	4(1)	430

^a Abbreviations: ν , IR spectral band monitored; SNR, signal-to-noise ratio; σ , estimated standard deviation; PFBS⁻, perfluoro-*n*-butanesulfonate; PFOS⁻, perfluoro-*n*-octanesulfonate; PMPA⁻, pinacolylmethylphosphonate. ^b Each uncoated-probe LOD was determined from sample and background spectra (1660 co-added scans each) collected over 10-minute intervals. ^c Each extractant-coated-probe LOD was determined from sample and background spectra (64 co-added scans each). The sample spectrum was collected after a 10-minute period during which analyte/NO₃⁻ or analyte/Cl⁻ anion exchange took place. ^d The silicon (Si) or diamond (Di) ATR crystal was coated by evaporation of 20 μ L of a 3 mM dichloromethane solution of DEC⁺NO₃⁻. ^e The ATR crystal was coated by evaporation of 20 μ L of a 1 mM dichloromethane solution of DEC⁺NO₃⁻. ^f The ATR crystal was coated by evaporation of 20 μ L of a 5 mM dichloromethane solution of DEC⁺Cl⁻.

The Limits of Detection for PMPA⁻

Shortly after we started our work on this project, we determined that the distilled-deionized LOD for PMPA⁻ using our methodology at the time was only 18 ppm, and we reported this value to the Army in October 2000.³⁵ Over the duration of the project, we worked hard to lower it, first to 1.8 ppm (April 2001), then to 630 ppb (Sept. 2002), and finally to 125 ppb (the current value). Therefore, our best 10-minute LOD for PMPA using the DEC⁺Cl⁻ coated diamond probe is 125 µg L⁻¹ with a *SNR* of 4 ± 1. The 10-minute LOD for PMPA⁻ in distilled-deionized water using the uncoated diamond probe 54 mg L⁻¹ with a *SNR* of 4 ± 1. The 10-minute LOD for PMPA⁻ in synthetic tap water using the DEC⁺Cl⁻-coated diamond probe is much higher, 36 mg L⁻¹ with a *SNR* of 4.0 ± 0.7. The 10-minute LOD for PMPA⁻ in synthetic tap water using the uncoated diamond probe 72 mg L⁻¹ with a *SNR* of 4 ± 1. The data are in the Tables and Figure below.

Table 14. Determination of 10-minute PMPA⁻ LOD using the DEC⁺Cl⁻-coated diamond probe^a

concentration, µg L ⁻¹	signal ^b	average signal (σ) ^c	average <i>SNR</i> ± error ^d
900	0.00392	0.00392(8)	21 ± 2
900	0.00383		
900	0.00401		
180	0.00119	0.00119(1)	6.2 ± 0.7
180	0.0012		
180	0.00118		
125	0.000675	0.0008(2)	4 ± 1
125	0.001112		
125	0.000668		
107	0.000259	0.00026(3)	1.4 ± 0.2
107	0.000224		
107	0.000308		

^a Distilled/deionized water. Each trial was done using the diamond probe coated with 20 µL of a 5 mM dichloromethane solution of DEC⁺Cl⁻. ^b Absorbance at 1046 cm⁻¹. ^c σ = Standard deviation. ^d Signal-to-noise ratio (*SNR*) where the average noise = 1.9(2) × 10⁻⁴ and the error was propagated from the signal and noise standard deviations.

At 125 $\mu\text{g L}^{-1}$ PMPA, each of the peaks had the following *SNRs*.

ν , cm^{-1}	<i>SNR</i> \pm error
1170	2.9 ± 0.5
1065	2.6 ± 0.6
1046	4 ± 1
1015	3 ± 1

Table 15. Determination of the PMPA⁻ 10-minute LOD using the uncoated diamond probe^a

concentration, mg L^{-1}	signal ^b	average signal (σ) ^c	average <i>SNR</i> \pm error ^d
90	0.0009263		9.3 ^e
72	0.000477	0.00054(5)	5 ± 1
72	0.000548		
72	0.000608		
54	0.000382	0.0004(1)	4 ± 1
54	0.000249		
54	0.000440		
54	0.000236		
54	0.000505		
54	0.000350		

^a Distilled/deionized water. Each 10-minute spectrum was the result of 1660 co-added scans. ^b Absorbance at 1042 cm^{-1} . ^c σ = Standard deviation. ^d Signal-to-noise ratio (*SNR*) where the average noise = $1.0(3) \times 10^{-4}$ and the error was propagated from the signal and noise standard deviations. ^e No error is listed for concentrations for which only one experiment was performed.

With 54 mg L^{-1} PMPA, each of the peaks had the following *SNRs*.

ν , cm^{-1}	<i>SNR</i> \pm error
1162	3 ± 1
1065	2 ± 1
1046	4 ± 1
1015	1.5 ± 0.5

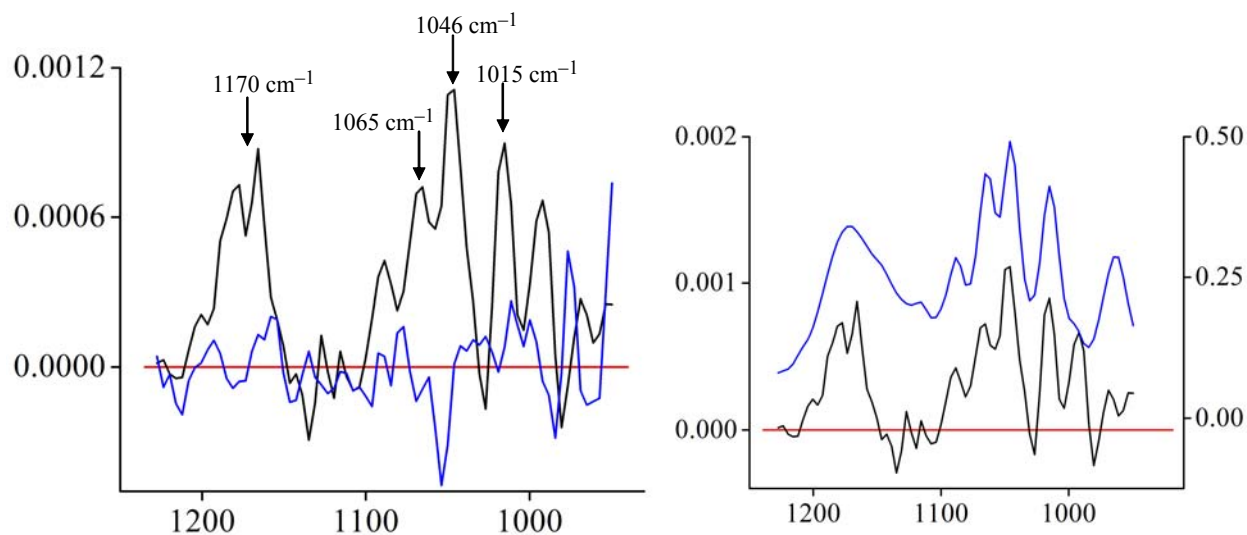


Figure 16 (left). Spectrum of $125 \mu\text{g L}^{-1}$ PMPA^{-} after 10 minutes in contact with the $\text{DEC}^{+}\text{Cl}^{-}$ -coated diamond probe is shown in black. A blank spectrum is shown in blue, and the baseline ($y = 0$) in red.

Figure 17 (right). Spectrum of the same $125 \mu\text{g L}^{-1}$ PMPA^{-} after 10 minutes in contact with the $\text{DEC}^{+}\text{Cl}^{-}$ -coated diamond probe is shown in black. A spectrum of 180mg L^{-1} PMPA^{-} after 10 minutes in contact with the $\text{DEC}^{+}\text{Cl}^{-}$ -coated diamond probe is overlaid in blue.

We prepared seven (7) batches of *synthetic tap water* in accordance with Janet Jensen's instructions (see Experimental Details). Several of these batches were used to determine the 10-minute PMPA^{-} LOD using the $\text{DEC}^{+}\text{Cl}^{-}$ film. Figure 18 shows ATR-FTIR spectra collected each minute for 15 min. during which PMPA^{-} was extracted from synthetic tap water by $\text{DEC}^{+}\text{Cl}^{-}$. Although the spectra are noisy, it is clear that extraction occurred. Figure 19 shows the first and last spectra for this particular PMPA^{-} detection experiment. The negative peak at ca. 1330cm^{-1} ($\nu(\text{NO})$) represents the loss of nitrate from the film.

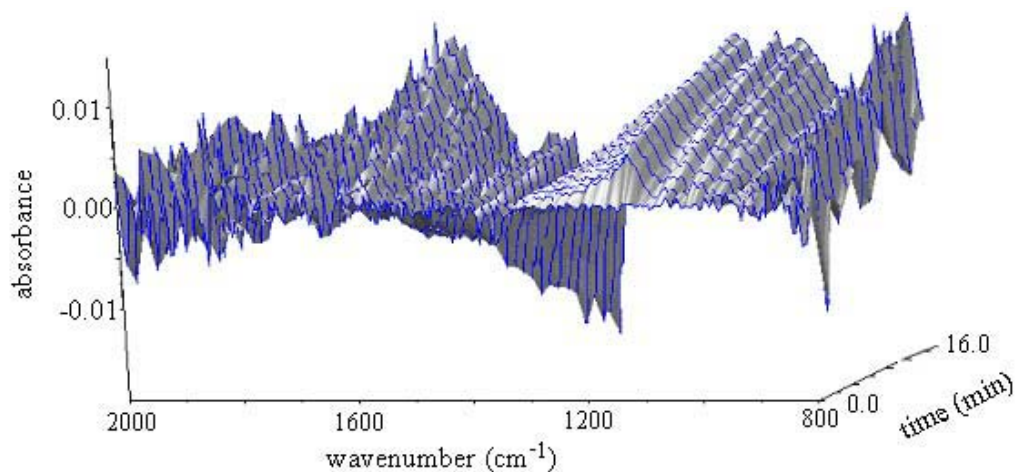


Figure 18. ATR-FTIR spectra recorded every minute for 15 minutes after the diamond probe coated by evaporation of 20 μL of a 5 mM dichloromethane solution of DEC^+Cl^- was immersed in synthetic tap water containing 90 mg L^{-1} PMPA^- (added as H(PMPA)).

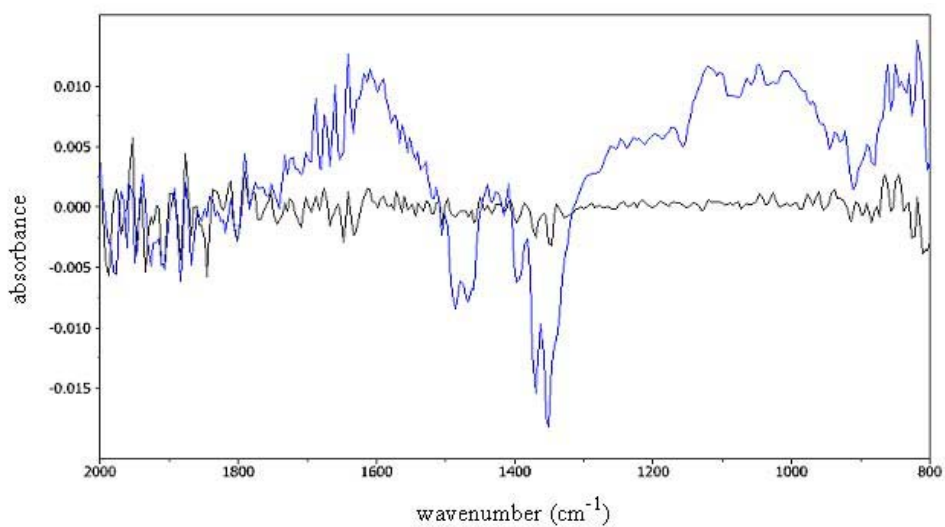


Figure 19. First and last spectra from the ATR-FTIR spectra shown in Figure 18.

Table 16. Determination of the 10-minute PMPA⁻ LOD in synthetic tap water using the DEC⁺Cl⁻-coated diamond probe^a

concentration, mg L ⁻¹	signal ^b	average signal (σ) ^c	average SNR \pm error ^d
90	0.01051	na	
54	0.00471	na	
36	0.007385	0.007(1)	4.0(7)
36	0.006003		
36	0.006905		
36	0.00914		
18	0.007071	0.005(1)	na ^e

^a Each trial was done using the diamond probe coated with 20 μ L of a 5 mM dichloromethane solution of DEC⁺Cl⁻. ^b Absorbance at 1112 cm⁻¹. ^c σ = Standard deviation. ^d Signal-to-noise ratio (SNR) where the average noise = $1.8(2) \times 10^{-3}$ and the error was propagated from the signal and noise standard deviations. ^e Due to the low absorbance for the last trial at 18 mg L⁻¹, which gives SNR < 2, this concentration was determined not to be the LOD.

Table 17. Determination of the 10-minute PMPA⁻ LOD in synthetic tap water using the uncoated diamond probe^a

concentration, mg L ⁻¹	signal ^b	average signal (σ) ^c	average SNR \pm error ^d
179	0.00218		27 ^e
90	0.000306	0.0004(1)	5 \pm 2
90	0.000381		
90	0.000544		
72	0.00026	0.00031(7)	4 \pm 1
72	0.000408		
72	0.000264		

^a Each 10-minute spectrum was the result of 1660 co-added scans. ^b Absorbance at 1042 cm⁻¹. ^c σ = Standard deviation. ^d Signal-to-noise ratio (SNR) where the average noise = $8(2) \times 10^{-5}$ and the error was propagated from the signal and noise standard deviations. ^e No error is listed for those concentrations for which only one experiment was performed.

With 72 mg L⁻¹ PMPA in synthetic tap water, each of the peaks had the following SNRs.

ν , cm ⁻¹	SNR \pm error
1162	7 \pm 3
1065	3 \pm 1
1046	4 \pm 1
1015	3 \pm 2

The Limits of Detection for ClO₄⁻

The 10-minute LOD for ClO₄⁻ using the silicon probe is 4 μg L⁻¹ with a *SNR* of 3.5 ± 0.8, and the 10-minute LOD for ClO₄⁻ using the diamond probe is 3 μg L⁻¹ with a *SNR* of 2.8 ± 0.6. The 30-minute LOD for ClO₄⁻ using the silicon probe is 2 μg L⁻¹ with a *SNR* of 3.7 ± 0.9. The 10-minute LOD for ClO₄⁻ using the uncoated diamond probe is 70 mg L⁻¹ with a *SNR* of 4 ± 1. The 10-minute LOD for ClO₄⁻ using the uncoated silicon probe is 80 mg L⁻¹ with a *SNR* of 4.0 ± 0.6. The 30-minute LOD for ClO₄⁻ using the uncoated silicon probe is 40 mg L⁻¹ with a *SNR* of 5 ± 1.

Table 18. Determination of 10-minute ClO₄⁻ LOD using the DEC⁺NO₃⁻-coated silicon probe^a

concentration, μg L ⁻¹	v(ClO) signal ^b	average signal (σ) ^c	average <i>SNR</i> ± error ^d
500	0.14018	0.13(1)	220 ± 40
500	0.10723		
500	0.13716		
100	0.04833	0.045(5)	75 ± 15
100	0.05136		
100	0.04753		
100	0.03943		
100	0.03894		
100	0.04422		
10	0.004475	0.0041(7)	7 ± 2
10	0.003065		
10	0.00466		
5	0.00163	0.0027(8)	5 ± 2
5	0.003282		
5	0.0032		
4	0.001715	0.0021(3)	3.5 ± 0.8
4	0.00212		
4	0.002556		

^a Distilled/deionized water. Each trial was done using the silicon probe coated with 20 μL of a 3 mM dichloromethane solution of DEC⁺NO₃⁻. ^b Absorbance at 1096 cm⁻¹. ^c σ = Standard deviation. ^d Signal-to-noise ratio (*SNR*) where the average noise = 1.9(3) × 10⁻⁴ and the error was propagated from the signal and noise standard deviations.

Table 19. Determination of 10-minute ClO_4^- LOD using $\text{DEC}^+\text{NO}_3^-$ -coated diamond probe^a

concentration, $\mu\text{g L}^{-1}$	v(ClO) signal ^b	average signal (σ) ^c	average <i>SNR</i> \pm error ^d
10	0.00173		9.1 ^e
5	0.000969		5.1
3	0.000666	0.00054(9)	2.8 \pm 0.6
3	0.000446		
3	0.000511		

^a Distilled/deionized water. Each trial was done using the diamond probe coated with 20 μL of a 3 mM dichloromethane solution of $\text{DEC}^+\text{NO}_3^-$. ^b Absorbance at 1096 cm^{-1} . ^c σ = Standard deviation. ^d Signal-to-noise ratio (*SNR*) where the average noise = $1.9(3) \times 10^{-4}$ and the error was propagated from the signal and noise standard deviations. ^e No error is listed for those concentrations for which only one experiment was performed.

Table 20. Determination of 30-minute ClO_4^- LOD using the $\text{DEC}^+\text{NO}_3^-$ -coated silicon probe^a

concentration, $\mu\text{g L}^{-1}$	v ClO signal ^b	average signal (σ) ^c	average <i>SNR</i> \pm error ^d
4	0.002964	0.0034(5)	6 \pm 1
4	0.003909		
2	0.002295	0.0022(4)	3.7 \pm 0.9
2	0.002212		
2	0.002196		
2	0.00273		
2	0.00127		
2	0.00231		

^a Distilled/deionized water. Each trial was done using the silicon probe coated with 20 μL of a 3 mM dichloromethane solution of $\text{DEC}^+\text{NO}_3^-$. ^b Absorbance at 1096 cm^{-1} . ^c σ = Standard deviation. ^d Signal-to-noise ratio (*SNR*) where the average noise = $1.9(3) \times 10^{-4}$ and the error was propagated from the signal and noise standard deviations.

Table 21. Determination of the 10-minute ClO_4^- LOD using the uncoated diamond probe^a

concentration, mg L ⁻¹	v ClO signal ^b	average signal (σ) ^c	average SNR \pm error ^d
1000	0.007595	0.0076(2)	84 \pm 28
1000	0.007488		
1000	0.007862		
200	0.0015	0.0014(1)	14 \pm 6
200	0.00156		
200	0.00124		
150	0.00121	0.0010(2)	10 \pm 4
150	0.00105		
150	0.000644		
100	0.0006999	0.0006(2)	6 \pm 3
100	0.000388		
100	0.000733		
100	0.000431		
80	0.00031	0.00035(7)	4.4 \pm 1.4
80	0.000287		
80	0.000450		
80	0.000497		
70	0.000358	0.00032(2)	4 \pm 1
70	0.000313		
70	0.000302		

^a Distilled/deionized water. Each 10-minute spectrum was the result of 1660 co-added scans. ^b Absorbance at 1108 cm⁻¹. ^c σ = Standard deviation. ^d Signal-to-noise ratio (SNR) where average noise = $9(3) \times 10^{-5}$ and the error was propagated from the signal and noise standard deviations.

Table 22. Determination of the 10-minute ClO_4^- LOD using the uncoated silicon probe^a

concentration, mg L ⁻¹	v ClO signal ^b	average signal (σ) ^c	average SNR \pm error ^d
100	0.000833	0.0010(1)	7 \pm 1
100	0.00111		
100	0.0011		
100	0.00114		
80	0.000652	0.00060(5)	4.0 \pm 0.6
80	0.000529		
80	0.000631		
70	0.000502	0.00044(8)	2.9 \pm 0.7
70	0.000489		
70	0.000317		

^a Distilled/deionized water. Each 10-minute spectrum was the result of 1660 co-added scans. ^b Absorbance at 1108 cm⁻¹. ^c σ = Standard deviation. ^d Signal-to-noise ratio (SNR) where average noise = $1.5(2) \times 10^{-4}$ and the error was propagated from the signal and noise standard deviations.

Table 23. Calculation of the 30-minute ClO_4^- LOD using the uncoated silicon probe^a

concentration, mg L^{-1}	ν ClO signal ^b	average signal (σ) ^c	average $\text{SNR} \pm \text{error}^d$
80	0.00125		12.5 ^e
50	0.000759	0.0007(1)	7 ± 2
50	0.000566		
40	0.000442	0.0005(1)	5 ± 1
40	0.000735		
40	0.00057		
40	0.000416		
30	0.00011	0.0002(1)	2 ± 1
30	0.000387		
30	0.0000305		

^a Distilled/deionized water. Each 10-minute spectrum was the result of 5000 co-added scans. ^b Absorbance at 1108 cm^{-1} . ^c σ = Standard deviation. ^d Signal-to-noise ratio (SNR) where average noise = $1.0(2) \times 10^{-4}$ and the error was propagated from the signal and noise standard deviations. ^e No error is listed for those concentrations for which only one experiment was performed.

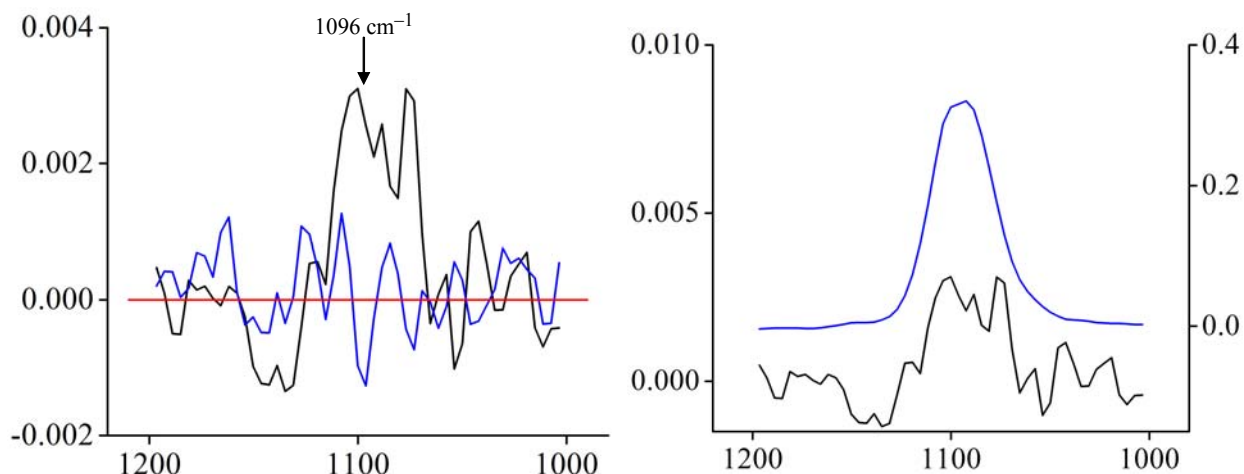


Figure 20 (left). Spectrum of $4 \mu\text{g L}^{-1} \text{ClO}_4^-$ after 10 minutes in contact with the $\text{DEC}^+\text{NO}_3^-$ -coated silicon probe is shown in black. A blank spectrum is shown in blue, and the baseline ($y = 0$) in red.

Figure 21 (right). Spectrum of the same $4 \mu\text{g L}^{-1} \text{ClO}_4^-$ after 10 minutes in contact with the $\text{DEC}^+\text{NO}_3^-$ -coated silicon probe is shown in black. A spectrum of $1000 \mu\text{g L}^{-1} \text{ClO}_4^-$ after 10 minutes in contact with the $\text{DEC}^+\text{NO}_3^-$ -coated silicon probe is overlaid in blue.

The Limits of Detection for ClO₃⁻

The 10-minute ClO₃⁻ LOD using the diamond probe is 17 μg L⁻¹ with a *SNR* of 3.2 ± 0.9 and the 10-minute ClO₃⁻ LOD using the silicon probe is 58.5 μg L⁻¹ with a *SNR* of 3.4 ± 0.6. The 10-minute ClO₃⁻ LOD using the uncoated diamond probe is 83.5 mg L⁻¹ with a *SNR* of 4 ± 1 and the 10-minute ClO₃⁻ LOD using the uncoated silicon probe is 167 mg L⁻¹ with a *SNR* of 3.0 ± 0.7.

Table 24. Determination of 10-minute ClO₃⁻ LOD using DEC⁺NO₃⁻-coated diamond probe^a

concentration, μg L ⁻¹	v(ClO) signal ^b	average signal (σ) ^c	average <i>SNR</i> ± error ^d
1670	0.05364		89 ^e
42	0.00422	0.0044(1)	8 ± 1
42	0.00451		
42	0.00441		
25	0.00354	0.0031(4)	5 ± 1
25	0.00292		
25	0.00273		
17	0.00211	0.0019(4)	3.2 ± 0.9
17	0.00224		
17	0.00134		
8.4	0.000837		1.4

^a Distilled/deionized water. Each trial was done using the diamond probe coated with 20 μL of a 3 mM dichloromethane solution of DEC⁺NO₃⁻. ^b Absorbance at 973 cm⁻¹. ^c σ = Standard deviation. ^d Signal-to-noise ratio (*SNR*) where the average noise = 6(1) × 10⁻⁴ and the error was propagated from the signal and noise standard deviations. ^e No error is listed for those concentrations for which only one experiment was performed.

For the 17 μg L⁻¹ chlorate trials on diamond, each peak had the following *SNRs*.

v (cm ⁻¹)	<i>SNR</i>
988	3.2 ± 0.7
973	3.2 ± 0.9

Table 25. Determination of the 10-minute ClO_3^- LOD using $\text{DEC}^+\text{NO}_3^-$ -coated silicon probe^a

concentration, $\mu\text{g L}^{-1}$	$\nu(\text{ClO})$ signal ^b	average signal (σ) ^c	average $\text{SNR} \pm \text{error}^d$
1670	0.05066		28 ^e
84	0.0109	0.0108(4)	5.4 ± 0.9
84	0.0112		
84	0.0103		
67	0.00831	0.008(1)	4.2 ± 0.8
67	0.00604		
67	0.00843		
58	0.00608	0.0062(4)	3.4 ± 0.6
58	0.00575		
58	0.00674		

^a Distilled/deionized water. Each trial was done using the silicon probe coated with 20 μL of a 3 mM dichloromethane solution of $\text{DEC}^+\text{NO}_3^-$. ^b Absorbance at 988 cm^{-1} . ^c σ = Standard deviation. ^d Signal-to-noise ratio (SNR) where the average noise = $1.8(3) \times 10^{-3}$ and the error was propagated from the signal and noise standard deviations. ^e No error is listed for those concentrations for which only one experiment was performed.

For the $58 \mu\text{g L}^{-1}$ chlorate trials on silicon, each peak had the following SNRs .

$\nu (\text{cm}^{-1})$	SNR
988	3.4 ± 0.6
973	3.6 ± 0.8

Table 26. Determination of the 10-minute ClO_3^- LOD using the uncoated diamond probe^a

concentration, mg L^{-1}	$\nu(\text{ClO})$ signal ^b	average signal (σ) ^c	average $\text{SNR} \pm \text{error}^d$
835	0.00654	0.0064(1)	49 ± 8
835	0.00619		
835	0.00642		
167	0.00123	0.00117(7)	9 ± 1
167	0.00110		
125	0.000638	0.00068(7)	5.2 ± 0.9
125	0.000627		
125	0.000774		
100	0.00078	0.0008(1)	6 ± 1
100	0.00091		
100	0.000662		
92	0.000574	0.00057(1)	4.4 ± 0.7
92	0.000585		
92	0.000561		
83.5	0.000362	0.0005(1)	4 ± 1
83.5	0.0005		
83.5	0.000658		

^a Each 10-minute spectrum was the result of 1660 co-added scans; ^b Absorbance at 973 cm^{-1} ; ^c σ = Standard deviation; ^d Signal-to-noise ratio (*SNR*) where the average noise = $1.3(2) \times 10^{-4}$ and the error was propagated from the signal and noise standard deviations.

Table 27. Determination of the 10-minute ClO_3^- LOD using the uncoated silicon probe.^a

concentration, mg L^{-1}	$\nu(\text{ClO})$ signal ^b	average signal (σ) ^c	average <i>SNR</i> \pm error ^d
8350	0.0407	0.0413(5)	83 ± 15
8350	0.041997		
8350	0.04122	0.0015(2)	3.0 ± 0.7
835	0.00496		
167	0.001561		
167	0.00118		
167	0.00161		
83.5	0.00074		1.5

^a Distilled/deionized water. Each 10-minute spectrum was the result of 1660 co-added scans. ^b Absorbance at 988 cm^{-1} ; ^c σ = Standard deviation. ^d Signal-to-noise ratio (*SNR*) where average noise = $5.0(9) \times 10^{-4}$ and the error was propagated from the signal and noise standard deviations.

^e No error is listed for those concentrations for which only one experiment was performed.

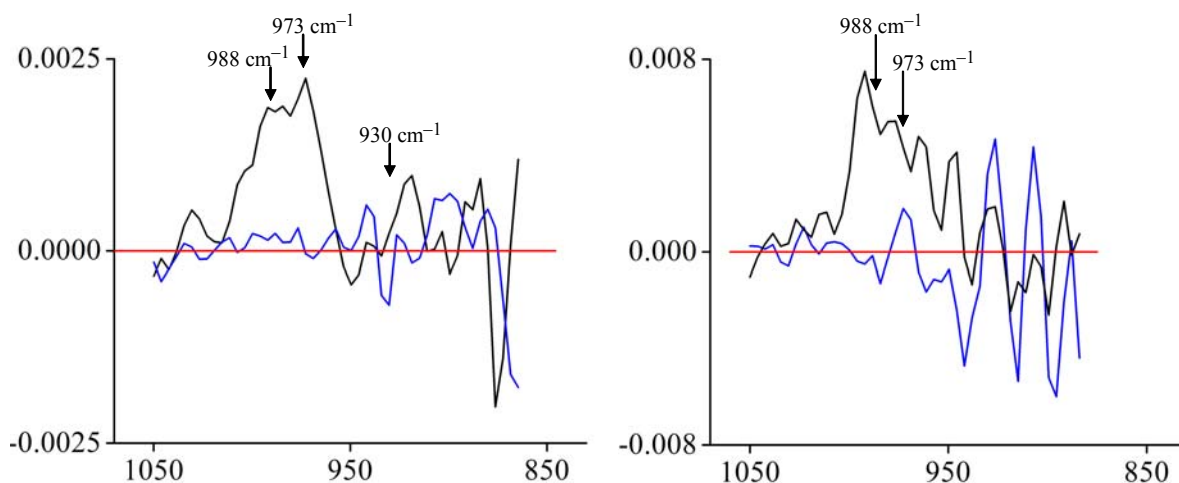


Figure 22. Spectrum of $17 \mu\text{g L}^{-1} \text{ClO}_3^-$ after 10 minutes in contact with the $\text{DEC}^+\text{NO}_3^-$ -coated diamond probe is shown in black. A blank spectrum is in blue, and the baseline ($y = 0$) in red.

Figure 23. Spectrum of $67 \mu\text{g L}^{-1} \text{ClO}_3^-$ after 10 minutes in contact with the $\text{DEC}^+\text{NO}_3^-$ -coated silicon probe is shown in black. A blank spectrum is in blue, and the baseline ($y = 0$) in red.

The Limits of Detection for PFOS⁻

The 10-minute PFOS⁻ LOD using the silicon probe is 30 $\mu\text{g L}^{-1}$ with a *SNR* of 3 ± 1 . The 10-minute PFOS⁻ LOD using the uncoated silicon probe is 5 mg L^{-1} with a *SNR* of 4 ± 1 .

Table 28. Determination of 10-minute PFOS⁻ LOD using the DEC⁺NO₃⁻-coated silicon probe^a

concentration, $\mu\text{g L}^{-1}$	signal ^b	average signal (σ) ^c	average <i>SNR</i> \pm error ^d
50	0.00444	0.0037(5)	10 ± 2
50	0.00358		
50	0.0033		
50	0.00334		
35	0.00304	0.0024(6)	6 ± 2
35	0.00245		
35	0.00157		
30	0.00105	0.0013(5)	3 ± 1
30	0.00196		
30	0.000772		
25	0.00059	0.0009(3)	2.4 ± 0.4
25	0.00132		
25	0.00084		

^a Distilled/deionized water. Each trial was done using the silicon probe coated with 20 μL of a 1 mM dichloromethane solution of DEC⁺NO₃⁻. ^b Absorbance at 1270 cm^{-1} . ^c σ = Standard deviation. ^d Signal-to-noise ratio (*SNR*) where the average noise = $3.9(6) \times 10^{-4}$ and the error was propagated from the signal and noise standard deviations.

For the 30 $\mu\text{g L}^{-1}$ PFOS trials, each peak had the following *SNRs*.

ν (cm^{-1})	<i>SNR</i>
1270	3 ± 1
1243	2 ± 1
1212	1.0 ± 0.8
1154	1.5 ± 0.8

Table 29. Determination of the 10-minute PFOS⁻ LOD using the uncoated silicon probe^a

concentration, mg L ⁻¹	signal ^b	average signal (σ) ^c	average SNR \pm error ^d
500	0.01535	0.012(2)	63 \pm 17
500	0.01106		
500	0.010385		
50	0.00203		11 ^e
25	0.00135		7
10	0.00115		6
5	0.000503	0.0008(2)	4 \pm 1
5	0.00101		
5	0.000745		

^a Distilled/deionized water. Each 10-minute spectrum was the result of 1660 co-added scans. ^b Absorbance at 1243 cm⁻¹. ^c σ = Standard deviation. ^d Signal-to-noise ratio (SNR) where average noise = 1.9(4) $\times 10^{-4}$ and the error was propagated from the signal and noise standard deviations. ^e No error is listed for those concentrations for which only one experiment was performed.

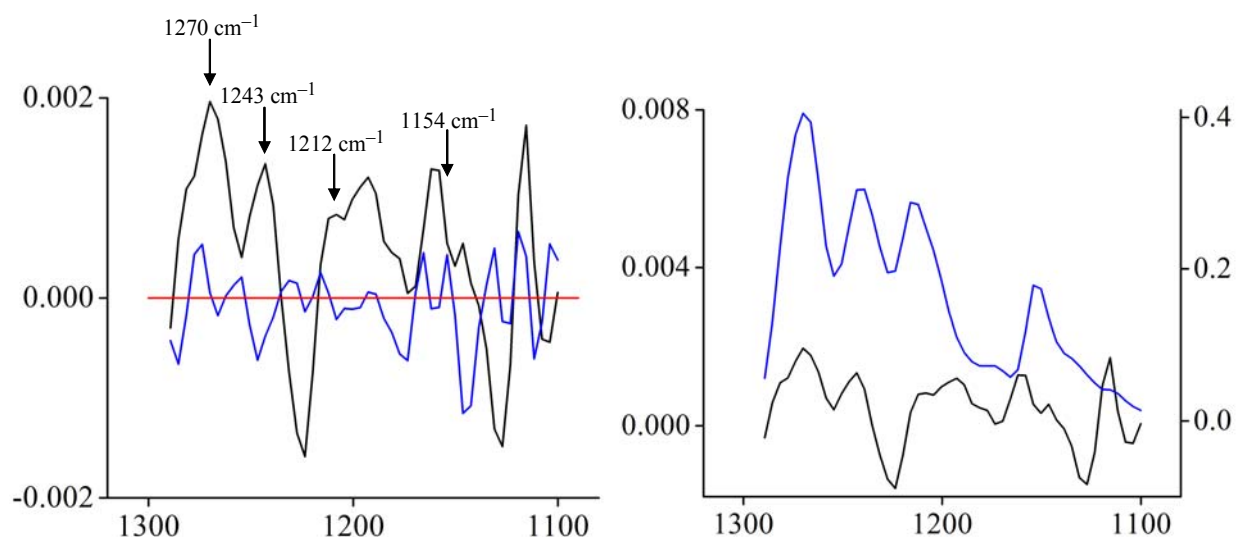


Figure 24 (left). Spectrum of 30 $\mu\text{g L}^{-1}$ PFOS after 10 minutes in contact with the DEC⁺NO₃⁻-coated silicon probe is shown in black. The blank spectrum is blue, and the baseline ($y = 0$) red.

Figure 25 (right). Spectrum of the same 30 $\mu\text{g L}^{-1}$ PFOS after 10 minutes in contact with the DEC⁺NO₃⁻-coated silicon probe is shown in black. A spectrum of 4990 $\mu\text{g L}^{-1}$ PFOS after 10 minutes in contact with the DEC⁺NO₃⁻-coated silicon probe (i.e., the more intense spectrum) is overlaid in blue.

The Limits of Detection for PFBS⁻

The 10-minute PFBS⁻ LOD using the silicon probe is 21 $\mu\text{g L}^{-1}$ with a *SNR* of 3.5 ± 0.8 . The 10-minute PFBS⁻ LOD using the uncoated silicon probe is 75 mg L^{-1} with a *SNR* of 3.5 ± 0.7 .

Table 30. Determination of 10-minute PFBS⁻ LOD using the DEC⁺NO₃⁻-coated silicon probe^a

concentration, $\mu\text{g L}^{-1}$	signal ^b	average signal (σ) ^c	average <i>SNR</i> \pm error ^d	
2990	0.40169	0.42(2)	910 \pm 130	
2990	0.41883			
2990	0.44954			
299	0.03178	0.0025(6)	69 ^e	
30	0.00205		5 \pm 1	
30	0.00202			
30	0.00263			
21	0.00158		0.0016(3)	3.5 \pm 0.8
21	0.0013			
21	0.00192			

^a Distilled/deionized water. Each trial was done using the silicon probe coated with 20 μL of a 1 mM dichloromethane solution of DEC⁺NO₃⁻. ^b Absorbance at 1270 cm^{-1} . ^c σ = Standard deviation. ^d Signal-to-noise ratio (*SNR*) where the average noise = $4.6(6) \times 10^{-4}$ and the error was propagated from the signal and noise standard deviations. ^e No error is listed for those concentrations for which only one experiment was performed.

For the 21 $\mu\text{g L}^{-1}$ PFBS trials, each of the peaks had the following *SNRs*.

ν (cm^{-1})	<i>SNR</i>
1270	3.5 \pm 0.8
1193	2.4 \pm 0.1
1131	5 \pm 1
1050	1.7 \pm 0.1

Table 31. Determination of the 10-minute PFBS⁻ LOD using the uncoated silicon probe^a

concentration, mg L ⁻¹	signal ^b	average signal (σ) ^c	average <i>SNR</i> \pm error ^d
1490	0.019705	0.01968(5)	68 \pm 12
1490	0.019723		
1490	0.01961		
149	0.00188	0.0017(2)	6 \pm 1
149	0.00152		
75	0.00087	0.0010(1)	3.5 \pm 0.7
75	0.001101		
75	0.001032		

^a Each 10-minute spectrum was the result of 1660 co-added scans. ^b Absorbance at 1254 cm⁻¹.

^c σ = Standard deviation. ^d Signal-to-noise ratio (*SNR*) where the average noise = $2.9(5) \times 10^{-4}$ and the error was propagated from the signal and noise standard deviations.

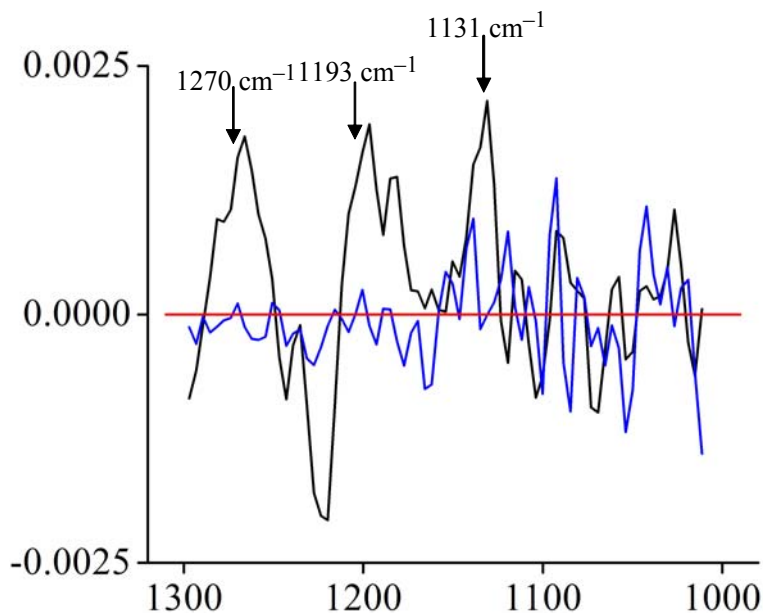


Figure 26. Spectrum of 21 $\mu\text{g L}^{-1}$ PFBS after 10 minutes in contact with the DEC⁺NO₃⁻-coated silicon probe is shown black. A blank spectrum is shown in blue, and the baseline ($y = 0$) in red.

The Limit of Detection for CF₃SO₃⁻ (triflate)

The 10-minute CF₃SO₃⁻ LOD using the DEC⁺NO₃⁻-coated silicon probe was 7.5 μg L⁻¹ with a SNR of 2.9 ± 0.5. The 10-minute CF₃SO₃⁻ LOD using the uncoated silicon probe was 45 mg L⁻¹ with a SNR of 3.7 ± 0.7.

Table 32. Determination of 10-minute CF₃SO₃⁻ LOD using DEC⁺NO₃⁻-coated silicon probe^a

concentration, μg L ⁻¹	signal ^b	average signal (σ) ^c	average SNR ± error ^d
15	0.00282	0.0037(9)	8 ± 2
15	0.00315		
15	0.00517		
15	0.00353		
10	0.00198	0.0024(3)	5.0 ± 0.8
10	0.00265		
10	0.00249		
7.5	0.0016	0.0014(2)	2.9 ± 0.5
7.5	0.00137		
7.5	0.00118		
7.5	0.00157		

^a Distilled/deionized water. Each trial was done using the silicon probe coated with 20 μL of a 1 mM dichloromethane solution of DEC⁺NO₃⁻. ^b Absorbance at 1266 cm⁻¹. ^c σ = Standard deviation. ^d Signal-to-noise ratio (SNR) where the average noise = 4.9(5) × 10⁻⁴ and the error was propagated from the signal and noise standard deviations.

For the 7.5 μg L⁻¹ triflate trials, each of the peaks had the following SNRs.

<i>v</i> (cm ⁻¹)	SNR
1266	2.9 ± 0.5
1154	2.0 ± 0.6
1034	3 ± 1

Table 33. Determination of the 10-minute CF_3SO_3^- LOD using the uncoated silicon probe^a

concentration, mg L^{-1}	signal ^b	average signal (σ) ^c	average $SNR \pm \text{error}^d$
1490	0.01467		113 ^e
745	0.007649	0.0075(1)	58 ± 13
745	0.007392		
149	0.00127	0.00136(9)	10 ± 2
149	0.00145		
75	0.000722		5.6
45	0.000542	0.00048(6)	3.7 ± 0.7
45	0.000406		
45	0.000485		

^a Distilled/deionized water. Each 10-minute spectrum was the result of 1660 co-added scans. ^b Absorbance at 1258 cm^{-1} . ^c σ = Standard deviation. ^d Signal-to-noise ratio (SNR) where average noise = $1.3(2) \times 10^{-4}$ and the error was propagated from the signal and noise standard deviations.

^e No error is listed for those concentrations for which only one experiment was performed.

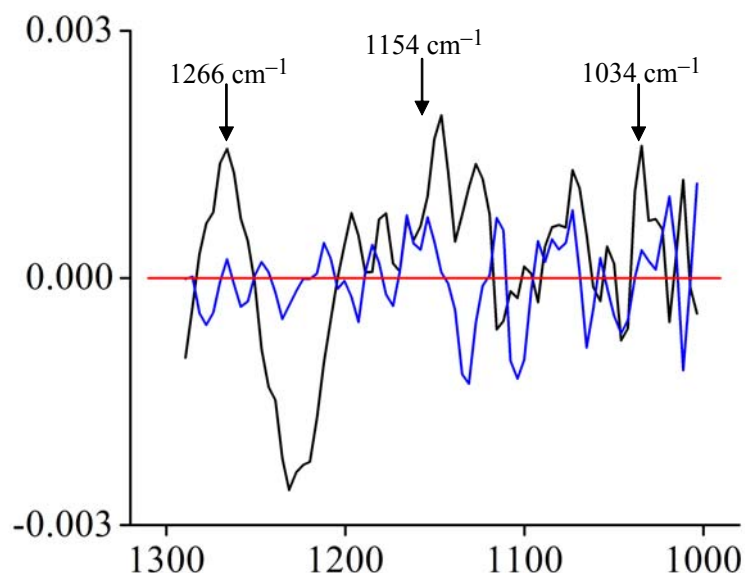


Figure 26. Spectrum of $7.5 \mu\text{g L}^{-1} \text{CF}_3\text{SO}_3^-$ after 10 minutes in contact with the $\text{DEC}^+\text{NO}_3^-$ -coated silicon probe is shown in black. A blank spectrum is shown in blue, and the baseline ($y = 0$) in red.

The Limits of Detection for BF₄⁻

The 10-minute BF₄⁻ LOD using the DEC⁺NO₃⁻-coated diamond probe was 5.2 µg L⁻¹ with a SNR of 4 ± 1. The 10-minute BF₄⁻ LOD using the uncoated diamond probe was 26 mg L⁻¹ with a SNR of 4 ± 1.

Table 34. Determination of the 10-minute BF₄⁻ LOD using DEC⁺NO₃⁻-coated diamond probe^a

concentration, µg L ⁻¹	signal ^b	average signal (σ) ^c	average SNR ± error ^d
8680	0.02286	0.027(3)	130.43 ^e
8680	0.2816		
8680	0.03000		
86.8	0.01284	0.015(3)	72.46 ^e
86.8	0.01653		
43.4	0.01156	na	
8.7	0.002785	0.0024(5)	11.59 ^e
8.7	0.002509		
8.7	0.001772		
7.8	0.001192	0.0013(4)	6.28 ^e
7.8	0.0009563		
7.8	0.002105		
7.8	0.001229		
7.8	0.001134		
7.8	0.001298		
6.9	0.0008776	0.00091(6)	4.40 ^e
6.9	0.000866		
6.9	0.0009771		
6.1	0.001378	0.0011(3)	5.31 ^e
6.1	0.0008075		
6.1	0.001026		
5.2	0.0009079	0.0007(2)	4 ± 1
5.2	0.0005393		
5.2	0.0006689		
5.2	0.0008404		
4.3	0.0006636	0.0007(4)	3.4 ^e
4.3	0.001194		
4.3	0.0009328		
4.3	0.0003878		
4.3	0.000238		
3.5	0.0003715	na	

^a Distilled/deionized water. Each 10-minute spectrum was recorded using the diamond probe coated with 20 μL of a 3 mM dichloromethane solution of $\text{DEC}^+\text{NO}_3^-$. ^b Absorbance at 1057 cm^{-1} . ^c σ = Standard deviation. ^d Signal-to-noise ratio (*SNR*) where the average noise = $2.1(4) \times 10^{-4}$ and the error was propagated from the signal and noise standard deviations. ^e Average *SNR* with error was not calculated for all concentrations.

Table 35. Determination of the 10-minute BF_4^- LOD using the uncoated diamond probe^a

concentration, mg L^{-1}	signal ^b	average signal (σ) ^c	average <i>SNR</i> \pm error ^d
868	0.010220	na	
86.8	0.001043	na	
43.4	0.0003998	0.0005(1)	7.14 ^e
43.4	0.0005355		
43.4	0.0002025		
43.4	0.0003607		
43.4	0.0005135		
34.7	0.0003727	0.0004(1)	5.71 ^e
34.7	0.0002941		
34.7	0.0004869		
34.7	0.0002721		
34.7	0.0002709		
34.7	0.0004905		
34.7	0.0006343		
26	0.0001963	0.00027(6)	4 \pm 1
26	0.0003061		
26	0.0003038		

^a Distilled/deionized water. Each 10-minute spectrum was the result of 1660 co-added scans.

^b Absorbance at 1073 cm^{-1} . ^c σ = Standard deviation. ^d Signal-to-noise ratio (*SNR*) where the average noise = $7(1) \times 10^{-5}$ and the error was propagated from the signal and noise standard deviations. ^e No error is listed for concentrations for which only one experiment was performed.

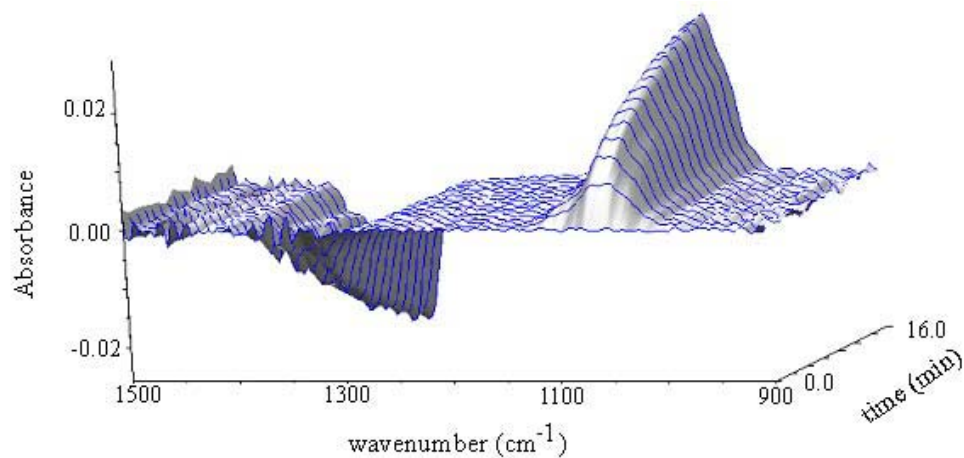


Figure 27. ATR-FTIR spectra recorded every minute for 15 minutes after the diamond probe coated by evaporation of 20 μL of a 3 mM dichloromethane solution of $\text{DEC}^+\text{NO}_3^-$ was immersed in 100 μM (8.7 mg L^{-1}) aqueous BF_4^- . The spectra show the loss of the $\nu(\text{NO}) \text{NO}_3^-$ band at ca. 1330 cm^{-1} and the appearance of the $\nu(\text{BF}) \text{BF}_4^-$ band at 1057 cm^{-1} .

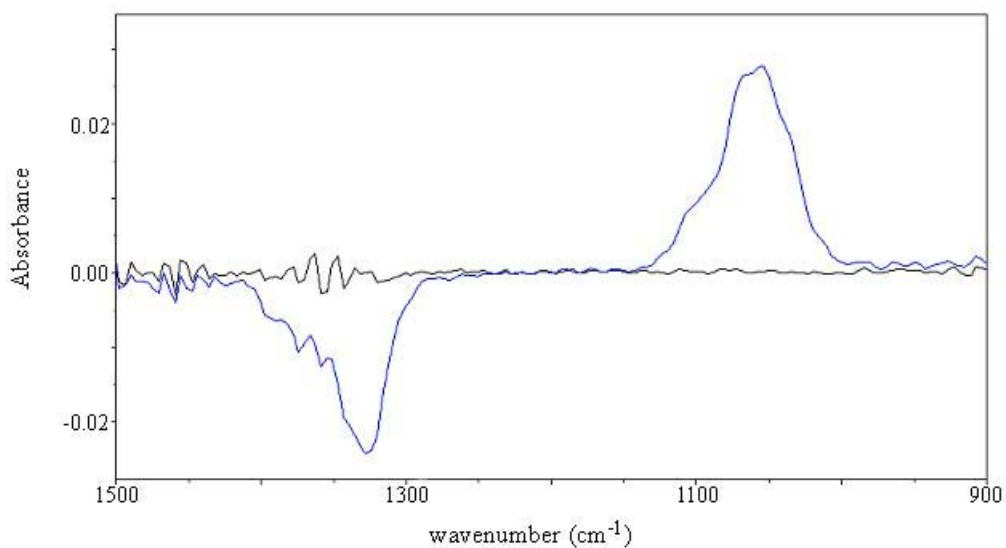


Figure 28. First and last spectra from the ATR-FTIR spectra shown in Figure 27.

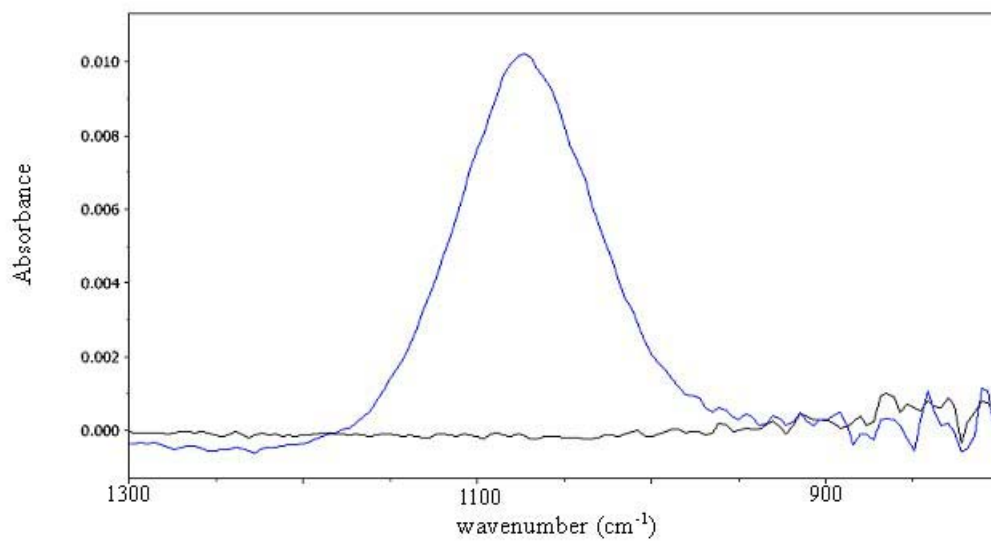


Figure 29. ATR-FTIR spectrum (1660 scans) of 10 mM (870 mg L^{-1}) aqueous BF_4^- ($\nu(\text{BF}) = 1057 \text{ cm}^{-1}$). A blank spectrum is also shown.

The Limits of Detection for PF₆⁻

The 10-minute PF₆⁻ LOD using the DEC⁺NO₃⁻-coated diamond probe was 86.4 μg L⁻¹ with a SNR of 3.1 ± 0.8. The 10-minute PF₆⁻ LOD using the uncoated diamond probe was 245 mg L⁻¹ with a SNR ratio of 3 ± 1.

Table 36. Determination of the 10-minute PF₆⁻ LOD using DEC⁺NO₃⁻-coated diamond probe^a

concentration, μg L ⁻¹	signal ^b	average signal (σ) ^c	average SNR ± error ^d
14400	0.3205	0.36(3)	80 ^e
14400	0.3774		
14400	0.3706		
1440	0.1447	0.15(1)	33.3 ^e
1440	0.1350		
1440	0.1482		
1440	0.1681	0.0162(6)	3.6 ^e
144	0.01606		
144	0.01686		
144	0.01569	0.017(6)	3.7 ^e
115	0.02044		
115	0.02095		
115	0.01061	0.014(2)	3.1(8)
86.4	0.01082		
86.4	0.01261		
86.4	0.01455		
86.4	0.01416		
86.4	0.01621	0.009(1)	2 ^e
72	0.01092		
72	0.007811		
72	0.01105		
72	0.009191		
72	0.008919		
72	0.008955		

^a Distilled/deionized water. Each 10-minute spectrum was recorded using the diamond probe coated with 20 μL of a 3 mM dichloromethane solution of DEC⁺NO₃⁻. ^b Absorbance at 841 cm⁻¹. ^c σ = Standard deviation. ^d Signal-to-noise ratio (SNR) where the average noise = 1.8(2) × 10⁻³ and the error was propagated from the signal and noise standard deviations.

^e Average SNR with error was not calculated for all concentrations.

Table 37. Determination of the 10-minute PF_6^- LOD using the uncoated diamond probe^a

concentration, mg L^{-1}	signal ^b	average signal (σ) ^c	average $\text{SNR} \pm \text{error}^{\text{d}}$
14400	0.1060	na	na
1440	0.01236	0.0121(4)	15.1 ^e
1440	0.01182		
720	0.006313	na	na
576	0.003954	na	na
432	0.003694	na	na
288	0.004200	0.0041(2)	5.1 ^e
288	0.003907		
245	0.002987	0.0030(4)	4 ± 1
245	0.003270		
245	0.002751		
245	0.002358		
245	0.003433		
230	0.002210	0.00243(8)	3 ^e
230	0.001659		
230	0.003670		
230	0.002981		
216	0.002101	na	
144	0.002849	na	

^a Distilled/deionized water. Each 10-minute spectrum was the result of 1660 co-added scans.

^b Absorbance at 861 cm^{-1} . ^c σ = Standard deviation. ^d Signal-to-noise ratio (SNR) where the average noise = $8(2) \times 10^{-4}$ and the error was propagated from the signal and noise standard deviations. ^e Average SNR with error was not calculated for all concentrations

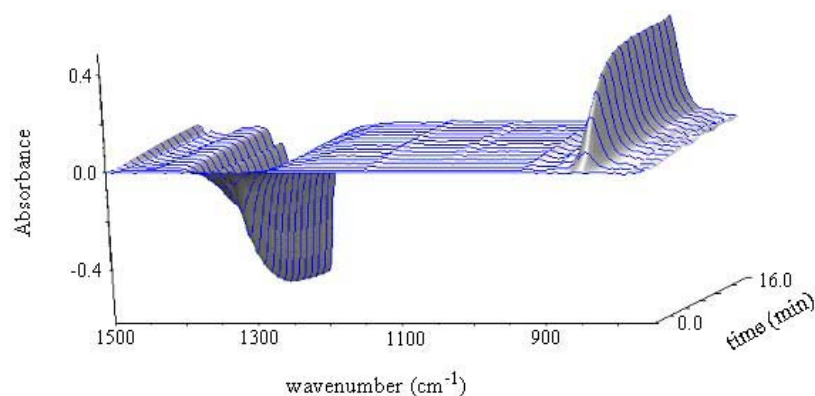


Figure 30. ATR-FTIR spectra recorded every minute for 15 minutes after the diamond probe coated by evaporation of 20 μL of a 3 mM dichloromethane solution of $\text{DEC}^+\text{NO}_3^-$ was immersed in 100 μM (14.4 mg L^{-1}) aqueous PF_6^- . The spectra show the loss of the $\nu(\text{NO}) \text{NO}_3^-$ band at ca. 1330 cm^{-1} and the appearance of the $T_{1u} \nu(\text{PF}) \text{PF}_6^-$ band at 841 cm^{-1} .

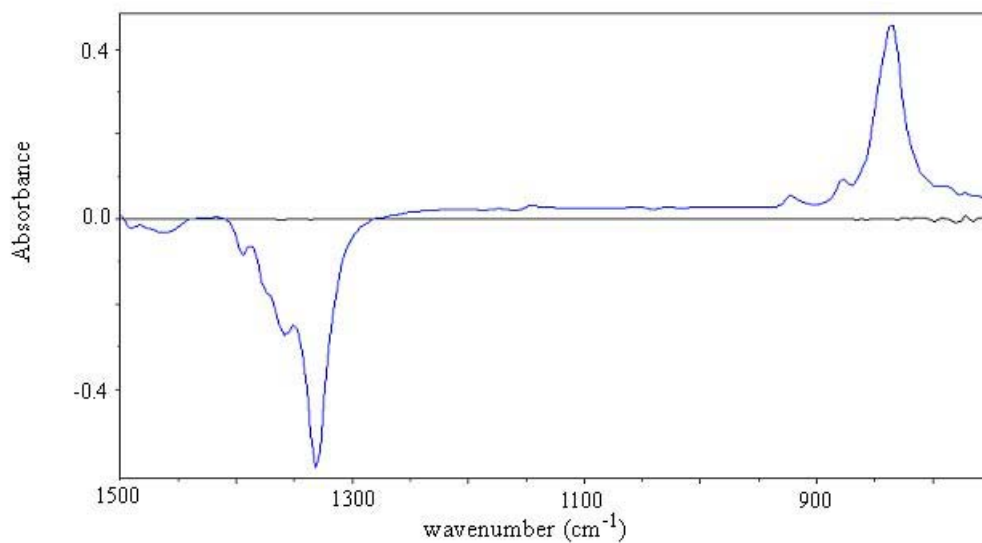


Figure 31. First and last spectra from the ATR-FTIR spectra shown in Figure 30.

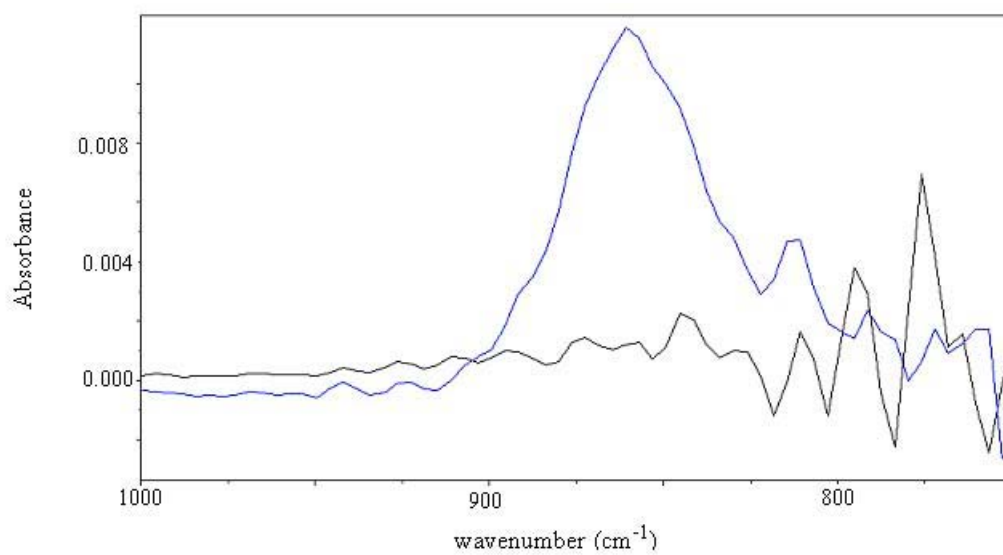


Figure 32. ATR-FTIR spectrum (1660 scans) of 10 mM (1440 mg L⁻¹) aqueous PF₆⁻ ($\nu(\text{PF}) = 861 \text{ cm}^{-1}$). A blank spectrum is also shown.

Discussion of LODs

The goal of this project was to demonstrate, despite popular belief to the contrary, that IR spectroscopy is a suitable analytical method for the detection and quantification of aqueous anionic pollutants such as cyanide and PMPA^- at sub-micromolar concentrations. The justification for the prejudice against analytical IR spectroscopy for trace analysis can be seen by examining the LODs for cyanide and those listed in Table 13, which are all in the low millimolar concentration range when using the uncoated ATR-FTIR probes. One advantage of analytical IR spectroscopy is the potential for simultaneous quantification and identification of a polyatomic analyte.

It was also our goal to develop a relatively simple IR methodology, one that could potentially be used by military lab technicians in the field, not only by skilled spectroscopists or materials scientists. This led to our reliance on replaceable thin-film coatings that were molecular anion-exchangers, designed to be insoluble in water but soluble in organic solvents to make the coating and subsequent cleaning of the ATR crystal as simple as possible. ATR probes with permanent, reusable anion-exchange coatings might improve reproducibility but would involve more sophisticated polymer-casting or sol-gel techniques for their preparation and could be subject to fouling over time. Although the focus of this work is on non-permanent films, some initial experiments were done exploring the possibility of recycling the ferrocene-based ion-exchange coating through a redox cycle which would allow a single film to be used multiple times.

We have shown that the sensitivity of a commercially-available ATR-FTIR spectrometer can be dramatically improved simply by applying a thin-film coating of an ion-exchange material to the surface of the ATR crystal. It was not our objective to design a method that would give LODs lower than any other analytical methods. We acknowledge that a more elaborate and time-consuming method such as solid phase extraction coupled with HPLC-ESIMS/MS can achieve the orders-of-magnitude lower LODs for many of the analytes we investigated.

Using the unmodified ATR probes, the LODs for cyanide and all of the anions listed in Table 13 are in the low millimolar range. Note that the 10-min LOD for PFOS⁻ with the uncoated probe, 0.01 mM, is 30 to 50 times lower than the uncoated-probe LODs for the shorter-chain-length sulfonate anions PFBS⁻ and CF₃SO₃⁻. This could be due to the more intense $\nu(\text{CF})$ bands of the longer perfluoroalkyl chain of PFOS⁻, but this does not explain why the LODs for PFBS⁻ and CF₃SO₃⁻ are essentially the same. The LODs listed in Table 13 for the unmodified ATR probes could be improved somewhat by increasing the number of co-added scans that constitute a single spectrum. As the number of scans per spectrum is increased, the *SNR* increases with the square root of the number of scans being signal averaged.³⁶ Increasing the scanning time from 10 minutes (1660 scans) to 30 minutes (5000 scans) should increase the *SNR* by a factor of 1.7. The LODs for ClO₄⁻ using the unmodified silicon probe after analysis times of 10 and 30 minutes are 0.8 and 0.4 mM, respectively. This two-fold decrease in LOD agrees well with theory. Although there is some advantage to collecting more scans per spectrum in order to lower the LOD, this must be balanced with the increased amount of time required for the analysis. Furthermore, there is a point of diminishing returns: a 60-minute LOD for ClO₄⁻ was not significantly different than the 30-minute LOD.

The LODs of the ATR-FTIR instrument used in this study were greatly improved by coating the ATR crystals. For example, the 10-minute LOD for ClO₄⁻ using the DEC⁺NO₃⁻-coated silicon probe was lowered by a factor of 20,000 to 0.04 μM (the uncoated silicon-probe LOD is 0.8 mM). Using the DEC⁺NO₃⁻- or DEC⁺Cl⁻-coated ATR probes, the LODs for all of the anions listed in Table 1 are in the sub-micromolar range. The increase in sensitivity of the coated ATR probes relative to the unmodified probes ranged from 170 for PFOS⁻ to 23,000 for ClO₄⁻.

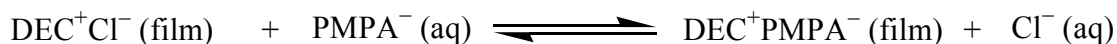
The LOD for ClO₄⁻ using the DEC⁺NO₃⁻-coated diamond ATR probe, 0.03 μM , is four orders of magnitude lower than the 1 mM aqueous ClO₄⁻ detected using Cr₂O₃-coated ZnSe ATR crystals.¹³ In fairness, we note that 1 mM was the concentration of perchlorate used for an experiment described in this reference; this concentration is not necessarily the LOD for the

Cr₂O₃-coated ATR crystal. Only two studies have reported the detection of low micromolar concentrations of aqueous anions by ATR-FTIR using coated ATR crystals. In one study, 1 μM aqueous sulfate was detected using a ZnSe ATR crystal coated with Fe₂O₃.⁵ In the other study, 1 μM aqueous carboxylate anions were detected with ZnSe ATR crystals coated with TiO₂.⁶ These LODs are up to two orders of magnitude higher than the sub-micromolar LODs listed in Table 13.

The silicon and diamond LODs for ClO₄⁻ and chlorate (ClO₃⁻) listed in Table 13 show that the detection limit of the anion can depend on the material of the ATR crystal. This is mainly because the IR throughput of the silicon ATR crystal decreases more significantly below 1000 cm⁻¹ than the throughput of the diamond crystal. Other minor factors might be the difference in evanescent wave penetration depths due to the differences in refractive indexes of diamond and silicon and the possibility of different film morphologies on the different ATR crystals. The decreased throughput of the silicon ATR crystal results in an increase in noise below 1000 cm⁻¹ for this optical material. The *SNR*'s for analytes that have IR bands below 1000 cm⁻¹, such as ClO₃⁻, are ca. four times smaller with the 30-bounce silicon probe than with the 18-bounce diamond probe for the same analyte concentration in spite of the greater number of internal reflections. Accordingly, the inherently lower noise level of the diamond probe below 1000 cm⁻¹ led to a significantly lower LOD for ClO₃⁻ relative to the silicon probe. Even ClO₄⁻, with ν(ClO) centered ca. 1100 cm⁻¹, has a slightly lower LOD with the diamond probe relative to the silicon probe.

The LODs for anions using extractant-coated ATR probes can be lowered by allowing the anion exchange to proceed for a longer time. Since the absorbance of the analyte peaks increased with time but the noise remained the same (because 64 co-added scans were collected regardless of the length of the anion-exchange time interval), the *SNR* was higher at longer extraction times. This resulted in a 30-minute LOD of 0.02 μM, which is two times lower than the 10-minute LOD of 0.04 μM. Given the error limits of these determinations, the two-fold lowering of the 30-minute LOD is probably within error of the expected three-fold decrease.

Lower LODs are possible at longer extraction times because the ion-exchange reaction is concentrating the analyte over time in the volume probed by the evanescent wave. The spectra in Figure 1 show the progress of the ion-exchange reaction of a film of $\text{DEC}^+\text{Cl}^-(s)$ with aqueous PMPA^- . This ion-exchange reaction is depicted in the equilibrium below.



This reaction is driven by the difference in hydration energies of the Cl^- and PMPA^- anions, which is larger than the difference in lattice energies of $\text{DEC}^+\text{Cl}^-(s)$ and $\text{DEC}^+\text{PMPA}^-(s)$ because the DEC^+ cation is very large. Ion-exchange reactions involving similar anions have been shown to be selective for the most weakly hydrated anion present in solution.^{19,37} Therefore, given a mixture of anions present in solution, only the most weakly hydrated anion should generally be detected by the extractant-coated ATR probe *at equilibrium*. Note that this ion exchange is selective only for monoanions; multiply-charged anions such as sulfate and phosphate were not extracted using DEC^+Cl^- or $\text{DEC}^+\text{NO}_3^-$.

Detection of Aqueous Permanganate (MnO_4^-)

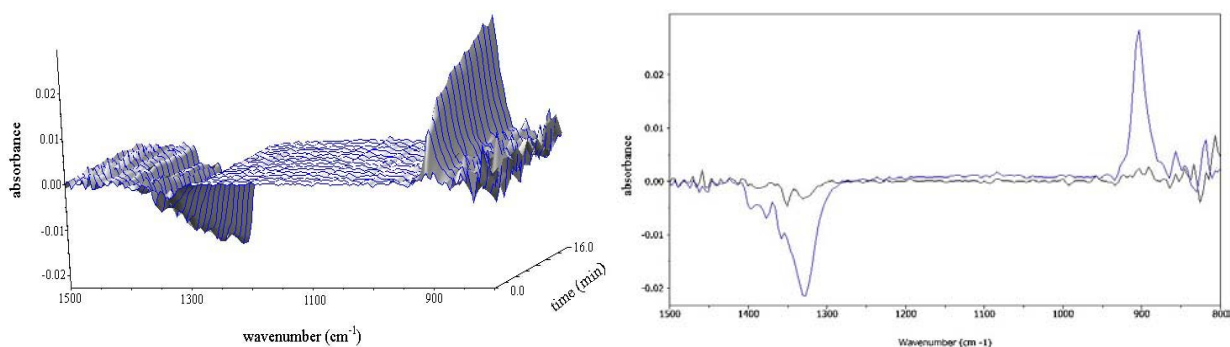


Figure 33. Detection of $100 \mu\text{M}$ (12 mg L^{-1}) MnO_4^- with the $\text{DEC}^+\text{NO}_3^-$ -coated diamond ATR probe.

Detection of the Perfluorocarboxylates $CF_3CO_2^-$, $C_7F_{15}CO_2^-$, and $C_{11}F_{23}CO_2^-$ in Water

Table 38. Extraction of $CF_3CO_2^-$ after 10 minutes in contact with the $DEC^+NO_3^-$ -coated diamond probe^a

concentration, mg L ⁻¹	signal ^b	average signal (σ) ^c	average SNR \pm error
11.4	0.3225	0.31(2)	
11.4	0.2869		
11.4	0.3072		
1.14	0.0539	0.07(2)	
1.14	0.0778		
1.14	0.0897		
0.114	0.0135	0.015(1)	
0.114	0.0145		
0.114	0.0159		
11.4	0.3225	0.31(2)	
11.4	0.2869		
11.4	0.3072		
1.14	0.0539	0.07(2)	
1.14	0.0778		
1.14	0.0897		
0.114	0.0135	0.015(1)	46 ^d
0.114	0.0145		

^a Distilled/deionized water. Each 10-minute spectrum was the result of 64 co-added scans.

^b Absorbance at 1690 cm⁻¹. ^c σ = Standard deviation. ^d approximate SNR = 46; therefore, the LOD may be 10 times lower than 0.114 mg L⁻¹, or ca. 12 μ g L⁻¹.

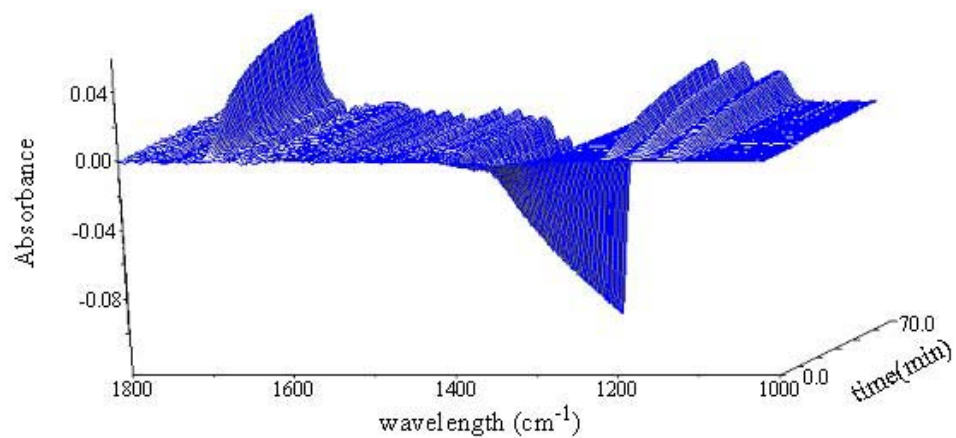


Figure 34. Extraction of $10 \mu\text{M}$ (1.1 mg L^{-1}) CF_3CO_2^- from distilled/deionized water using a film of $\text{DEC}^+\text{NO}_3^-$ on the diamond ATR probe formed by evaporation of $20 \mu\text{L}$ of a 3 mM dichloromethane solution of $\text{DEC}^+\text{NO}_3^-$. Note the disappearance of the $\nu(\text{NO}) \text{NO}_3^-$ peak at 1330 cm^{-1} and the appearance of the $\nu(\text{CO}) \text{CF}_3\text{CO}_2^-$ peak at 1690 cm^{-1} .

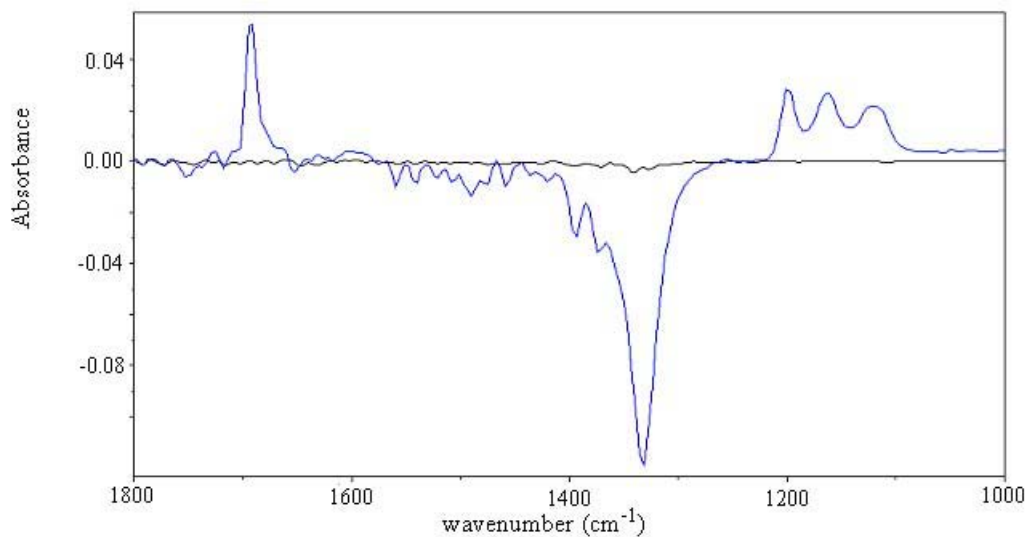


Figure 35. First and last ATR-FTIR spectra of the series of spectra shown in Figure 34.

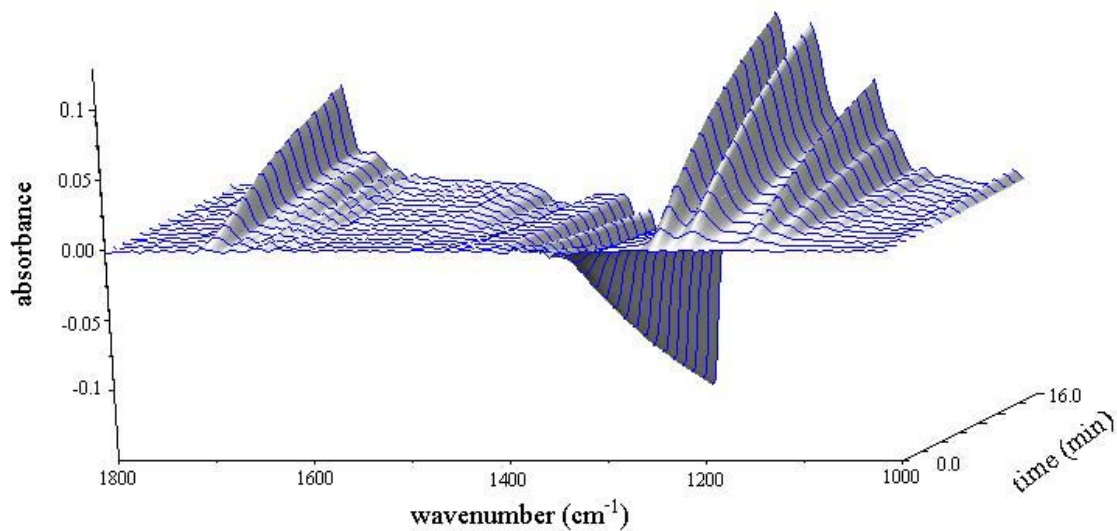


Figure 36. Extraction of 12.4 μM (5.1 mg L^{-1}) $\text{C}_7\text{F}_{15}\text{CO}_2^-$ from distilled/deionized water using a film of $\text{DEC}^+\text{NO}_3^-$ on the diamond ATR probe formed by evaporation of 20 μL of a 3 mM dichloromethane solution of $\text{DEC}^+\text{NO}_3^-$. Note the disappearance of the $\nu(\text{NO}) \text{NO}_3^-$ peak at 1330 cm^{-1} and the appearance of the $\nu(\text{CO}) \text{C}_7\text{F}_{15}\text{CO}_2^-$ peak at 1690 cm^{-1} .

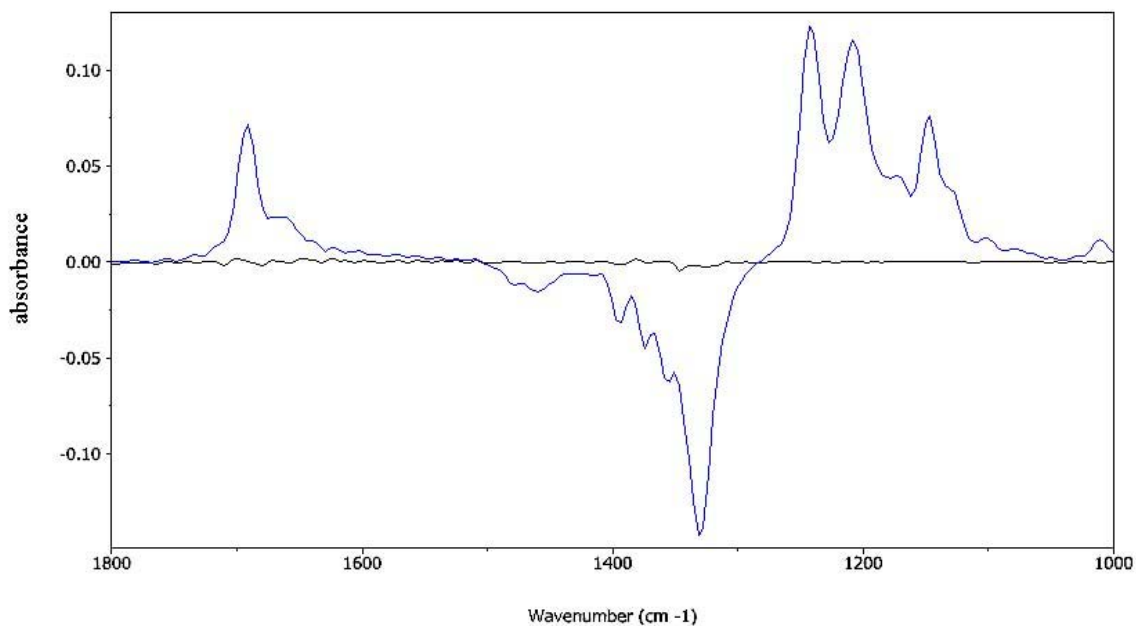


Figure 37. First and last ATR-FTIR spectra of the series of spectra shown in Figure 36.

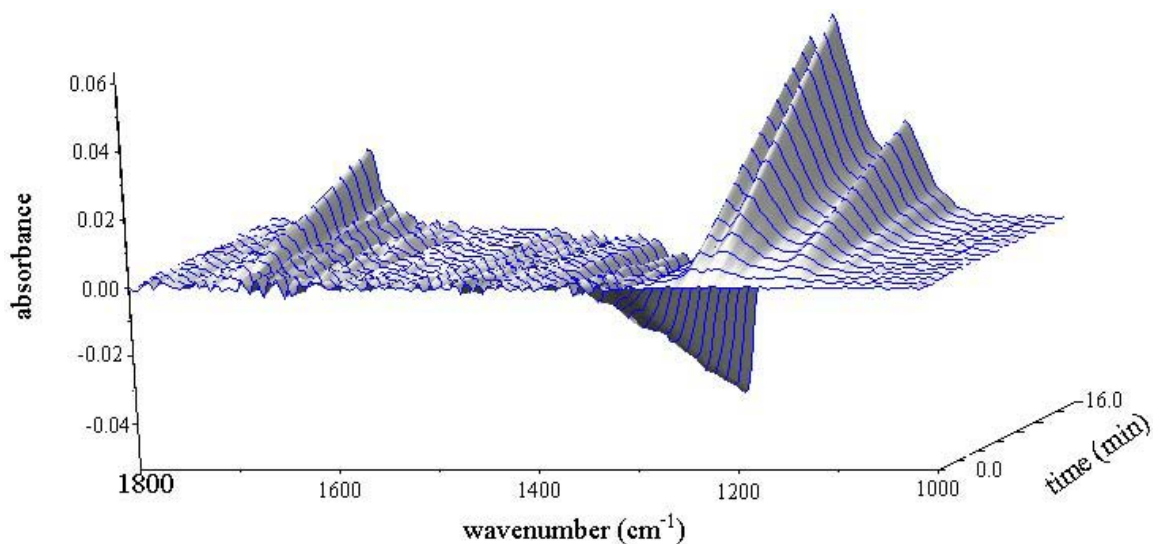


Figure 38. Extraction of 18.9 μM (11.6 mg L⁻¹) C₁₁F₂₃CO₂⁻ from distilled/deionized water using a film of DEC⁺NO₃⁻ on the diamond ATR probe formed by evaporation of 20 μL of a 3 mM dichloromethane solution of DEC⁺NO₃⁻. Note the disappearance of the ν(NO) NO₃⁻ peak at 1330 cm⁻¹ and the appearance of the ν(CO) C₁₁F₂₃CO₂⁻ peak at 1695 cm⁻¹.

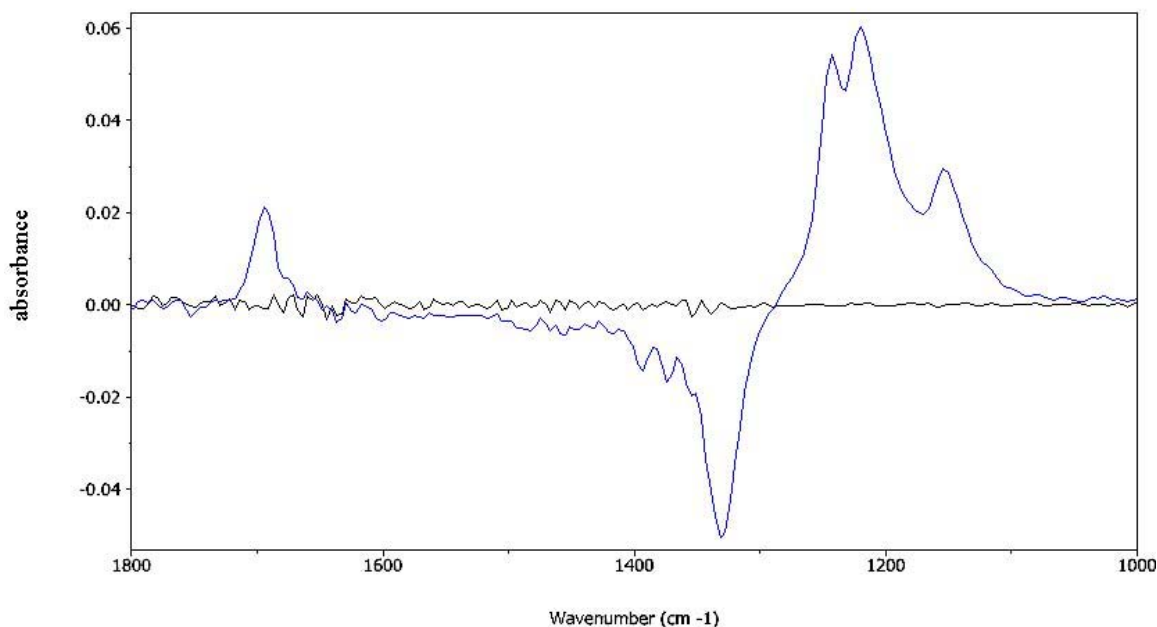


Figure 39. First and last ATR-FTIR spectra of the series of spectra shown in Figure 38.

Calibration Curves for PMPA⁻, ClO₄⁻, and PFOS⁻

Table 39. Data for the March 2002 PMPA calibration curve using 5 mM DEC⁺Cl⁻ on the silicon probe.

concentration, mg L ⁻¹	average dA/dt at 1061 cm ⁻¹	1 sigma	RSD ^a
1.8	0.00127	0.00009	7
18	0.0035	0.0002	6
72	0.0092	0.0005	5
126	0.017	0.001	6
180	0.022	0.002	9

^a Relative standard deviation.

Three trials were done at each concentration.

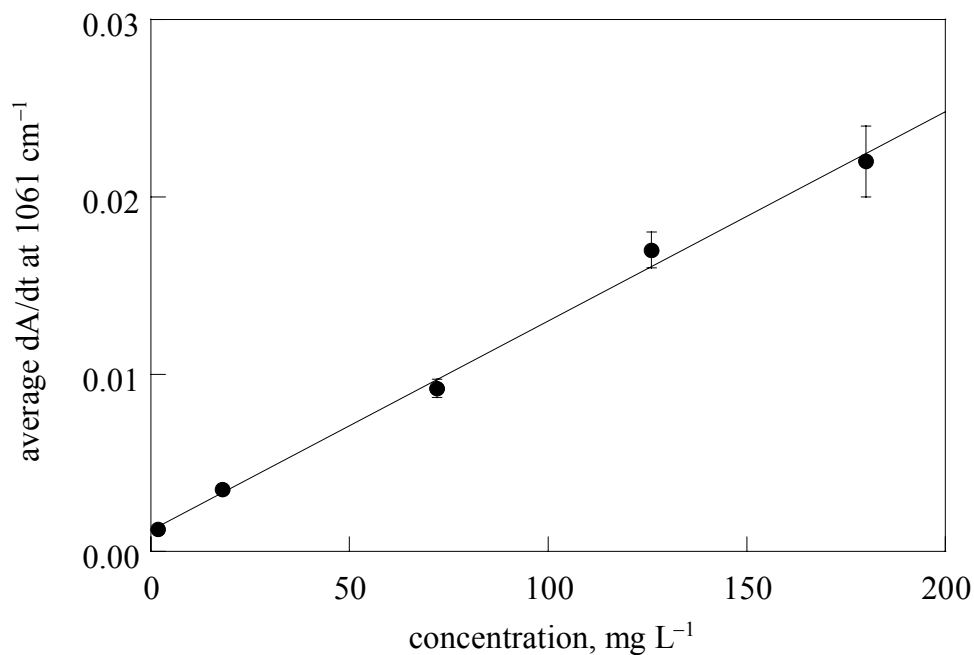


Figure 40. PMPA calibration curve made March 2002. The films were made on the silicon probe from 20 μ L of a 5 mM dichloromethane solution of DEC⁺Cl⁻. The error bars represent \pm one standard deviation. The equation of the line is: $y = 0.000118(5)x + 0.0012(5)$.

Table 40. Data for the April 2003 PMPA calibration curve using 5 mM DEC⁺Cl⁻ on the diamond probe.

concentration, mg L ⁻¹	average dA/dt at 1046 cm ⁻¹	1 sigma	RSD ^a
0.18	1.00E-04	1.00E-05	10
0.9	0.00049	3.00E-05	6
1.8	0.001	1.00E-04	10
18	0.009	0.002	22

^a Relative standard deviation.

Three trials were done at each concentration except 18 mg L⁻¹ where four trials were done.

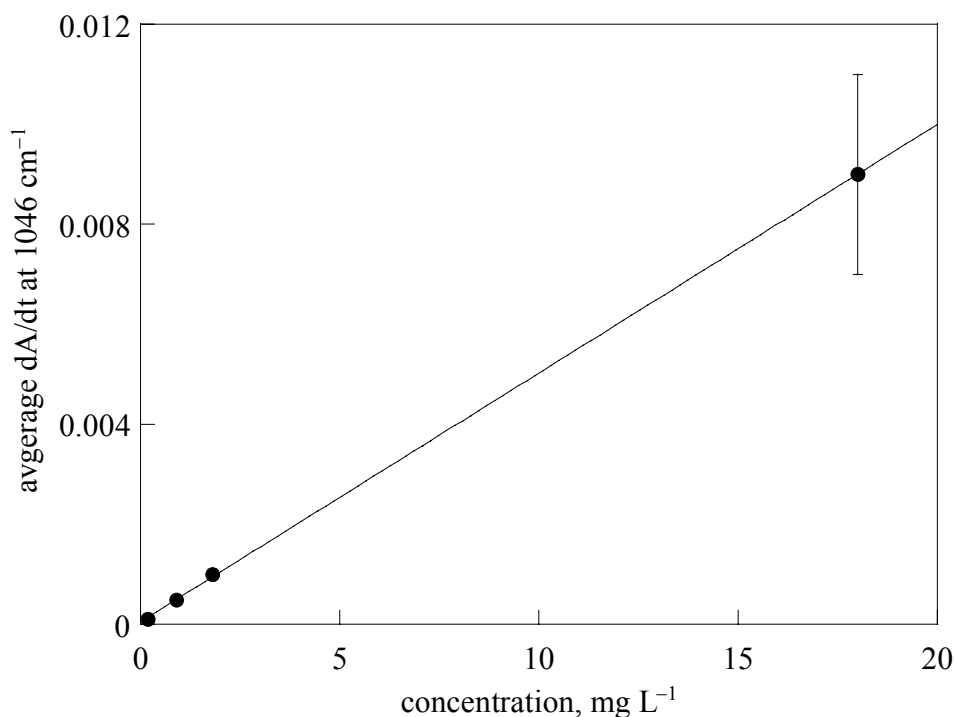


Figure 41. PMPA calibration curve made April 2003. The films were made on the diamond probe from 20 μ L of a 5 mM dichloromethane solution of DEC⁺Cl⁻. The error bars represent \pm one standard deviation. The equation of the line is: $y = 0.000497(3)x + 0.00005(3)$.

Table 41. Data for the July 2003 PMPA calibration curve using 5 mM DEC⁺Cl⁻ on the diamond probe.

concentration, mg L ⁻¹	average dA/dt at 1046 cm ⁻¹	1 sigma	3 sigma	RSD ^a
0.18	0.00011	0.00002	0.00006	18
0.54	0.00038	0.00002	0.00006	5
0.9	0.00059	0.00005	0.00025	8
1.26	0.0009	0.00005	0.00025	6
1.8	0.0012	0.0002	0.0006	17
3.6	0.00229	0.00007	0.00021	3
5.4	0.0035	0.0002	0.0006	6
7.2	0.00383			
9	0.00411			
18	0.0079			

^a Relative standard deviation.

Three trials were done the concentration range 0.18 to 5.4 mg L⁻¹. Only 1 trial was done at the higher concentrations of 7.2 to 18 mg L⁻¹.

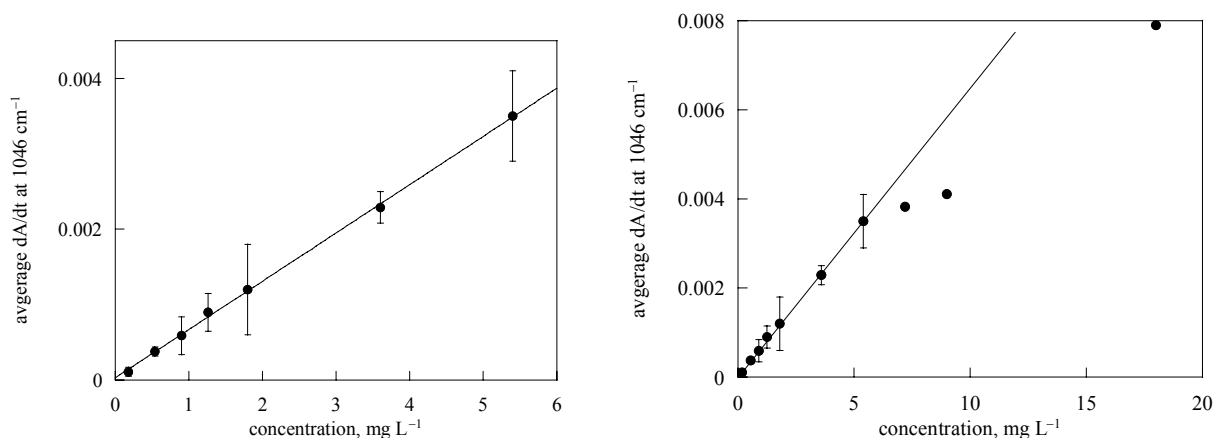


Figure 42. PMPA calibration curve made July 2003. The films were made on the diamond probe from 20 μ L of a 5 mM dichloromethane solution of DEC⁺Cl⁻. The error bars represent \pm three standard deviations. The equation of the line is: $y = 0.000640(9)x + 0.00003(2)$. The line in the left graph is the same as the linear fit for the right graph.

Table 42. Data from all trials at all concentrations for the July 2003 ClO₄⁻ calibration curve.

conc., $\mu\text{g L}^{-1}$	dA/dt at 1096 cm^{-1}	average dA/dt	1 sigma	RSD ^a	3 sigma
0	4.83E-05	0.00008	0.00003	38	0.00009
0	0.000116				
0	6.03E-05				
0	8.85E-05				
4	0.000189	0.00023	0.00003	13	0.00009
4	0.000224				
4	0.000263				
5	0.000242	0.00026	0.00004	15	0.00012
5	0.000226				
5	0.000325				
5	0.000242				
10	0.000432	0.00048	0.00003	6	0.00009
10	0.000496				
10	0.000523				
10	0.000486				
25	0.000743	0.0009	0.0001	11	0.0003
25	0.00086				
25	0.001115				
25	0.000996				
35	0.001135	0.00122	0.00006	5	0.00018
35	0.001275				
35	0.001265				
50	0.001728	0.00188	0.00009	5	0.00027
50	0.001911				
50	0.001952				
50	0.001941				
60	0.002291	0.0021	0.0002	10	0.0006
60	0.002282				
60	0.001835				
70	0.00256	0.0025	0.0002	8	0.0006
70	0.002256				
70	0.002588				
80	0.002816	0.00272	0.00009	3	0.00027
80	0.002596				
80	0.002747				
90	0.003104	0.0032	0.0001	3	0.0003
90	0.003321				
90	0.003089				
100	0.003481	0.0033	0.0003	9	0.0009
100	0.003452				
100	0.002854				
100	0.003552				
500	0.010894	0.0103	0.0009	9	0.0027
500	0.009131				

500	0.009725				
500	0.011488				
1000	0.016539	0.0171	0.0009	5	0.0027
1000	0.0163				
1000	0.01832				
1500	0.018136	0.0179	0.0007	4	0.0021
1500	0.018627				
1500	0.017003				

^a Relative standard deviation (RSD).

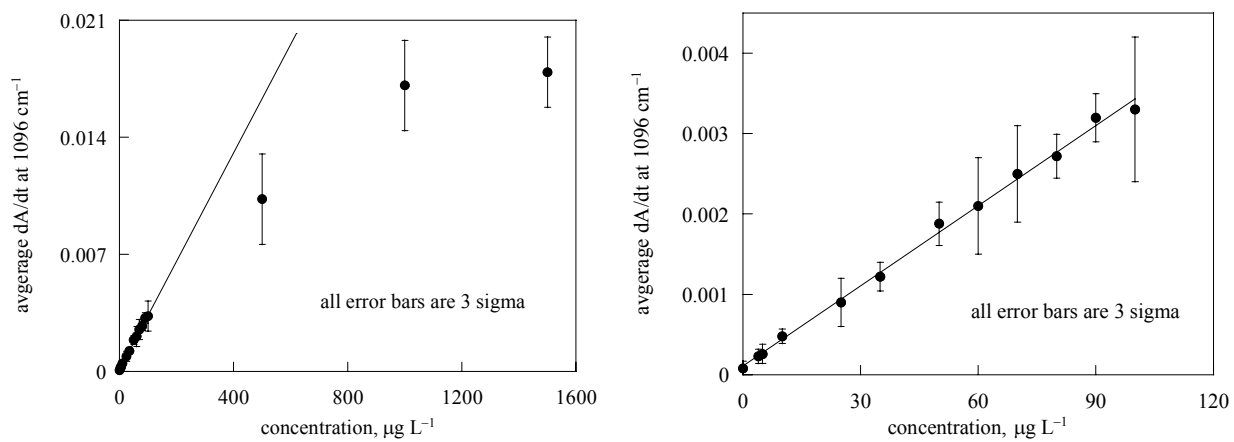


Figure 43. This graph was made July 2003. Perchlorate calibration curve made from the silicon probe coated with 20 μL of a 3 mM dichloromethane solution of $\text{DEC}^+\text{NO}_3^-$. Error bars represent \pm three standard deviations. The equation for the above line is $y = 3.32(6) \times 10^{-3}x + 1.1(3) \times 10^{-4}$. The line shown in the left graph is the same as the linear fit in the right graph.

Table 43. Data for the July 2003 PFOS calibration curve using 1 mM DEC⁺NO₃⁻ on the silicon probe.

concentration, $\mu\text{g L}^{-1}$	average dA/dt at 1270 cm^{-1}	1 sigma	3 sigma	RSD ^a
2495	0.0115	0.0008	0.0024	7
998	0.004534			
499	0.0033	0.0001	0.0003	3
449	0.0027	0.0002	0.0006	7
349	0.0023	0.0001	0.0003	4
250	0.0017	0.0002	0.0006	12
150	0.00115	0.00006	0.00018	5
50	0.00039	0.00006	0.00018	15
30	0.00019	0.00005	0.00015	26
0	-0.00005	0.00003	0.00009	60

^a Relative standard deviation.

Three trials were done at 449, 349, and 150 $\mu\text{g L}^{-1}$; four trials were done at 2495 $\mu\text{g L}^{-1}$; one trial was done at 998 $\mu\text{g L}^{-1}$; all remaining concentrations had six trials.

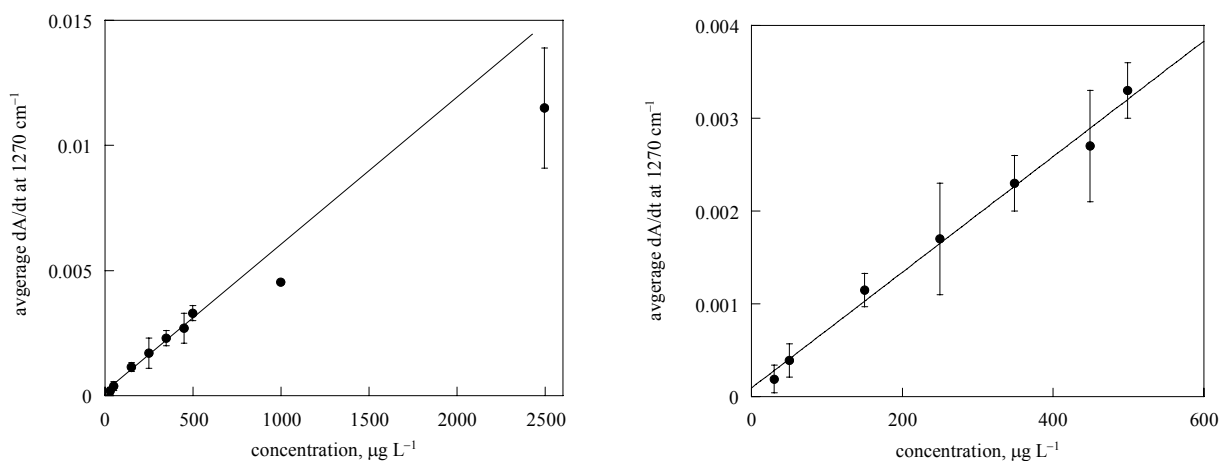
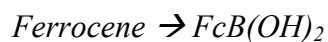


Figure 44. PFOS calibration curve made July 2003. The films were made on the silicon probe from 20 μL of a 1 mM dichloromethane solution of DEC⁺NO₃⁻. The error bars represent \pm one standard deviation. The equation of the line is: $y = 6.2(3) \times 10^{-6}x + 9(8) \times 10^{-5}$. The line in the left graph represents the linear fit of the right graph.

Synthesis of aza-DEC and aza-DEC⁺NO₃⁻



Initially, the first steps toward the synthesis of azaDEC⁺Cl⁻ involved the conversion of ferrocene to the boronic acid from which the ferrocenyl phthalimide was then generated. {Montserrat, *J. Chem. Res.*, (5), 1995, 336-337} Ferrocene was dissolved in carbon disulfide and boron tribromide was added. The mixture was refluxed under nitrogen for a day. Once 24 hours had passed, the reaction was cooled to 0°C and added to 2M NaOH (also at 0°C). The CS₂ layer was discarded and the aqueous layer was washed with ether. The ether layer was acidified with 2M HCl (0°C) and a yellow-orange precipitate was collected and washed with water (26% yield).

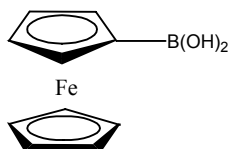


Figure 45. Ferrocenyl boronic acid

NMR data obtained in d₆-acetone for the ferrocenyl boronic acid are in good agreement with that reported by Floris and Illuminati. {Floris, Barbara and Illuminati, Gabriello. *J. Organomet. Chem.*, **1978**, 150, 101-113} ESI-MS data of the product was obtained in acetonitrile and it shows the predominant species is FcB(OH)₂ (m/z 230) with an unknown impurity that has an m/z 274.

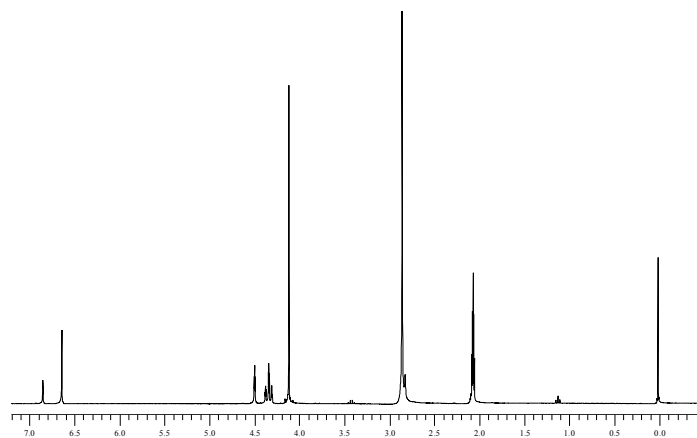


Figure 46. ^1H NMR spectra of $\text{FcB}(\text{OH})_2$ in d_6 -acetone. Peak at 2.9 ppm is water and at 2.1 ppm is solvent.

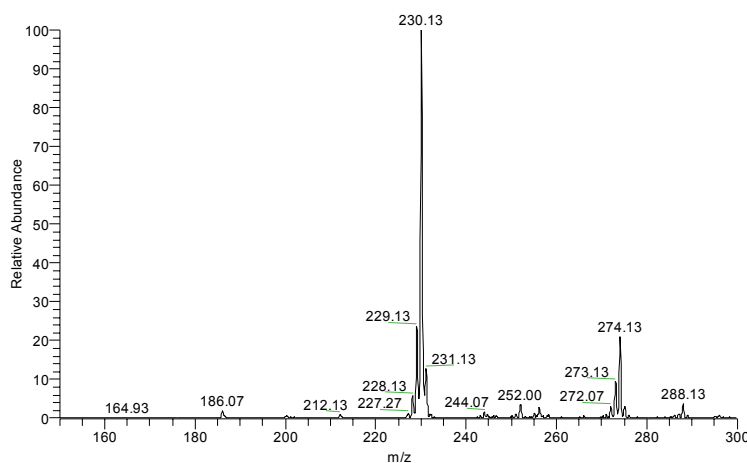


Figure 47. ESI-MS data of $\text{FcB}(\text{OH})_2$ in acetonitrile.

$\text{FcB}(\text{OH})_2 \rightarrow \text{Fcphthalimide}$

In order to generate ferrocenyl phthalimide from ferrocenyl boronic acid, {Bilstein, et al. *Organometallics*, **1999**, *18*, 4325-36} copper phthalimide had to first be generated by mixing copper sulfate and 4 equivalents of potassium phthalimide. The resulting blue solid was collected and rinsed with water and ethanol. Once generated, 2 equivalents of $\text{Cu}(\text{phthalimide})$ and

FcB(OH)₂ were mixed and refluxed in dry acetone. The reaction mixture was allowed to cool to room temperature at which point it was diluted with diethyl ether and then filtered. The filtrate was washed with KOH, H₂O, CH₃COOH, and water again. It was then dried over magnesium sulfate and a red brown solid was collected (11.6% crude yield). NMR of the product (Figure 48) in CDCl₃, however, did not agree with the literature values given by Bildstein and co-workers.

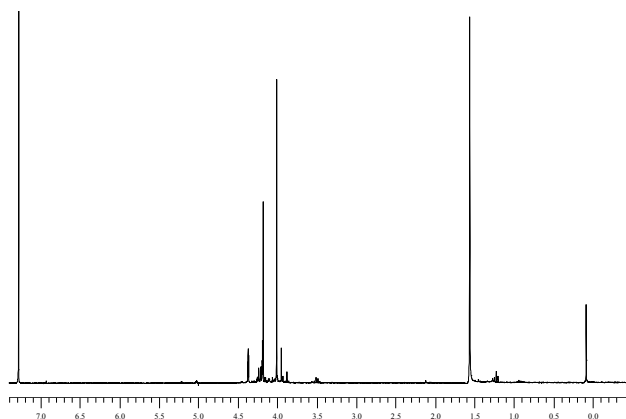


Figure 48. ¹H NMR of crude Fcphthalimide in CDCl₃.

Analysis of the NMR data indicates that the characteristic phthalimide proton peaks, which should appear at 7.72 and 7.86 ppm, are not present. The product that was obtained exhibits no significant peaks in that region. Mass spectral analysis of the compound did not show the expected Fcphthalimide peak at m/z 331.02, either. Nor was any starting material observed. It was, therefore, obvious that attempts to generate the compound through the ferrocenyl phthalimide were going to be problematic.

New Synthetic Route to Generate Ferrocenyl Phthalimide

After searching the literature for alternate routes to Fc(phthalimide) (Figure 49) it was decided to follow the synthesis set forth by Bildstein and co-workers in 1999. The synthesis

simply involves refluxing ferrocenyl bromide with phthalimide in the presence of Cu_2O in pyridine.

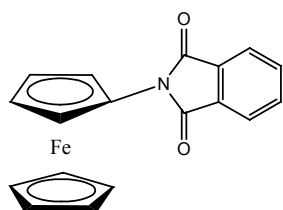


Figure 49. ferrocenyl phthalimide

The materials were added together in a schlenk flask under nitrogen in the glove box. The solution is red/brown in color. After 48-76 hours (depending on the scale of reaction), the pyridine is evaporated and hexanes are then used to triturate the resulting solid. The solid is filtered and rinsed with hexanes to remove any unreacted bromoferrocene. The filter paper containing the solid is then washed with ether until all solid is dissolved in solution. The ether is then evaporated and cold ethanol is added to the resulting solid. The mixture is heated until all solid dissolves (occasional hot filtering with ethanol is required), and then allowed to slowly cool to RT. Occasionally the resulting solution is also put into the freezer to facilitate collection of the red crystals. Three synthetic preps were carried out for this compound and the yields ranged from 30-70%. ^1H NMR and MS data for the compound are shown in Figures 50 and 51, respectively, and indicate that a pure product was obtained.

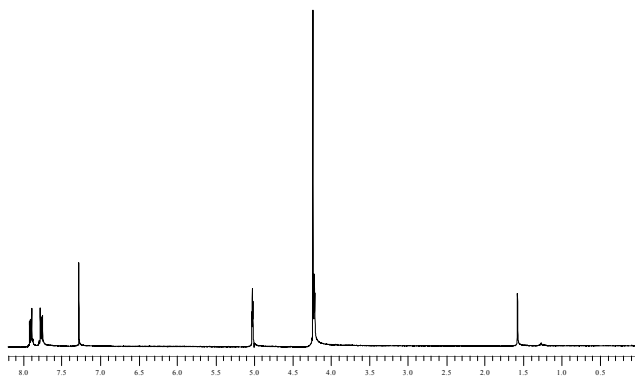


Figure 50. ^1H NMR of Fcphthalimide in CDCl_3 .

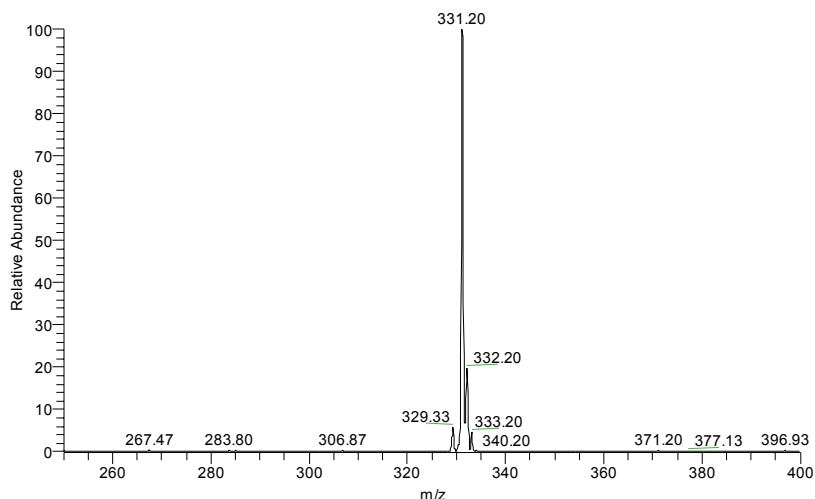


Figure 51. ESI-MS of Fcphthalimide prep taken in acetonitrile.

Alkylation of Fcphthalimide

Having successfully generated the ferrocenyl phthalimide at this point, alkylation of the cyclopentadienyl rings at the 1', 3, and 3' positions (Figure 52) was undertaken. Synthetic procedures developed by former Strauss group members for the alkylation of DEC were followed.

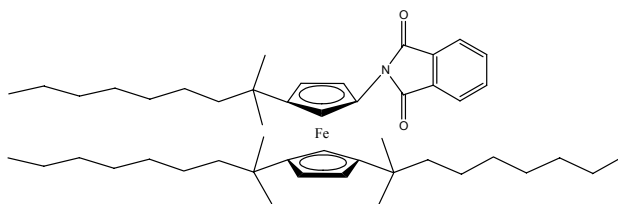


Figure 52. 1-phthalimide-1',3,3'-tri(2-methyl-2-nonyl)ferrocene.

Before alkylation, 2-methyl-2-chloro-nonane was generated by stirring 2-methyl-2-nonanol with concentrated HCl overnight. The resulting product was passed over a dry silica column to purify and was stored in the dark. The NMR data for this product in d_6 -benzene can be seen in Figure 53. After this, 2-chloro-2-methyl-nonane (7.4 fold equivalents over Fc) was added

to ZnCl_2 (3 fold excess over Fc) in a 3-neck round bottom flask under N_2 . The trialkylated Fc(phthalimide) was dissolved in dichloromethane and put into an addition funnel attached to the round bottom flask. The resulting contraption was carefully removed from the glove box and set up with a condenser under nitrogen. While stirring, the Fcphthalimide is added to the 3-neck RB, slowly over an hour. The resulting orange/red/brown solution is then refluxed for 48-96 hours (depending on scale of reaction). Following this, the solution is removed from heat and allowed to cool. It is then washed with an equal volume of 10% HCl, followed by one wash with 1M NaOH, and 2 washes with deionized/distilled water. The organic layer was collected and the dichloromethane was evaporated resulting in an orange/brown oil. Attempts to recrystallize have been unsuccessful to this point. Five synthetic preps of this material have been carried out to date and the crude yields are typically around 70-80%.

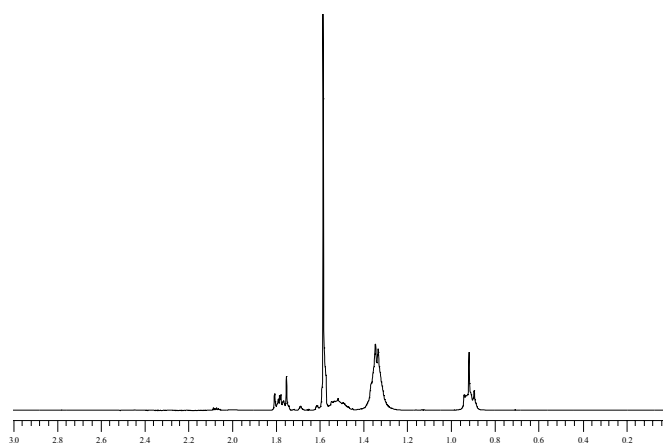


Figure 53. ^1H NMR of 2-chloro-2-methyl-nonane in d_6 -acetone.

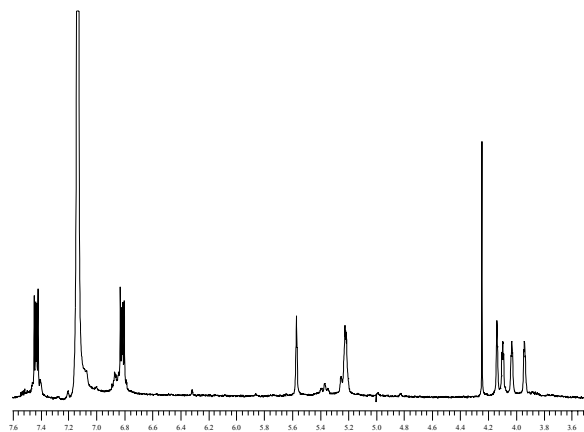


Figure 54. ^1H NMR of trialkylated ferrocenyl phthalimide in d_6 -benzene. Only Cp and phthalimide proton regions are shown due to the complexity observed in the alkyl region.

NMR spectra of the prep show expected quartets at 6.82 and 7.45 ppm for the phthalimide protons. Due to the substitution on the cyclopentadienyl rings the peaks from 3.9-4.2 ppm and at 5.2 ppm and 5.6 ppm correspond to the six remaining Cp protons. The peak at 7.15 ppm is the solvent and the peak at 4.3 ppm is the signal for remaining dichloromethane in deuterated benzene.

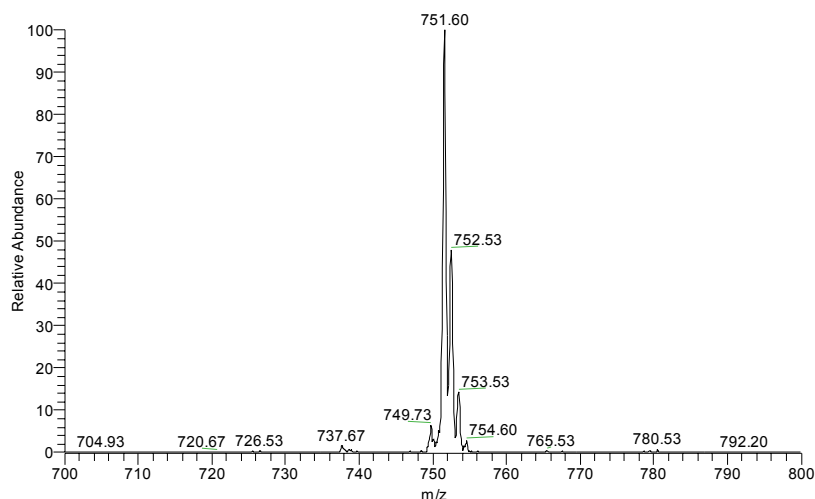


Figure 55. ESI-MS of trialkylated ferrocenyl phthalimide in dichloromethane.

The ESI-MS of the compound shows a single peak at m/z 751.60. One of the synthetic preps of this compound, however, showed a peak at m/z 611 in small abundance. This molecular weight species corresponded to bisalkylated ferrocenyl phthalimides in which one of the positions of the Cp ring did not undergo alkylation. In the MS this particular signal was not very intense, but comparison with NMR of the same compound showed a significant amount of product which was not fully alkylated. Therefore, the amount of time which the reaction is allowed to proceed varied depending on the scale of the reaction.

Reduction of phthalimide to NH_2

Without recrystallization of the alkylated ferrocenyl phthalimide compound generated in the previous step, reduction of the phthalimide moiety to NH_2 was carried out. The oil was dissolved in ethanol and the resulting solution was purged with nitrogen. Under nitrogen, hydrazine hydrate (40-50 fold excess over Fc) was added to the flask with a syringe. The reduction reaction was allowed to reflux for 2-3 hours, after which time it was cooled and deionized/distilled water was added. The product was extracted into ether and dried over sodium sulfate. The ether was evaporated off and the resulting orange/brown oil was stored under nitrogen. If not careful to store under nitrogen product may appear to become purple, though structural characterization (MS and NMR) show no difference between the different colored products. The synthesis for this compound has been carried out 3 times to date and the crude yields were observed to be as high as 92%. Attempts at recrystallization for this product were also unsuccessful. The 1H NMR and ESI-MS data are shown in Figures 57 and 58.

Analysis of the 1H NMR of the compound shows that the peaks characteristic of phthalimide observed did in fact disappear (spinning side bands are what appear to be in their positions). The alkylated region was ignored in the analysis of the synthesis due to its complexity. The MS data for the compound indicated that the sample was relatively pure.

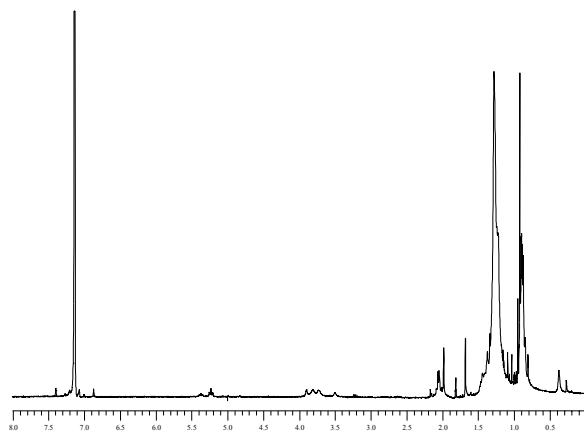


Figure 57. ^1H NMR of trialkylated ferrocenyl amine in d_6 -benzene.

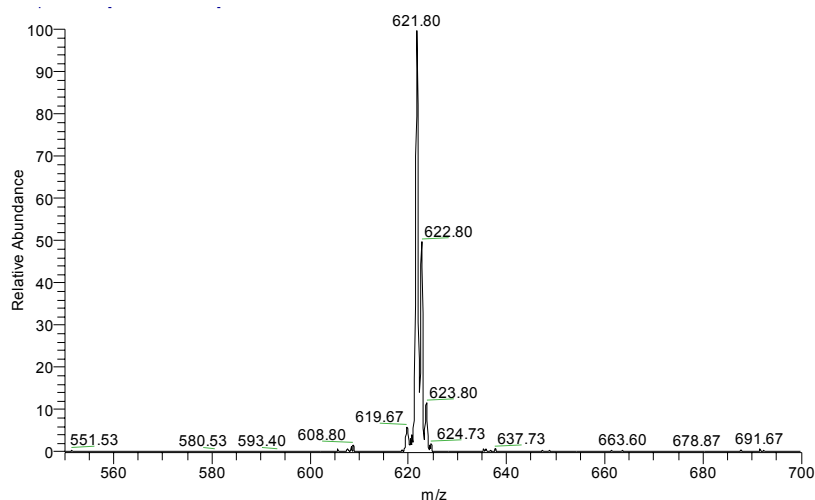


Figure 58. ESI-MS of the trialkylated ferrocenyl amine.

N-alkylation of trialkylated ferrocenyl amine

Based on conversations with peers at Colorado State University the N-alkylation was set up using 1:2 MeOH/DCM as solvent, 1.3 equivalents of heptaldehyde over the alkylated ferrocenyl amine, and 10-15 fold excess of sodium cyanoborohydride over the ferrocenyl amine. The starting materials, along with the alkylated ferrocenyl amine, were added together under N_2 in the glove box. The reaction mixture was then stirred at room temperature under N_2 and

appeared to be complete after 2-3 hours (based on ESI-MS). The resulting solution was red/brown at this point and then NaOH was added to give pH 10. The resulting product was extracted into dichloromethane which was then evaporated to give the red/brown oil that was obtained. Attempts at recrystallization for this product were not carried out and the resulting crude product was directly used in the final synthetic step towards azaDEC⁺Cl⁻. The N-alkylation was carried out 4 times and crude yields varied between 47 and 95%. ¹H NMR and ESI-MS are shown in Figures 59 and 60, respectively.

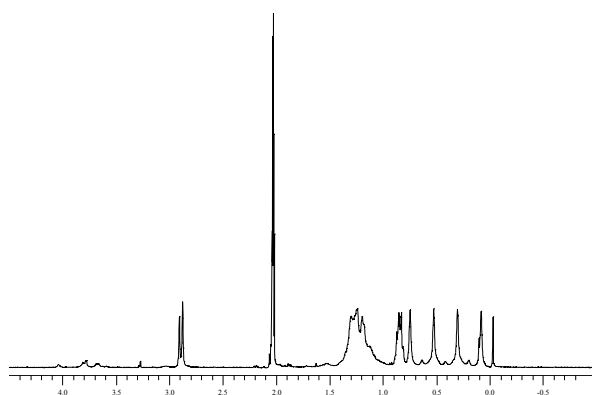


Figure 59. ¹H NMR of N-alkylated trialkylated ferrocenyl amine in d₆-acetone.

At this point NMR was not heavily relied on for analysis, however, it did show that the starting material was no longer present. Analysis by ESI-MS in dichloromethane indicates that a relatively pure product was obtained.

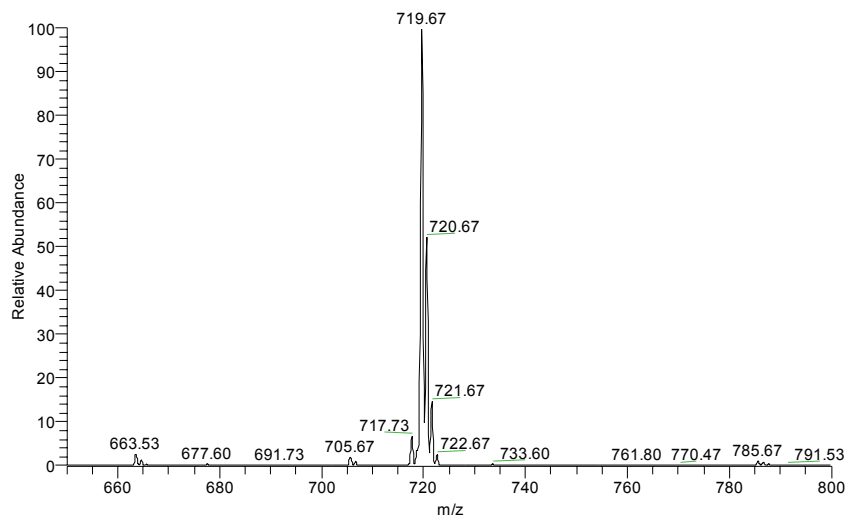


Figure 60. ESI-MS (in dichlorobenzene) of N-alkylation.

Exhaustive N-methylation to generate azaDEC⁺Cl⁻

The final step in our synthesis of azaDEC⁺Cl⁻ (Figure 61) involved determining the conditions under which the N-alkylated complex could be methylated.

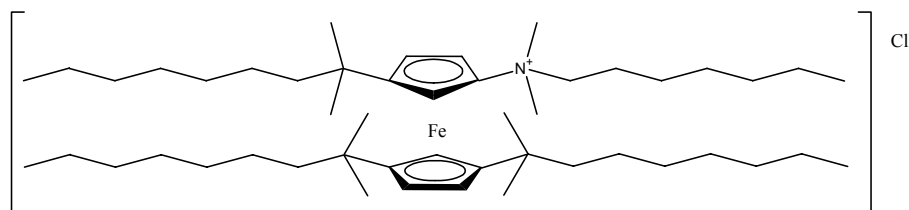


Figure 61. The compound azaDEC⁺Cl⁻

Based on Sommers, JOC, 1970, 35(5), 1558 and conversations with peers at CSU, 2-3 equivalents of 2,6-lutidine was added to the N-alkylated oil obtained in the previous section. Using methyl iodide as the solvent, methylation of the nitrogen occurred with stirring at room temperature over roughly a week. Other methods for methylation were attempted with no success, including:

- 1) using acetone as the solvent with MeI present in 10 fold excess
- 2) using methyl triflate as the methylating agent
- 3) using dimethyl sulfate as the methylating agent/solvent.

This reaction and resulting product were not monitored by NMR but solely by ESI-MS. This technique shows that the reaction proceeds through conversion first to the mono-methylated product (m/z 733) and then to the bis-methylated quaternary nitrogen (m/z 748).

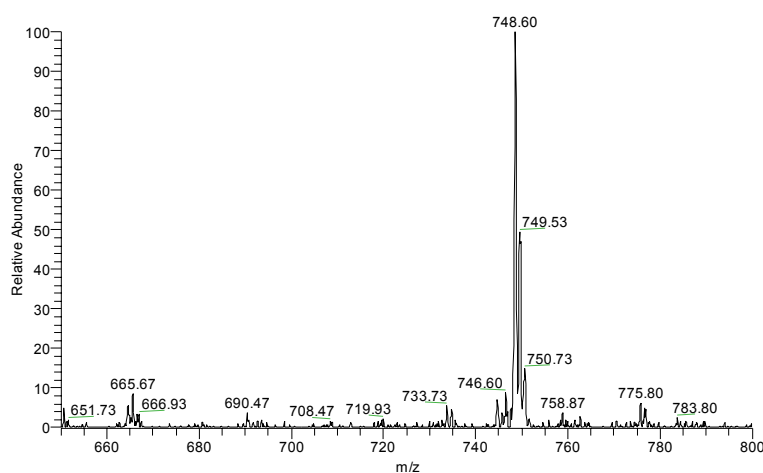
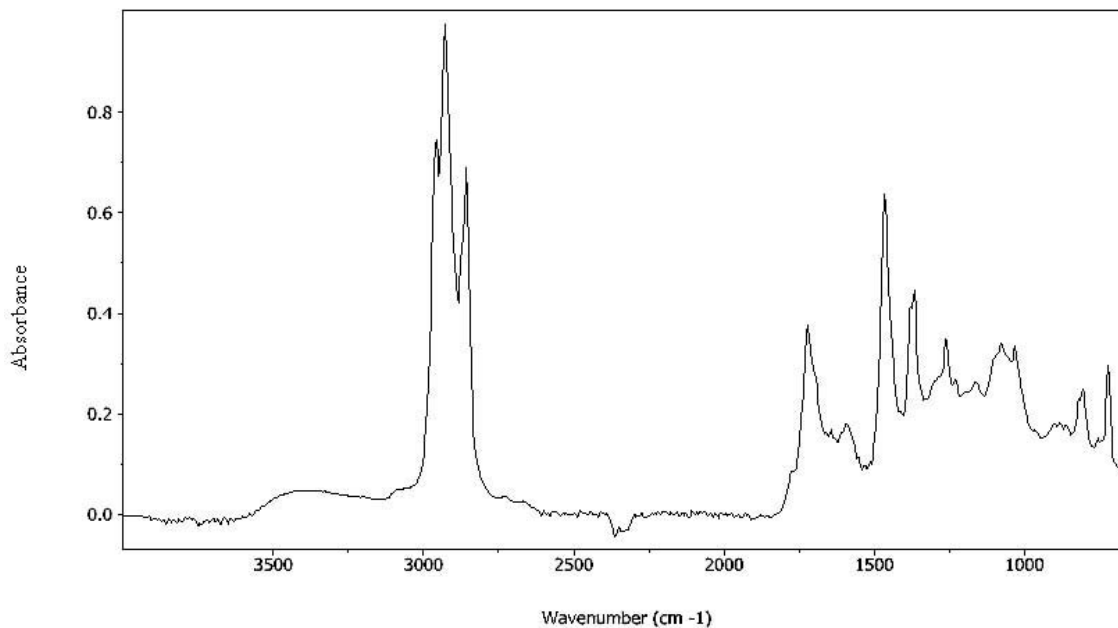


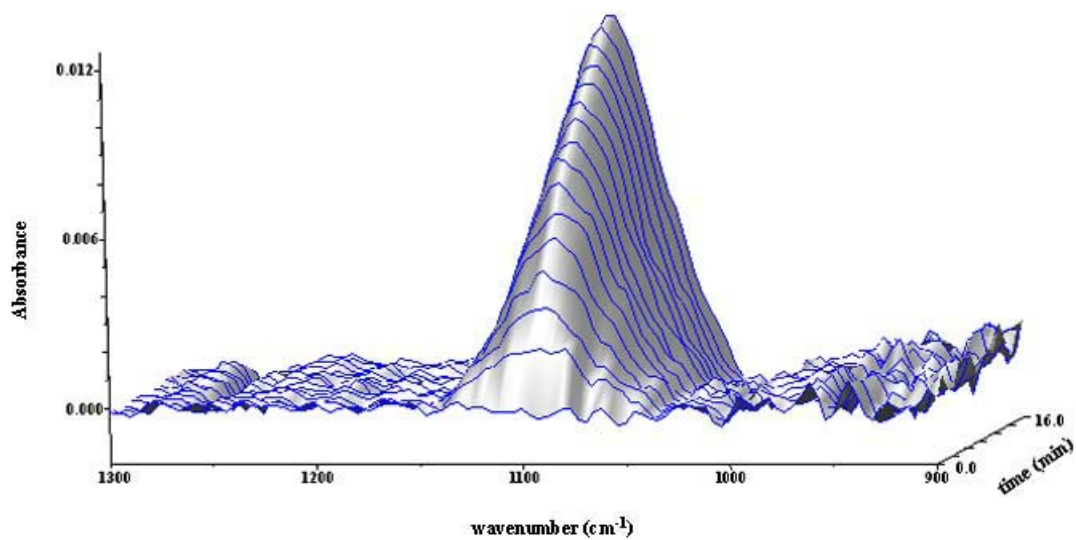
Figure 62. ESI-MS in acetonitrile of azaDEC⁺Cl⁻.

Though the synthetic prep actually generates azaDEC⁺I⁻, anion exchange of I⁻ for Cl⁻ and NO₃⁻ was achieved through vigorous shaking with numerous aliquots of HgCl₂/NaCl or NaNO₃. Disappearance of the iodide anion was monitored in the negative ion mode of ESI-MS. Once the azaDEC⁺Cl⁻ compound was generated, though not 100% pure, initial experiments were carried out to determine its effectiveness in the extraction of PMPA.

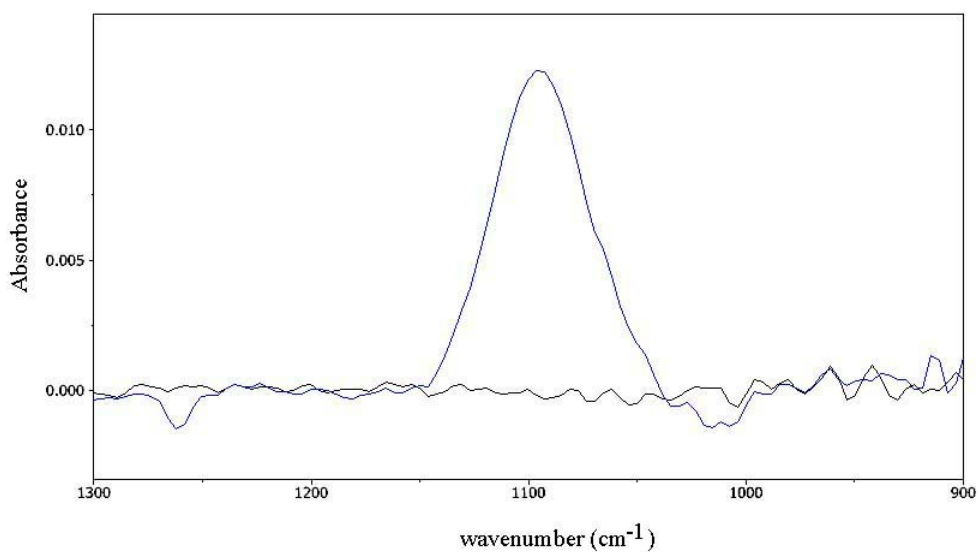
azaDEC⁺Cl⁻ Extraction of ClO₄⁻ and PMPA

Once the synthesis of azaDEC⁺X⁻ had been achieved initial experiments were carried out with the oily substance in order to test its ability to detect any anions. The first set of experiments were unsuccessful at exhibiting the extraction of PMPA as monitored by ATR-FTIR. This was believed to be due to the incomplete anion exchange of iodide for chloride. After more exhaustive efforts at exchanging the anions, the following experiments were successful. The first figure below shows a spectrum of the film itself and the second and third figures show the extraction of 10µM perchlorate with the new ferrocenyl film. It is important to keep in mind that the film is of a complex that is an oil and does contain minor impurities. LOD analysis was not carried using this compound for the analysis of perchlorate, it was simply a diagnostic run done to test the new complex.

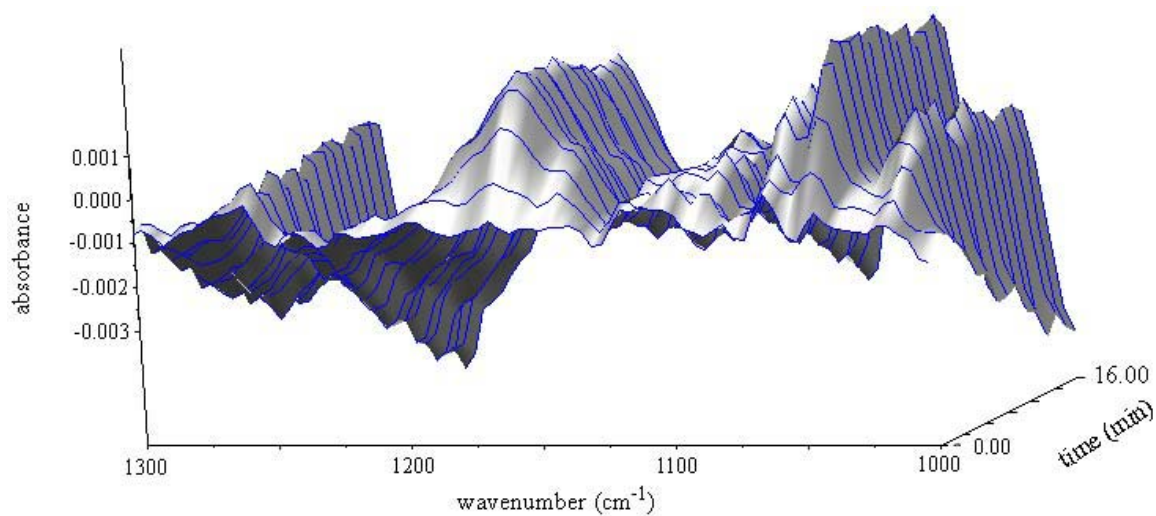




The first and last spectra for this reaction are shown below.



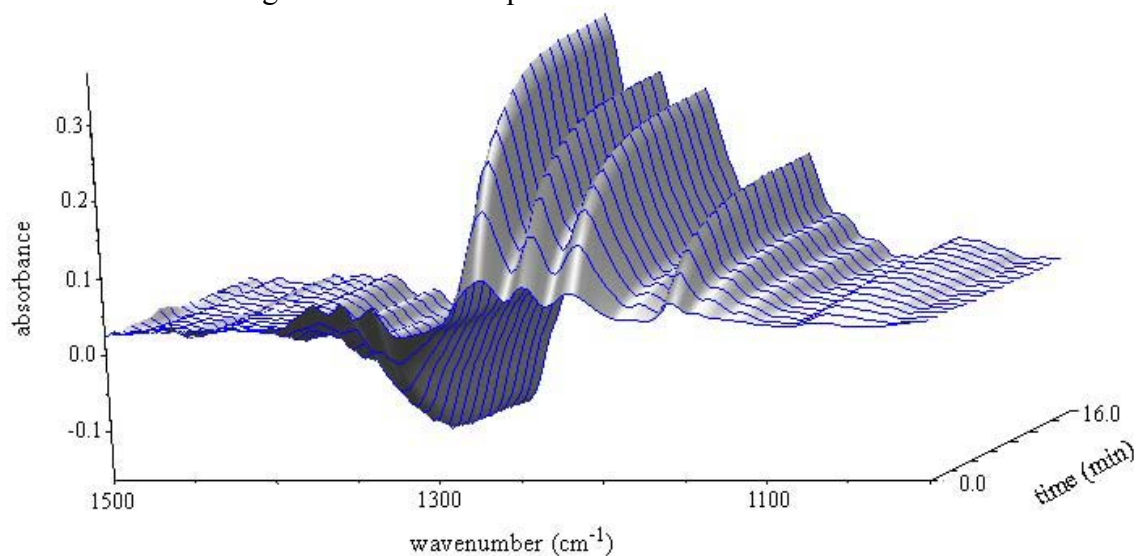
Having shown that the new ferrocenyl compound is effective in the extraction of anions, we then tested its use in the detection of 10 μM PMPA. A representative reaction using the new film is shown below. This reaction resulted in a *SNR* of approximately 10.



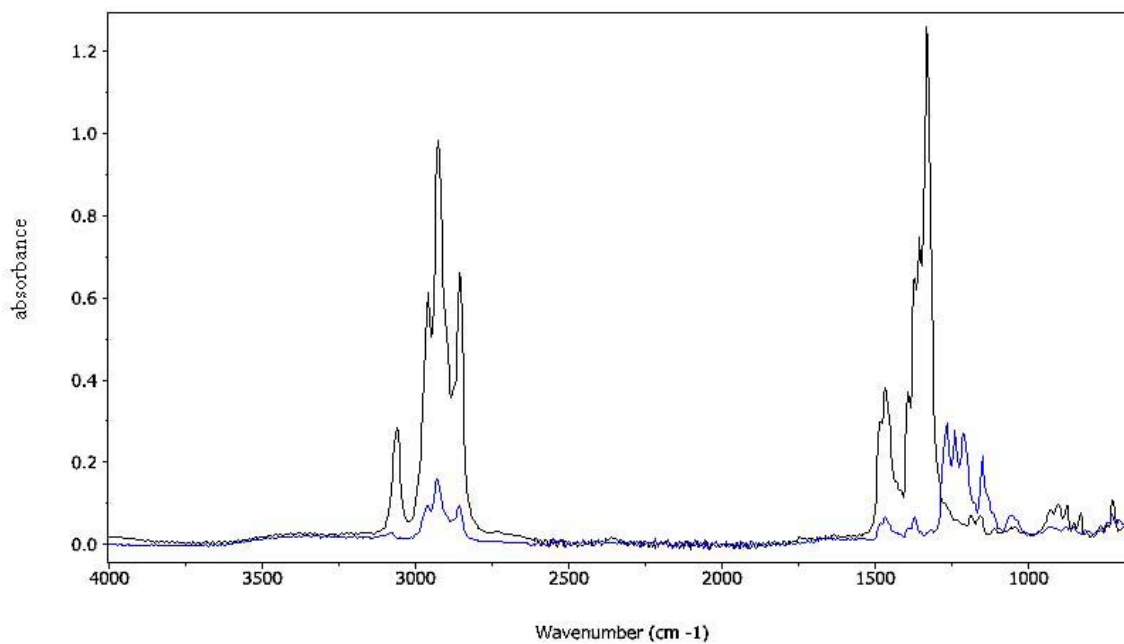
The analysis of the new compound also involved investigation of 100 μM PMPA ($SNR \sim 86$), and 50 μM PMPA ($SNR \sim 76$). Though these numbers are approximate it is clear that the LOD using this compound, which is challenging to recrystallized, will be higher than the LOD with DEC^+Cl^- (0.7 μM , 125 ppb).

Crystallization of $\text{DEC}^+\text{PFOS}^-$ and $\text{DEC}^+(1\text{-Me-CB}_{11}\text{F}_{11})^-$

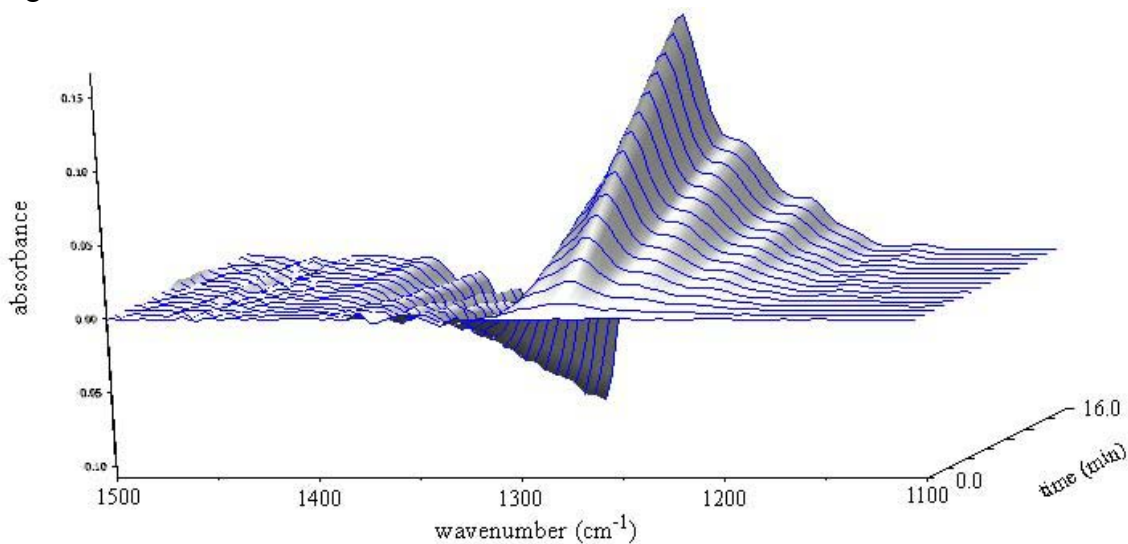
Attempts to generate crystals of DEC^+ with PFOS^- and $1\text{-Me-CB}_{11}\text{F}_{11}^-$ have been undertaken. Before trying to recrystallized the materials reactions were carried out to observe the extraction of the anions with $\text{DEC}^+\text{NO}_3^-$, and spectra of the films before and after extraction were also collected. The first figure shown here represents the extraction of PFOS^- .



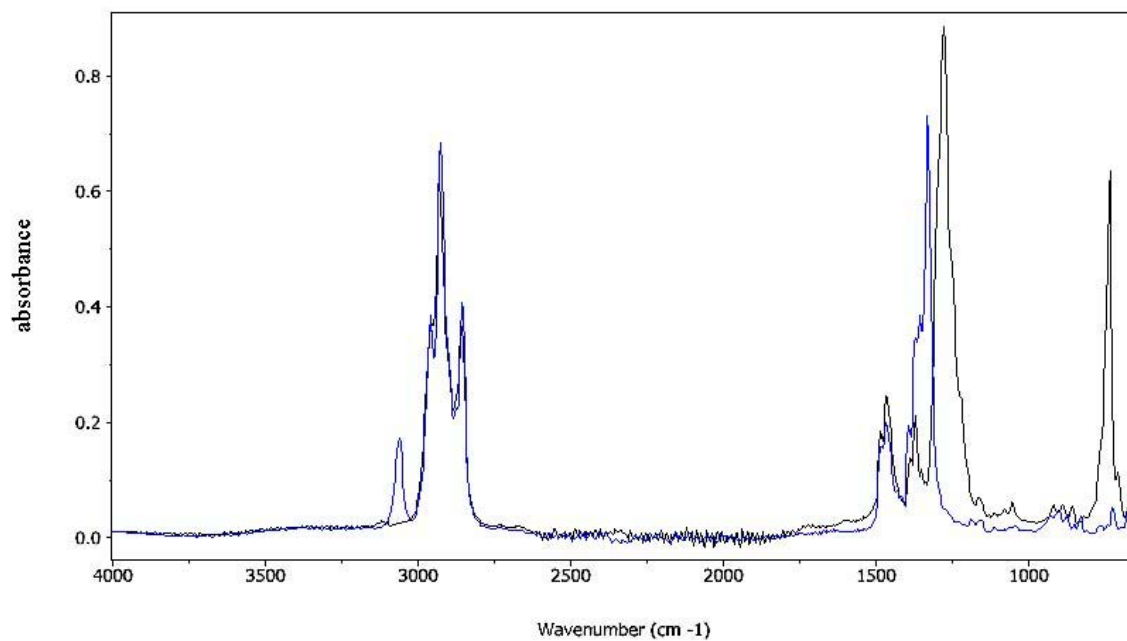
This figures compares films of $\text{DEC}^+\text{NO}_3^-$ (black) and $\text{DEC}^+\text{PFOS}^-$ (blue). Dilution occurred during anion exchange.



Here are similar experiments carried out with $1\text{-MeCB}_{11}\text{F}_{11}^-$. The first figure is again the extraction of $6\ \mu\text{M}$ carborane with $\text{DEC}^+\text{NO}_3^-$. As is apparent from the reaction shown, LOD analysis of the carborane in the film would more than likely be in the nanomolar concentration range.



This figure compares spectra of the films containing the different anions, NO_3^- (blue) and $1\text{-MeCB}_{11}\text{F}_{11}^-$ (black).



Currently, attempts are being made at recrystallizing these complexes for X-ray analysis. The most promising solvent system involves dissolving the complex in toluene and slowly allowing hexane to mix with the system.

References

- (1) Strauss, S. H.; Odom, M. A.; Hebert, G. N.; Clapsaddle, B. J. *J. Am. Water Works Assoc.* **2002**, *94*, 109;
- (2) Gehring, J. W.; Rindner, R. M.; Seals, W. "Design of a Deluge System to Extinguish Lead Azide Fires," Southwest Research Institute, 1978.
- (3) Hebert, G. N.; Odom, M. A.; Bowman, S. C.; Strauss, S. H. *Anal. Chem.* **2003**, *submitted for publication*.
- (4) Moody, C. A.; Hebert, G. N.; Strauss, S. H.; Field, J. A. *J. Environ. Monit.* **2003**, *5*, 341.
- (5) Hug, S. J. *J. Colloid Interface Sci.* **1997**, *188*, 415.
- (6) Weisz, A. D.; Rodenas, L. G.; Morando, P. J.; Regazzoni, A. E.; Blesa, M. A. *Catal. Today* **2002**, *76*, 103.
- (7) Duckworth, O. W.; Martin, S. T. *Geochim. Cosmochim. Acta* **2001**, *65*, 4289.
- (8) Elzinga, E. J.; Peak, D.; Sparks, D. L. *Geochim. Cosmochim. Acta* **2001**, *65*, 2219.
- (9) Borda, M. J.; Strongin, D. R.; Schoonen, M. A. *Spectrochim. Acta, Part A* **2003**, *59*, 1103.
- (10) Peak, D.; Luther, G. W., III; Sparks, D. L. *Geochim. Cosmochim. Acta* **2003**, *67*, 2551.
- (11) Voegelin, A.; Hug, S. J. *Envir. Sci. Technol.* **2003**, *37*, 972.
- (12) Jakusch, M.; Janotta, M.; Mizaikoff, B. *Anal. Chem.* **1999**, *71*, 4786.
- (13) Degenhardt, J.; McQuillan, A. J. *Langmuir* **1999**, *15*, 4595.
- (14) Dobson, K. D.; McQuillan, A. J. *Spectrochim. Acta, Part A* **1999**, *55*, 1395.
- (15) Dobson, K. D.; McQuillan, A. J. *Langmuir* **1997**, *13*, 3392.
- (16) Wijnja, H.; Schulthess, C. P. *Soil Sci. Soc. Am. J.* **2001**, *65*, 324.
- (17) Sheals, J.; Sjoberg, S.; Persson, P. *Envir. Sci. Technol.* **2002**, *36*, 3090.

- (18) Kellner, R.; Zippel, E.; Pungor, E.; Toth, K.; Lindner, E. In *Comtemporary Electroanalytical Chemistry*; Ivaska, A., Lewenstam, A., Sara, R., Eds.; Plenum Press: New York, 1990; 223.
- (19) Clark, J. F.; Clark, D. L.; Whitener, G. D.; Schroeder, N. C.; Strauss, S. H. *Environ. Sci. Technol.* **1996**, *30*, 3124.
- (20) Clapsaddle, B. J.; Clark, J. F.; Clark, D. L.; Gansle, K. M.; Gash, A. E.; Chambliss, C. K.; Odom, M. A.; Miller, S. M.; Anderson, O. P.; Hughes, R. P.; Strauss, S. H. *Inorg. Chem.* **2003**, *manuscript in preparation*.
- (21) Hebert, G. N.; Odom, M. A.; Craig, P. S.; Dick, D. L.; Strauss, S. H. *J. Environ. Monit.* **2002**, *4*, 90.
- (22) Mercier, J.-P.; Morin, P.; Dreux, M.; Tambute, A. *Chromatographia* **1998**, *48*, 529.
- (23) Harrick, N. J. *Internal Reflection Spectroscopy*; Interscience: New York, 1967.
- (24) Urban, M. W. *Attenuated Total Reflectance Spectroscopy of Polymers. Theory and Practice*; American Chemical Society: Washington DC, 1996.
- (25) Parsons, M. L. *J. Chem. Educ.* **1969**, *46*, 290.
- (26) Kaiser, H. *Anal. Chem.* **1970**, *42*, 26A; Long, G. L.; Winefordner, J. D. *Anal. Chem.* **1983**, *55*, 712A; Williams, T. W.; Salin, E. D. *Anal. Chem.* **1988**, *60*, 725.
- (27) *Spectrochim. Acta, Part B* **1978**, *33*, 241.
- (28) *Spectrochim. Acta, Part B* **1978**, *33*, 248.
- (29) Boumans, P. W. J. M. *Spectrochim. Acta, Part B* **1978**, *33*, 625.
- (30) *Anal. Chem.* **1980**, *52*, 2242.
- (31) Winefordner, J. D.; McCarthy, W. J.; St. John, P. A. *J. Chem. Educ.* **1967**, *44*, 80; McCarthy, W. J. In *Advances in Analytical Chemistry and Instrumentation*; Reilley, C. N., McLafferty, F. N., Eds.; Wiley-Interscience: New York, 1971; 493; Glaser, J. A.; Foerst, D. L.; McKee, G. D.; Quave, S. A.; Budde, W. L. *Environ. Sci. Technol.* **1981**, *15*, 1426; Faber, K.; Lorber, A.; Kowalski, B. R. *J. Chemom.* **1997**, *11*, 419.
- (32) St. John, P. A.; McCarthy, W. J.; Winefordner, J. D. *Anal. Chem.* **1967**, *39*, 1495.

- (33) Parsons, M. L.; Winefordner, J. D. *Appl. Spectrosc.* **1967**, *21*, 368; Ingle, J. D., Jr. *Anal. Chem.* **1975**, *47*, 1217.
- (34) Wilhite, R. N.; Ellis, R. F. *Appl. Spectrosc.* **1963**, *17*, 168.
- (35) Odom, M. A.; Hebert, G. N.; Clapsaddle, B. J.; Strauss, S. H. In *Proceedings of the First Joint Conference on Point Detection, Williamsburg, VA, October 2000*; Science and Technology Corporation: Hampton, VA, 2001; 158.
- (36) Griffiths, P. R.; de Haseth, J. *Fourier Transform Infrared Spectrometry*; John Wiley & Sons: New York, 1986.
- (37) Chambliss, C. K.; Martin, C. R.; Strauss, S. H.; Moyer, B. A. *Solvent Extr. Ion Exch.* **1999**, *17*, 553.